

AD-A093 800

HARRIS CORP MELBOURNE FLA

F/G 17/4

RAPID ACQUISITION OF SPREAD SPECTRUM SIGNALS. (U)

DEC 80 M J BOUVIER, H E WALLS, R W BOYD

DAAG29-80-C-0005

UNCLASSIFIED

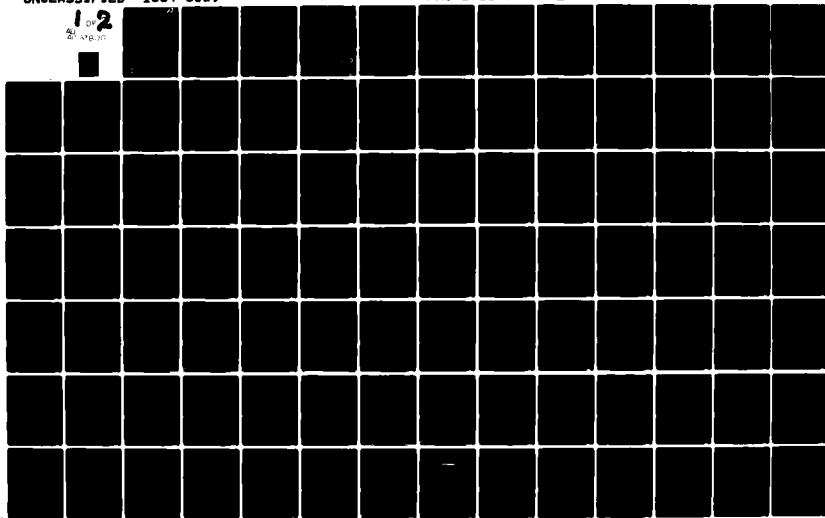
1634-8019

ARO-17105.1-A-EL

NL

1 of 2

2 pages



D

LEVEL II

1634-8019

4

AD A093800

**RAPID ACQUISITION OF
SPREAD SPECTRUM SIGNALS**

DECEMBER 1980

CONTRACT # DAAG29-80-C-0005

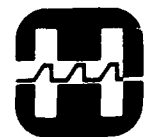
FINAL REPORT
FOR PERIOD
OCTOBER 1979 TO OCTOBER 1980

ARMY RESEARCH OFFICE
RESEARCH TRIANGLE PARK
NORTH CAROLINA 27709

S DTIC ELECTE D
JAN 15 1981
D

DDC FILE COPY

DISTRIBUTION STATEMENT A
Approved for public release;
Distribution Unlimited



HARRIS

HARRIS CORPORATION Government Information Systems Division
P.O. Box 94000 Melbourne, Florida 32901 • U.S.A. • Tel. (305) 727-5009

81 1 12 332

UNCLASSIFIED

SECURITY CLASSIFICATION OF THIS PAGE (When Data Entered)

REPORT DOCUMENTATION PAGE		READ INSTRUCTIONS BEFORE COMPLETING FORM
1. REPORT NUMBER 19) 17105.1-A-EL	2. GOVT ACCESSION NO. AD-A093800	3. RECIPIENT'S CATALOG NUMBER 7
4. TITLE (and Subtitle) Rapid Acquisition of Spread Spectrum Signals, I	5. TYPE OF REPORT & PERIOD COVERED Final Report. 29 Oct 79 - 28 Oct 80	
	6. PERFORMING ORG. REPORT NUMBER	
7. AUTHOR(s) M. J. Bouvier, Jr. H. E. Walls R. W. Boyd	8. CONTRACT OR GRANT NUMBER(s) DAAG29-80-C-0095K	
9. PERFORMING ORGANIZATION NAME AND ADDRESS Harris Corporation Melbourne, FL 32901	10. PROGRAM ELEMENT, PROJECT, TASK AREA & WORK UNIT NUMBERS 12-17-1	
11. CONTROLLING OFFICE NAME AND ADDRESS U. S. Army Research Office Post Office Box 12211 Research Triangle Park, NC 27709	12. REPORT DATE 11) Dec 80	
	13. NUMBER OF PAGES 158	
14. MONITORING AGENCY NAME & ADDRESS (if different from Controlling Office)	15. SECURITY CLASS. (of this report) Unclassified	
	15a. DECLASSIFICATION/DOWNGRADING SCHEDULE	
16. DISTRIBUTION STATEMENT (of this Report) Approved for public release; distribution unlimited.		
17. DISTRIBUTION STATEMENT (of the abstract entered in Block 20, if different from Report) NA		
18. SUPPLEMENTARY NOTES The view, opinions, and/or findings contained in this report are those of the author(s) and should not be construed as an official Department of the Army position, policy, or decision, unless so designated by other documentation.		
19. KEY WORDS (Continue on reverse side if necessary and identify by block number) spread spectrum signals signal acquisition waveforms communications		
20. ABSTRACT (Continue on reverse side if necessary and identify by block number) This investigation has focused on the fundamental principles of the acquisition process, mathematically quantifying potential acquisition performance as a function of (1) receiver structures and devices, (2) spreading waveforms and (3) specially structured acquisition signals. Certainly the most obvious conclusion is that MF devices offer a relatively straightforward means (for DS systems at least) of achieving two to three orders-of-magnitude improvement in acquisition time. These magnitudes of improvement are quite significant for reacquisition operations.		

1634-8019

RAPID ACQUISITION OF SPREAD SPECTRUM SIGNALS

M. J. BOUVIER, JR.
H. E. WALLS
R. W. BOYD

DECEMBER 1980

CONTRACT # DAAG29-80-C-0005

FINAL REPORT
FOR PERIOD
OCTOBER 1979 TO OCTOBER 1980

ARMY RESEARCH OFFICE
RESEARCH TRIANGLE PARK
NORTH CAROLINA 27709

DTIC
ELECTE
S D
JAN 15 1981
D

DISTRIBUTION STATEMENT A

Approved for public release;
Distribution Unlimited

Table of Contents

<u>Section</u>	<u>Title</u>	<u>Page</u>
1.0	Introduction.....	1-1
1.1	Statement of the Problem.....	1-1
1.2	Objectives of the Study.....	1-3
1.3	Organization of the Report.....	1-4
2.0	Mean Search Time.....	2-1
2.1	Example: Direct Serial Search.....	2-5
3.0	Serial Search Techniques.....	3-1
3.1	Single Integration.....	3-1
3.2	Double Integration.....	3-11
3.3	Sequential Detection.....	3-18
3.4	Doppler Limitations.....	3-34
4.0	Parallel Search Operations.....	4-1
5.0	Matched Filter Technology.....	5-1
5.1	CCD.....	5-1
5.2	Digital Correlator.....	5-3
5.3	SAW Convolver.....	5-3
5.3.1	Effects of Doppler and Random Phase Variations.....	5-5
5.4	Hybrid Array Correlator.....	5-24
6.0	Direct Serial Search versus Matched Filter Search.....	6-1
7.0	Comparison of DS, FH and FH/DS.....	7-1
7.1	Direct Sequence.....	7-1
7.2	Frequency Hop.....	7-1
7.2.1	Direct Search of FH.....	7-3
7.2.2	MF for FH.....	7-4
7.3	Frequency Hop/Direct Sequence.....	7-9
7.3.1	Direct Search.....	7-9
7.3.2	Matched Filter.....	7-13
8.0	Basic Acquisition Strategies.....	8-1
8.1	Search Methods.....	8-2
8.2	The Data Transmission Method.....	8-4
8.3	The Combined Search and Data Transmission Method.....	8-5
8.4	Example.....	8-6

Table of Contents (Continued)

<u>Section</u>	<u>Title</u>	<u>Page</u>
8.5	The Optimum Combined Method.....	8-8
8.6	Conclusions.....	8-10
9.0	Code Validity Interval Techniques.....	9-i
9.1	Hard Edge CVI.....	9-1
9.2	Soft Edge CVI.....	9-2
9.3	Acquisition Characteristics.....	9-4
10.0	Summary.....	10-1
11.0	Recommendations for Future Work.....	11-1
APPENDIX A	FH Acquisition by ASEAT.....	A-1
APPENDIX B	Component Codes.....	B-1
APPENDIX C	Timing Uncertainty at Reacquisition.....	C-1
APPENDIX D	Optical Processing.....	D-1

List of Illustrations

<u>Number</u>	<u>Title</u>	<u>Page</u>
2.1-1	Direct Serial Search for PN Code Acquisition.....	2-6
2.1-2	Acquisition Performance.....	2-10
2.1-3	Average Number of Cells Searched, False Alarms and Acquisition Time Versus Dwell Time.....	2-11
2.1-4	Comparison of "Approximation" and "Actual" Optimum SNR_{ED}	2-14
3.1-1	Noncoherent Fixed Dwell Time Acquisition Model.....	3-2
3.1-2	Acquisition Performance.....	3-6
3.1-3	Acquisition Performance.....	3-7
3.1-4	Acquisition Performance.....	3-8
3.1-5	Acquisition Performance.....	3-10
3.2-1	Noncoherent Double Dwell Time Acquisition Model.....	3-11
3.2-2	Acquisition Performance.....	3-15
3.2-3	Acquisition Performance.....	3-16
3.3-1	Block Diagram of Sequential Detector.....	3-21
3.3-2	Acquisition Performance.....	3-22
3.3-3	Miss Probability Versus S/N with Random Start Phase....	3-23
3.3-4	Effect of Lower Threshold on Mean-Time-to-Dismiss (No Signal).....	3-24
3.3-5	Effect of External Accumulator on Dismissal Time.....	3-25
3.3-6	Effect of Lower Threshold on Mean-Time-to-Dismiss (No Signal) (Approximation).....	3-27
3.3-7	Acquisition Performance.....	3-28
3.3-8	Acquisition Performance.....	3-30
3.3-9	Acquisition Performance.....	3-31
3.4-1	Noncoherent Detector.....	3-34
4.0-1	Acquisition Performance.....	4-6
5.1-1	511-Stage CCD Matched Filter.....	5-2
5.2-1	64-Bit Digital Correlator.....	5-4
5.3-1	SAW Beamwidth Compression Convolver.....	5-6
5.3.1-1	SAW Convolver.....	5-8

List of Illustrations (Con't)

<u>Number</u>	<u>Title</u>	<u>Page</u>
5.3.1-1A	Normalized Function for Output of Convolver with the Input and Reference Waveforms Being 10 μ s Pulses.....	5-12
5.3.1-2	Normalized Correlation Function for Output of Convolver with the Input and Reference Waveforms Being 10 μ s Pulses with 10 KHz of Doppler.....	5-13
5.3.1-3	Normalized Correlation Function for Output of Convolver with the Input and Reference Waveforms Being 10 μ s Pulses with 50 KHz of Doppler.....	5-14
5.3.1-4	Normalized Correlation Function for Output of Convolver with the Input and Reference Waveforms Being 10 μ s Pulses with 50 KHz of Doppler.....	5-15
5.3.1-5	Loss in Convolver Peak Output Due to Doppler for the Input and Reference Waveforms Being 10 μ s Pulses.....	5-16
5.3.1-6	Normalized Mean Square Value of Convolver Output with Random Phase Input.....	5-19
5.3.1-7	Normalized Mean Square Value of Convolver Output with Random Phase Input.....	5-20
5.3.1-8	Normalized Mean Square Value of Convolver Output with Random Phase Input.....	5-21
5.3.1-9	Normalized Mean Square Value of Convolver Output with Random Phase Input.....	5-22
5.3.1-10	Loss in Convolver Mean Square Output Due to Doppler and Random Phase Variations.....	5-23
5.4-1	Hybrid Array Correlator Concept.....	5-25
5.4-2	Correlator Cell of Hybrid Array Correlator.....	5-28
6.0-1	Multiply and Integrate Correlator Receiver.....	6-1
6.0-2	Direct Serial Search.....	6-2
6.0-3	MF for DS Acquisition.....	6-3
6.0-4(a)	Direct Serial Search.....	6-4
6.0-4(b)	Matched Filter Search.....	6-5
7.2-1	Basic FH Transmitter.....	7-2
7.2.1-1	Direct Search for FH Acquisition.....	7-3
7.2.2-1	MF for FH Acquisition.....	7-4
7.2.2-2	Advanced FH Pattern.....	7-5
7.2.2-3	Undelayed Samples.....	7-7
7.2.2-4	Delayed Samples.....	7-7

List of Illustrations (Con't)

<u>Number</u>	<u>Title</u>	<u>Page</u>
7.3-1	Basic FH/DS Transmitter.....	7-10
7.3.1-1	Direct Search of FH/DS.....	7-11
7.3.2-1	MF Receiver for FH/DS.....	7-14
7.3.2-2	Summary of Acquisition Performances.....	7-15
8.4-1	Performance of the Combined Method.....	8-9
9.1-1	Processing Gain Loss in Hard Edge CVI System.....	9-3
9.2-1	Processing Gain Loss in Soft Edge CVI System.....	9-5
A-1	FH Acquisition by ASEAT.....	A-2
C-1	Timing Uncertainties.....	C-4
D-1	Time-Integrating Correlator.....	D-3

SECTION 1.0
INTRODUCTION

1.0 INTRODUCTION

This report presents the results of the "Rapid Acquisition of Spread Spectrum Study" which was performed between October 1979 and October 1980 under Army Research Office contract number DAAG29-80-C-0005.

1.1 Statement of the Problem

Tactical Communications provide the backbone for the Command and Control functions in today's military systems; however, this communications is being threatened by the increased capabilities of enemy electronic countermeasures which could deny the availability of critical communications during a stressed situation. The continued development and deployment of anti-jam (AJ) systems employing Spread Spectrum communications is necessary to counter this electronic threat. Most spread spectrum systems derive their spreading signal, either directly or indirectly, from a pseudonoise (PN) sequence generator. In order to despread the received signal, and subsequently recover the transmitted data, the receiver's PN generator must be synchronized with the transmitter's PN generator. The process of achieving this synchronization is commonly called acquisition. Rapid acquisition of timing synchronization is essential for tactical communication systems involving dynamic platforms in highly flexible operational scenarios. But addressing spread spectrum acquisition in the military environment also imposes the conflicting constraint that protection against intelligent jamming not be unduly compromised during the acquisition process.

The performance of any acquisition or reacquisition strategy is a function of the timing uncertainty, hardware complexity and code randomness. Many systems choose to periodically reduce code randomness via short codes, fixed preambles, dedicated acquisition intervals, etc. in order to achieve a desired acquisition time. However, this compromise increases the vulnerability to smart jammers which may make this approach acceptable only for acquisition in a benign environment. Other means of reducing acquisition time are generally at the expense of more costly and/or more complex hardware. For example, a more accurate time standard, or a second receiver (such as GPS) for external time synchronization, can be used to reduce time uncertainty. The large number of variables, some of which are scenario based and some technology based, makes it convenient from both a concept viewpoint and a design viewpoint to identify three categories of acquisition:

Initial Acquisition

- Initial System Operations
- Initial Network Entry

} Scenario Dependent

"Coarse" Reacquisition

- Network Entry
- Silent Running

} Scenario and
Technology Dependent

"Fine" Reacquisition

- TDMA
- Noise Unlocks
- LOS Outage

} Technology
Dependent

Initial acquisition is acquisition in the truest sense - initial establishment of timing synchronization from total timing uncertainty. In general it is the most difficult and most time consuming, and the one most sensitive to scenario. Initial system operations require acquisition of system timing as only one part of the overall operation of establishing communications and must be accompanied by terminal deployment, antenna pointing, and other setup functions. Thus, the initial timing acquisition may be done in a relatively leisure fashion if it is not the pacing item. Also, in some scenarios, initial acquisition is performed in a benign environment such that AJ performance is not required during this mission phase and, therefore, may be accommodated by use of a short repetitive code or even a "pre-launch" hard wire connection. Initial entry of a platform into a communication network may require a complete initial acquisition operation or only a "coarse" reacquisition or "adjustment of timing" operation depending upon whether or not a priori knowledge of the network's timing is available to the platform.

Reacquisition from "coarse" timing uncertainty is required at the completion of operational modes referred to as "silent running" or "dead reckoning". In these modes a vehicle is navigated to a target area by an onboard system with the communication link "silent" and upon arriving at the area the link must be rapidly established in a heavy ECM environment. Reacquisition strategy and performance for these modes are obviously both scenario dependent (i.e., availability of position estimates, etc.) and technology dependent (i.e., clock stability, reacquisition hardware, etc.).

The third category of timing acquisition is that of reacquisition from "fine" timing uncertainty, and is the acquisition operation most often

performed in tactical communication systems. It is performed after relatively short periods of link outage which occur between bursts in TDMA systems or as a result of noise or LOS produced losses-of-lock. The timing uncertainty is small; rapid reacquisition is required; and reacquisition performance is basically only a function of receiver technology.

1.2 Objectives of the Study

The technical proposal upon which the study was based identified four specific objectives; all four objectives were achieved during the study. The first objective was to establish the performance of an existing acquisition technique which would serve as a standard by which to judge the techniques developed during the study. The sequential detection acquisition technique was identified as the standard so that the first objective was:

Objective 1: Establish the acquisition performance of the sequential detection algorithm for a realistic set of operating conditions.

The theory and performance of the sequential detection algorithm are presented in Section 3, along with those of the other serial search techniques. Sequential detection is shown to provide an acquisition time advantage of two to four times over the others at the low signal-to-noise ratios commonly encountered in tactical AJ data links. The second, and primary, objective of the study was to identify acquisition techniques which can provide significantly more rapid acquisition than the sequential detection technique, with a stated goal of 1000 times improvement. As stated in the proposal:

Objective 2: Postulate and evaluate new techniques for rapid acquisition - goal of X1000 improvement.

The matched filter (MF) devices described in Section 5 provide one key to orders-of-magnitude improvement in acquisition time. The performances of direct search and MF based acquisition systems are compared in Section 6 and an example presented there indicates a 2000 times advantage for the MF system. The use of special acquisition protocols or strategies, which are presented in Section 8, can provide many orders-of-magnitude improvement in acquisition time. These techniques are particularly applicable to initial acquisition or to reacquisition with extremely large time uncertainty. With limited time uncertainty the Code Validity Interval (CVI) methods discussed in Section 9 permit data demodulation without any reacquisition operation. These techniques are quite attractive for application to tactical AJ data links in which bursty

type messages are transmitted between dynamic platforms in a highly flexible operational scenario.

Another means of achieving more rapid acquisition is by choice of spreading waveform - the subject of the third objective.

Objective 3: Exploit the rapid acquisition potential of FH/DS signals.

The acquisition performances of FH and FH/DS are established and compared to that of DS in Section 7. The FH and FH/DS waveforms can be utilized to reduce acquisition time by several orders-of-magnitude and thus can be considered to be acquisition aids. Basically FH systems gain the advantage as a consequence of the fact that the timing resolution required in these systems for data demodulation is much coarser than that required in DS systems. Therefore, the timing uncertainty remaining at the completion of the acquisition process is greater. If the data link must provide a highly accurate range estimate, as is common in DS applications, then timing must be resolved to the same degree in the FH system and the DS system, and the FH system does not exhibit any acquisition time advantage.

As stated in the proposal the emphasis was to be on rapid acquisition concepts and that results were not to be constrained by present day hardware limitations. However, a secondary objective was:

Objective 4: Implications to hardware development.

The key hardware item for improved acquisition performance is the MF. This is a rapidly developing technology but today's state-of-the-art devices (described in Section 5) cannot fully satisfy the requirements. The major deficiency is the limited integration time or "length", which limits the processing gain.

1.3 Organization of the Report

The basic approach taken in this study to identify rapid acquisition techniques has been to postulate, characterize and compare: (1) receiver structures and devices, (2) spreading waveforms and (3) special acquisition protocols or strategies, and then to identify those characteristics which can potentially be exploited to provide a rapid acquisition capability. The objective has been to identify orders of magnitude of potential improvement in acquisition performance over presently employed direct search acquisition methods. At the same time the need to limit the vulnerability to intelligent jammers has been a recognized requirement.

All of the concepts presented in this report are applicable, in general, to all three categories of acquisition. However, it is recognized that it is entirely impractical to consider establishing initial synchronization (starting from total timing uncertainty) directly from the fully random spreading waveforms commonly employed in military communication systems. Pragmatically, true initial acquisition can be accomplished in an operationally acceptable amount of time only if the randomness of the spreading waveform is reduced which implies some potential reduction in AJ protection against "very smart" jammers. Methods for achieving this trade-off are specifically addressed in Sections 8 and 9; the other sections of the report are primarily applicable to the "coarse" and/or "fine" acquisition processes. Section 2 presents a heuristic derivation of a previously obtained expression for mean acquisition time. The advantage of the heuristic development is that it permits greater insight into the underlying interactions between system parameters such as detection probability, false alarm probability, dwell time and signal-to-noise ratio. In addition, the problem is formulated there as a general search problem in order to emphasize the broad applicability of the results. In Section 3 the performances of the direct serial search techniques of single and double integration and sequential detection are evaluated and compared under common operating conditions. The obvious extension to parallel search operations is considered in Section 4. Ideally one would expect the acquisition time to decrease linearly with the number of parallel search devices employed; however, the results presented indicate that this advantage is not fully realizable. The limitation arises from the fact that if all parallel devices are stepped ahead synchronously then all of the devices are tied up whenever any one incurs a false alarm.

The rapidly emerging technology of matched filter (MF) devices is expected to play a key role in the implementation and performance of future spread spectrum systems, both for acquisition and data demodulation. Characteristics of typical state-of-the-art MF devices which shown promise for spread spectrum applications (Charge Couple Devices, SAW Convolvers, Digital Correlators and the Hybrid Array Correlator presently under development at Harris). are briefly described in Section 5. Section 6 compares MF-based acquisition techniques to the direct search techniques with the intent of both illustrating the potential acquisition gains available with MFs and providing some insight into the underlying conceptual differences between the direct search and MF techniques. Section examines the influence of the spreading waveform on acquisition performance, presenting basic acquisition structures and performance characteristics for direct sequence (DS), frequency hop (FH) and combined FH/DS spreading waveforms. FH has some-

times been proposed as an acquisition aid for DS systems and this issue is thoroughly examined. Special acquisition protocols or strategies are presented and analyzed in Section 8. These techniques are primarily of interest for acquisition with extremely large timing uncertainty such as initial acquisition and the trade-off between acquisition time and randomness in the spreading waveform is addressed here. Sections 6, 7 and 8 are tied together in that Section 6 considers acquisition performance as a function of receiver hardware, Section 7 as a function of spreading waveform and Section 8 as a function of special strategies. Section 9 describes a signaling technique which does not normally require any reacquisition operation in the normal sense but, as would be expected, suffers some increase in vulnerability to smart jamming. The main body of the report concludes with a summary of the study results, Section 10, and recommendations for future work, Section 11.

Appendix A describes an Autogressive Spectral Estimation Acquisition Technique (ASEAT) for acquisition of FH signals. The technique has a very rapid acquisition capability but requires that a linear feedback shift register be used for generating the FH addresses. This makes the system very vulnerable to a relatively unsophisticated jammer so that this technique is inappropriate for military spread spectrum systems, at least in its present state of development. Component codes, described in Appendix B, offer a means of introducing structure into a DS spreading signal in such a way that it can be exploited by the receiver to reduce acquisition time. Of course, this structure (reduced randomness) carries with it some potential reduction in smart jammer immunity, but these codes do represent an alternative to other structured waveform methods such as conventional short codes. Appendix C discusses the sources of timing error and their relative contributions to the total timing uncertainty during periods of link outage. Appendix D discusses optical processing techniques which have the potential for providing better MF performance than the more conventional MF approaches. These techniques warrant further study to establish their applicability to military spread spectrum systems as acquisition as well as data demodulation devices.

SECTION 2.0
MEAN SEARCH TIME

2.0 MEAN SEARCH TIME

An expression for the mean time to acquire a pseudonoise (PN) spread spectrum signal was developed in [1] using a Markov chain model. In this section a heuristic approach is used, resulting in the same expression, in order to obtain greater insight into the acquisition process and to more readily identify the underlying trade-off between the probability of acquisition detection and probability of false alarm. In addition, the formulation of the problem is generalized somewhat to emphasize the fact that the result is applicable to a larger class of search problems than acquisition of PN spread spectrum signals.

In the general context of a search through some uncertainty region containing q cells, one of which is the correct cell, define

- q = Number of cells in the uncertainty region
- P_D = Probability of detection when at the correct location
- P_{FA} = Probability of false alarm (false detection)
- C = Average number of cells searched for detection
- Q = Average number of false alarms during the search
- K = Number of time units of false alarm penalty
- $R = C + KQ$ = Average total number of time units in the search
- τ_D = Search (dwell) time at each cell
- \bar{T} = Average search time

It is assumed that there is no a priori knowledge of the location of the correct cell within the uncertainty region, and, at least initially, that there is only one searcher. The procedure is to repeatedly search through the entire uncertainty region until the correct cell is detected. On each search through the region each cell is tested only once but the order is arbitrary. In fact the order may be rearranged prior to each new search through the region.

The mean time to detect the location of the correct cell is determined as follows. The probability that the correct cell is detected on the i^{th} search through the uncertainty region is

$$P[\text{Detection on } i^{\text{th}} \text{ Search}] = P_D(1 - P_D)^{i-1}$$

which is the geometric probability law. For this probability law the mean number of trials required for detection is $1/P_D$ which implies that the correct cell is detected, on the average, on the $(1/P_D)^{\text{th}}$ search through the uncertainty region.

Therefore, on the average, there are $(1/P_D - 1)$ unsuccessful searches through the q-cell region, or

$$\left(\frac{1}{P_D} - 1\right) q \quad (2.0-1)$$

cells searched unsuccessfully prior to the final search of the region. The search will terminate on the next search through the region at the location of the correct cell. With the location uniformly distributed throughout the region the mean location is at

$$\frac{q+1}{2} \quad (2.0-2)$$

Therefore the average total number of cells searched is the sum of (2.0-1) and (2.0-2),

$$\begin{aligned} C &= \left(\frac{1}{P_D} - 1\right) q + \left(\frac{q+1}{2}\right) \\ &= \frac{(2 - P_D)q + P_D}{2 P_D} \end{aligned} \quad (2.0-3)$$

To consider the effect of false alarms on the search process, note that of the C cells searched $1/P_D$ are correct so that there is a possibility of a false alarm on $(C - 1/P_D)$ cells. The number of false alarms, n_{FA} , which occur in $n = (C - 1/P_D)$ trials follows a Binomial probability law,

$$P \left[\begin{array}{c} n_{FA} \text{ False Alarms} \\ \text{in } n \text{ Trials} \end{array} \right] = \binom{n}{n_{FA}} P_{FA}^{n_{FA}} (1 - P_{FA})^{n - n_{FA}}$$

$$n_{FA} = 0, 1, 2, \dots, n$$

The mean of the Binomial probability law is

$$\overline{n_{FA}} = n P_{FA}$$

so that the mean number of false alarms during the search is

$$\begin{aligned} Q &= \left(C - \frac{1}{P_D}\right) P_{FA} \\ &= \left[\frac{(2 - P_D)q + P_D - 2}{2 P_D} \right] P_{FA} \end{aligned} \quad (2.0-4)$$

For each false alarm a penalty of K time units is incurred so that the average total number of time units spent in the search process is

$$\begin{aligned}
 R &= C + KQ \\
 &= \frac{(2 - P_D)q + P_D + K[(2 - P_D)q + P_D - 2] P_{FA}}{2 P_D}
 \end{aligned}$$

which can be manipulated into

$$R = \frac{2 + (2 - P_D)(q - 1)(1 + K P_{FA})}{2 P_D} \quad (2.0-5)$$

The mean search time is therefore

$$\begin{aligned}
 \bar{T} &= R \tau_D \\
 &= \left[\frac{2 + (2 - P_D)(q - 1)(1 + K P_{FA})}{2 P_D} \right] \tau_D \quad (2.0-6)
 \end{aligned}$$

which is the mean acquisition time expression obtained in [1].

The importance of the heuristic derivation presented here is that the effects of missed detections and false alarms can be readily identified as individual contributions to the mean acquisition time. Consequently the trade-offs between P_D , P_{FA} and τ_D can be examined at a more fundamental level. For example (2.0-3) from (2.0-4) it is seen that the total average number of cells, C, searched is a function only of P_D whereas the average number of false alarms, Q, is a function of both P_D and P_{FA} . For P_D very small

$$C \cong \frac{q}{P_D}$$

(many searches through the uncertainty region) and

$$Q \cong \frac{q-1}{P_D} P_{FA}$$

which for $q \gg 1$ is

$$Q \cong \frac{q}{P_D} P_{FA}$$

Under these conditions Q is relatively large since there are a large number of opportunities (cells searched) for false alarms. On the other hand if P_D is

close to unity then

$$C \cong \frac{q+1}{2}$$

(acquisition on the first search through the uncertainty region) and

$$Q \cong \frac{q-1}{2} P_{FA}$$

so that the number of false alarms is relatively small since there are not many opportunities for false alarms. These dependences on P_D and P_{FA} are intuitively obvious but it is convenient to have them quantitatively expressed for system design and analysis purposes. The trade-offs between P_D , P_{FA} and τ_D will be examined in detail in the next section in the context of PN code acquisition.

The other parameter in the C , Q and \bar{T} expressions is the number of cells in the uncertainty region q . The three expressions are in fact linear functions of q , a fact which is emphasized by rewriting them as

$$C = \left(\frac{2 - P_D}{2 P_D} \right) q + \left(\frac{1}{2} \right)$$

$$Q = \left[\frac{(2 - P_D) P_{FA}}{2 P_D} \right] q + \left[\frac{(P_D - 2) P_{FA}}{2 P_D} \right]$$

$$\bar{T} = \left[\frac{(2 - P_D)(1 + K P_{FA}) \tau_D}{2 P_D} \right] q + \left[\frac{P_D \tau_D + (P_D - 2) K P_{FA} \tau_D}{2 P_D} \right]$$

Obviously C and Q and the resulting mean search time \bar{T} can be reduced by reducing q . In a PN code driven spread spectrum system with total timing uncertainty, q is the length of the PN code or some multiple of it. Reducing the length of the code to reduce acquisition time increases the vulnerability to intelligent jammers, and protection against jamming, particularly intelligent jamming, is the main objective in many spread spectrum applications. Another means of reducing the mean search time is by defining the uncertainty region such that some a priori preference is given to the location of the correct cell within the region. However, this may also increase the vulnerability to intelligent jammers. Basically protection against intelligent jamming requires uncertainty in the transmitted signal as viewed by the jammer but this same uncertainty is present in the signal as viewed by an unsynchronized friendly receiver. From the jamming point of view the uncertainty translates into protection; from the acquisition point of view it translates into long acquisition time. The obvious

conclusion is that for reduced acquisition time the emphasis must be on reducing the dwell time τ_D . The rapidly developing matched filter technologies will undoubtedly make major contributions in this area.

One other obvious means of reducing the mean search time is by employing more than one searcher. If S searchers are employed then in theory C , Q and \bar{T} are reduced by a factor of S . However, in practice this linear reduction is usually not realized. The problem is that parallel search operations are usually implemented such that the search devices are synchronously stepped through their respective portions of the uncertainty region. Consequently any time one search device suffers a false alarm all pay the false alarm penalty. As the number of parallel devices becomes large the false alarm penalty becomes a limiting factor.

2.1 Example: Direct Serial Search

Consider the single dwell time, noncoherent detector PN code acquisition model shown in Figure 2.1-1. After mixing the received signal with the local PN code reference the resulting signal is filtered, envelope detected and sampled every τ_D seconds where

$$\tau_D = \frac{1}{B_{ED}}$$

The sample value is then compared to a decision threshold. If a "hit" results the system conducts a verification test for $K\tau_D$ seconds which results in either a verified acquisition or a dismissed false alarm. When either a "no hit" decision results from the threshold decision or a false alarm is dismissed the PN code reference is stepped one chip or less and a new sample value generated τ_D seconds later. This search procedure continues until acquisition is achieved. Typically the PN code reference is stepped in half-chip increments so that q is twice the code length. When the incoming PN signal and local reference are not in alignment the input to the envelope detector is assumed to be bandlimited white Gaussian noise of power N ; when the PN signals are aligned the input is assumed to be a sinusoid of peak amplitude A_0 plus bandlimited white Gaussian noise of power N . Under these assumptions the samples are Rayleigh distributed in the noise only case

$$p_{x|n}(x) = \frac{x}{N} e^{-x^2/2N} \quad x \geq 0$$

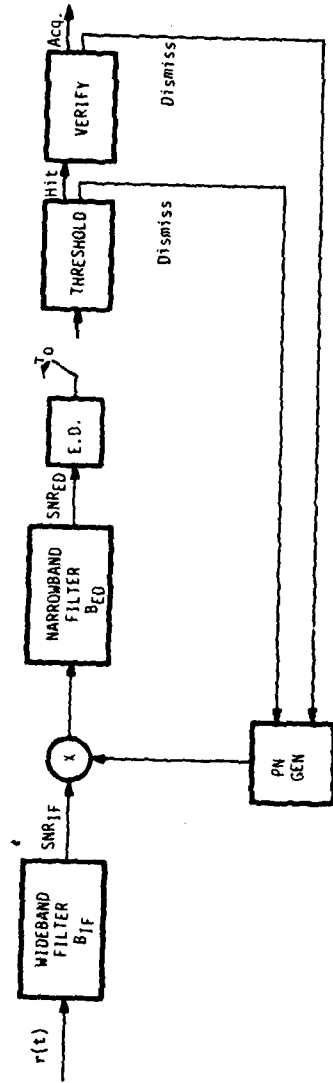


Figure 2.1-1.
Direct Serial Search for PN Code Acquisition

so that the false alarm probability is

$$P_{FA} = e^{-V_T^2/2N} \quad (2.1-1)$$

where V_T is the decision threshold. Expressing V_T in terms of P_{FA}

$$V_T = \sqrt{-2N \ln P_{FA}} \quad (2.1-2)$$

For the signal plus noise case the samples are Ricean distributed but this distribution is difficult to work with analytically so that the approximation [2]

$$P_{x|s+n}(x) \cong \sqrt{\frac{x}{2\pi A_0 N}} e^{-(x-A_0)^2/2N} dx, \quad x \geq 0$$

will be used, with the result that

$$P_D \cong \int_{V_T}^{\infty} \sqrt{\frac{x}{2\pi A_0 N}} e^{-(x-A_0)^2/2N} dx \quad (2.1-3)$$

This approximation to P_D is quite good whenever the predetection SNR is somewhat greater than unity. In the following analyses less accurate approximations will be required at some points to obtain results which are simple enough to be useful in system design. The accuracy of these results will be tested by considering the results obtained from the approximation in (2.1-3) as "exact" results, with a change of variable (2.1-3) becomes

$$P_D = \frac{1}{\sqrt{\pi}} \int_{\frac{V_T}{\sqrt{2N}} - \frac{A_0}{\sqrt{2N}}}^{\infty} \left(\frac{u}{A_0/\sqrt{2N}} + 1 \right)^{\frac{1}{2}} e^{-u^2} du$$

but from (2.1-2)

$$\frac{V_T}{\sqrt{2N}} = \sqrt{-\ln P_{FA}} \quad (2.1-4)$$

and $A_0/\sqrt{2N}$ is the SNR at the input to the envelope detector in the signal plus noise case,

$$\text{SNR}_{ED} = \frac{A_0}{\sqrt{2N}} \quad (2.1-5)$$

so that

$$P_D = \frac{1}{\sqrt{\pi}} \int_{\sqrt{-\ln P_{FA}} - \sqrt{\text{SNR}_{ED}}}^{\infty} \left(\frac{u}{\sqrt{\text{SNR}_{ED}}} + 1 \right)^{\frac{1}{2}} e^{-u^2} du \quad (2.1-6)$$

This expression provides the trade-off between P_D and P_{FA} needed to examine C, Q, and \bar{T} , with SNR_{ED} as an additional system parameter. The predetection SNR is in fact a function of τ_D since

$$\begin{aligned} \text{SNR}_{ED} &= \left(\frac{B_{IF}}{B_{ED}} \right) \text{SNR}_{IF} \\ &= (B_{IF} \tau_D) \text{SNR}_{IF} \end{aligned}$$

With the notation

$$\alpha \triangleq B_{IF} \text{SNR}_{IF}$$

which has units (sec^{-1}), then

$$\text{SNR}_{ED} = \alpha \tau_D \quad (2.1-7)$$

Values for a typical PN spread spectrum system may be

$$\begin{aligned} \text{SNR}_{IF} &= -20 \text{ dB} \\ B_{IF} &= 10 \text{ MHz} \end{aligned}$$

so that a typical value of α is

$$\alpha = 10^5 \text{ sec}^{-1}$$

Using (2.1-7) the mean acquisition time normalized by α to a unitless quantity, can be expressed in terms of the predetection SNR as

$$\alpha \bar{T} = \frac{2 + (2 - P_D)(q - 1)(1 + K P_{FA})}{2 P_D} \bullet \text{SNR}_{ED} \quad (2.1-8)$$

This normalized mean acquisition time is plotted in Figure 2.1-2 as a function of SNR_{ED} for several values of P_{FA} and with

$$q = 1000$$

$$K = 5$$

It is seen that at lower values of SNR_{ED} acquisition time can be reduced by allowing a higher P_{FA} whereas at higher values of SNR_{ED} acquisition time is somewhat insensitive to P_{FA} . In all cases an optimum value of SNR_{ED} exists (with a corresponding optimum value of τ_D), with performance more sensitive to SNR_{ED} at lower values of P_{FA} . Figure 2.1-3 provides for a more detailed examination of the effects of dwell time on the acquisition process. In the lower range of τ_D a small increase in τ_D produces a large decrease in the average number of cells searched, C , due to the corresponding increase in P_D . The average number of false alarms, Q , also decreases simply because there are less opportunities to make a false alarm. With both C and Q decreasing, the average acquisition time decreases rapidly even though the dwell time is increasing. For values of τ_D in the vicinity of 55 the rate at which C and Q are decreasing with increasing τ_D is reduced (implying that P_D is approaching unity) so that \bar{T} flattens out. As τ_D increases beyond this region C and Q remain essentially constant (slowly approaching their minimum values corresponding to $P_D=1$) so that \bar{T} increases linearly with τ_D .

These results indicate an optimum value of SNR_{ED} , with a corresponding optimum value of τ_D , and with \bar{T} exhibiting a relatively sharp null about the optimum value for large SNR_{ED} s. Expressions for these optimum values can be obtained by defining

$$x \triangleq \sqrt{SNR_{ED}} \quad (2.1-9)$$

so that

$$\tau_D = \frac{1}{\alpha} x^2 \quad (2.1-10)$$

and finding the value of x which minimizes

$$\bar{T} = \frac{2 + (2 - P_D)(q - 1)(1 + K P_{FA})}{2 P_D} \frac{x^2}{\alpha} \quad (2.1-11)$$

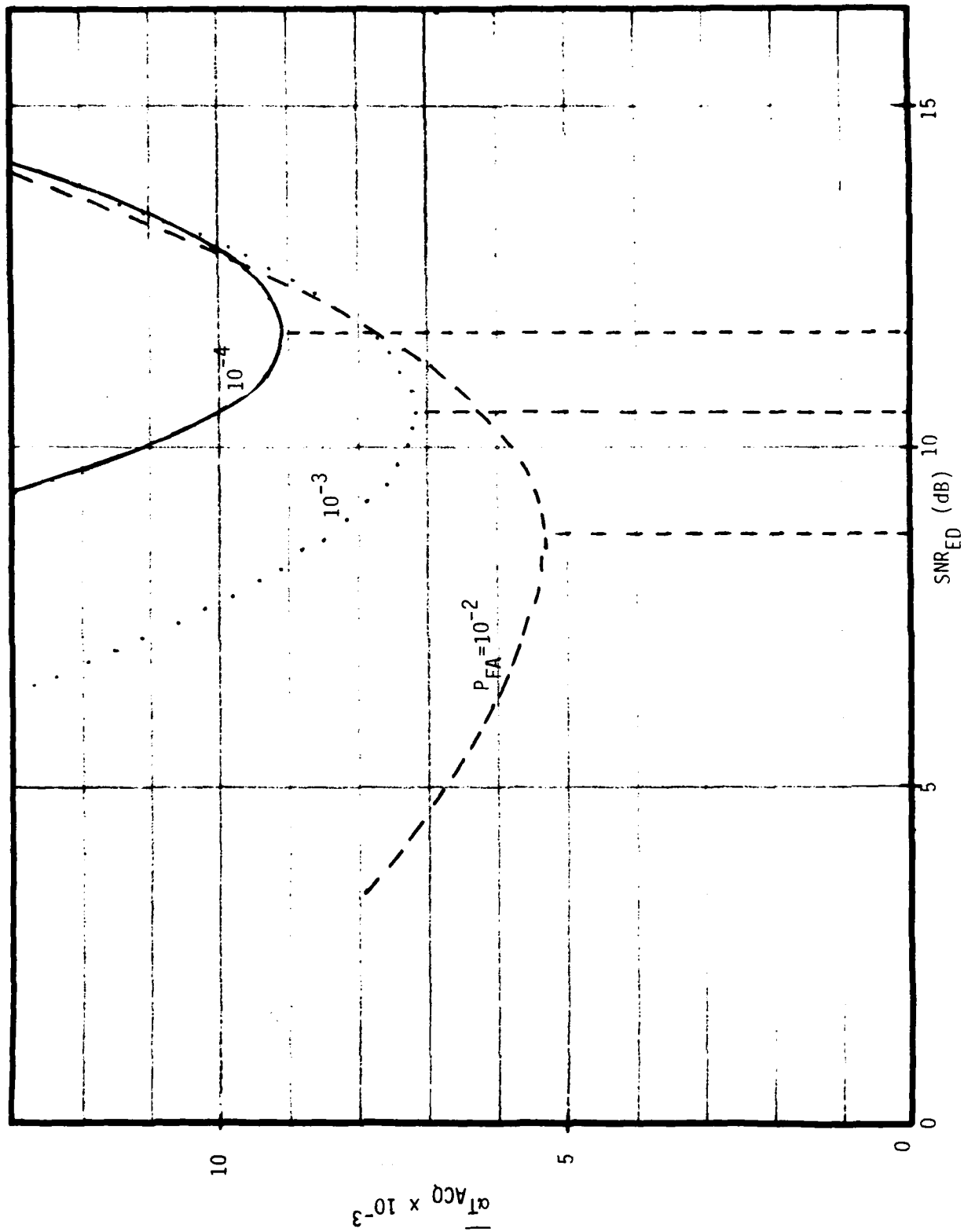


Figure 2.1-2.

Acquisition Performance

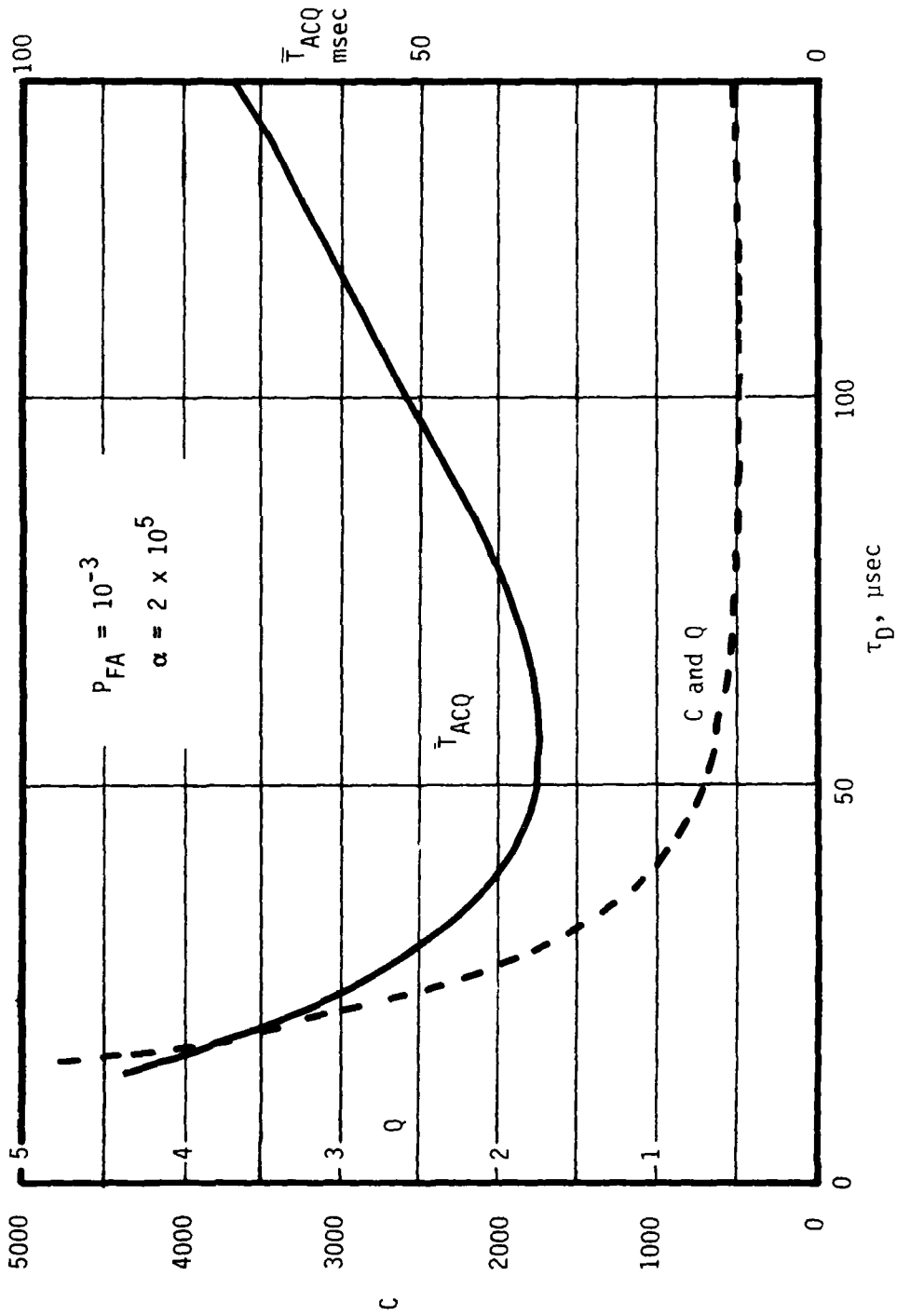


Figure 2.1-3. Average Number of Cells Searched, False Alarms and Acquisition Time Versus Dwell Time

keeping in mind that P_D is a function of x . Differentiating \bar{T} with respect to x , setting equal to zero and defining

$$\beta \triangleq (q - 1)(1 + K P_{FA}) \quad (2.1-12)$$

yields

$$\left[x \frac{d P_D}{dx} - 2 P_D + \frac{\beta}{\beta+1} P_D^2 \right]_{x = x_{opt}} = 0 \quad (2.1-13)$$

The approximation for P_D used earlier is

$$P_D \cong \int_{V_T}^{\infty} \sqrt{\frac{u}{2\pi A_0 N}} e^{-(u-A_0)^2/2N} du \quad (2.1-14)$$

A less accurate approximation which will yield simpler results is the Gaussian approximation to (2.1-14) [2]

$$P_D \cong \int_{V_T}^{\infty} \frac{1}{\sqrt{2\pi N}} e^{-(u-A_0)^2/2N} du \quad (2.1-15)$$

which can be further approximated by [3]

$$P_D \cong \frac{1}{\sqrt{2\pi}} \frac{\sqrt{N}}{V_T - A_0} e^{-(V_T - A_0)^2/2N} \quad (2.1-16)$$

In terms of the optimization parameter x this becomes

$$P_D \cong \frac{1}{2\sqrt{\pi}} \frac{1}{\sqrt{-\ln P_{FA}} - x} e^{-\left(\sqrt{-\ln P_{FA}} - x\right)^2} \quad (2.1-17)$$

Using (2.1-17) in (2.1-13) and defining

$$Y \triangleq \sqrt{-\ln P_{FA}} - x_{opt} \quad (2.1-18)$$

yields

$$4Y^3 - 4Y^2 + 2Y + \frac{\beta}{(\beta+1)\sqrt{\pi}} e^{-Y^2} = -2\sqrt{-\ln P_{FA}} \quad (2.1-19)$$

For specific values of P_{FA} and

$$\beta \triangleq (q - 1)(1 + K P_{FA})$$

numerical techniques can be employed to solve (2.1-19) for γ and that

$$\text{SNR}_{\text{ED opt}} = \left(\sqrt{-\ln P_{\text{FA}}} - \gamma \right)^2 \quad (2.1-20)$$

and

$$\tau_{\text{D opt}} = \frac{\text{SNR}_{\text{ED opt}}}{\alpha} \quad (2.1-21)$$

The optimum SNR_{ED} as determined from (2.1-19) (labeled "approximation") is compared in Figure 2.1-4 with the optimum value as determined by iterative evaluations of (2.1-8) using the more exact approximation for P_{D} given in (2.1-6) (labeled "actual"). It is seen that the "approximation" somewhat over estimates the "actual" value at the higher values of P_{FA} . But as noted earlier the minimum is quite broad for the higher values of P_{FA} so that the "approximate" optimum SNR_{ED} should provide a sufficiently accurate estimate for system design.

The foregoing considered the minimization of mean acquisition time by selection of the predetection SNR or, correspondingly, dwell time. The system designer may also have the option of selecting the P_{FA} so as to minimize \bar{T} . This requires the minimization of \bar{T} with respect to SNR_{ED} and P_{FA} . With

$$Z \triangleq \sqrt{-\ln P_{\text{FA}}} \quad (2.1-22)$$

and, as before,

$$X \triangleq \sqrt{\text{SNR}_{\text{ED}}}$$

differentiating \bar{T} with respect to X and setting equal to zero, and with respect to Z and setting equal to zero yields

$$\left[X \frac{\partial P_{\text{D}}}{\partial X} - 2 P_{\text{D}} + \frac{\beta}{\beta+1} P_{\text{D}}^2 \right] \Bigg|_{\substack{X = X_{\text{opt}} \\ Z = Z_{\text{opt}}}} = 0 \quad (2.1-23)$$

and

$$\left\{ -q \frac{\partial P_{\text{D}}}{\partial Z} + (q-1)K \left[P_{\text{D}} \frac{\partial P_{\text{FA}}}{\partial Z} - P_{\text{FA}} \frac{\partial P_{\text{D}}}{\partial Z} \right] + (q-1)K P_{\text{D}}^2 \frac{\partial P_{\text{FA}}}{\partial Z} \right\} \Bigg|_{\substack{X = X_{\text{opt}} \\ Z = Z_{\text{opt}}}} = 0 \quad (2.1-24)$$

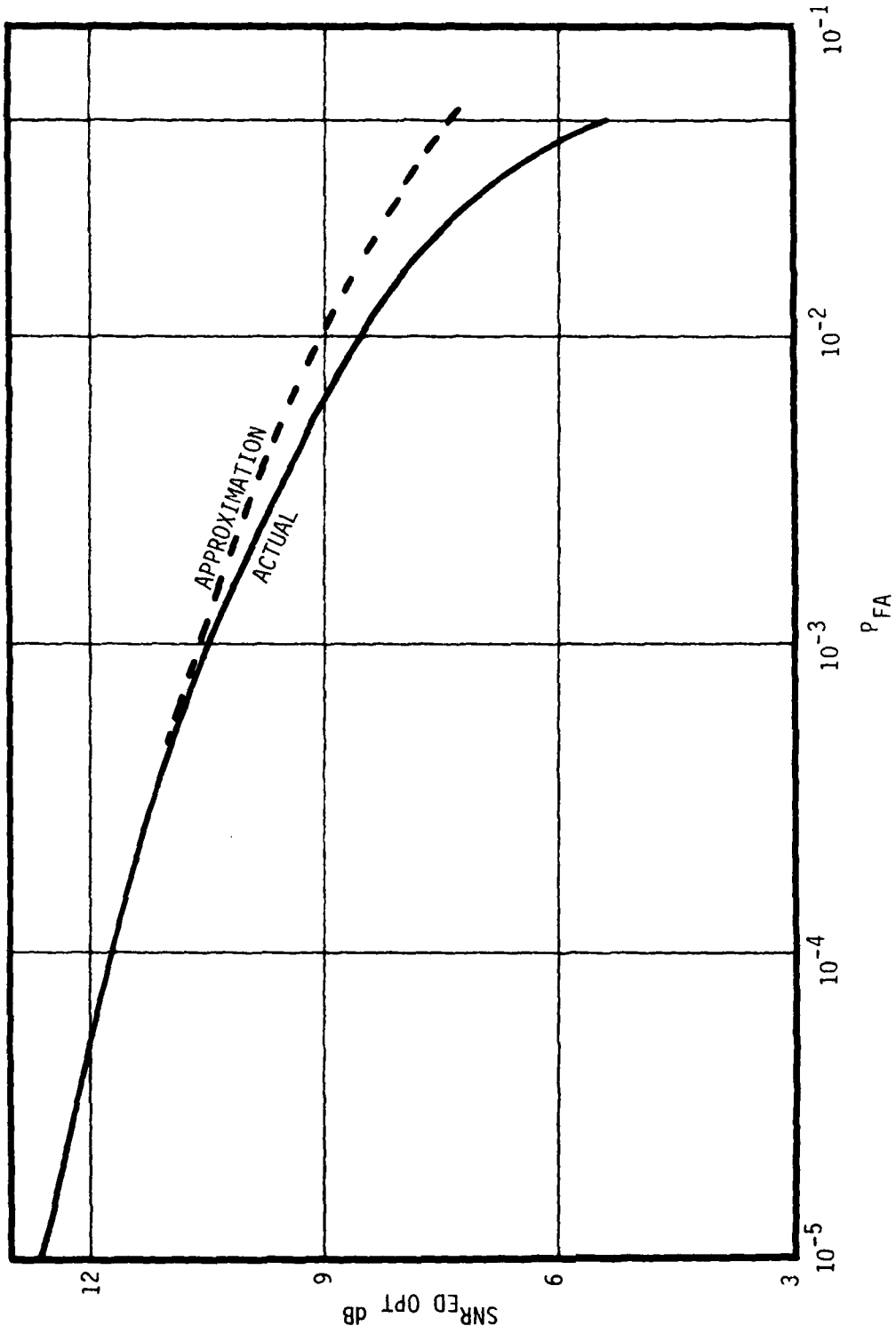


Figure 2.1-4. Comparison of "Approximation" and "Actual" Optimum SNR_{ED}

where

$$\frac{\partial P_D}{\partial X} = \frac{1}{2\sqrt{\pi}} \left[\frac{1}{Z-X} - 2 \right] e^{-(X-Z)^2} \quad (2.1-25a)$$

$$\frac{\partial P_{FA}}{\partial X} = 0 \quad (2.1-25b)$$

$$\frac{\partial P_D}{\partial Z} = \frac{1}{2\sqrt{\pi}} \left[\frac{-1}{Z-X} - 2 \right] e^{-(X-Z)^2} \quad (2.1-25c)$$

$$\frac{\partial P_{FA}}{\partial Z} = -2Z e^{-Z^2} \quad (2.1-25d)$$

and β is now

$$\beta = (q - 1)(1 + K e^{-Z^2}) \quad (2.1-26)$$

The resulting pair of equations which must be solved simultaneously to obtain X_{opt} and Z_{opt} is

$$4(Z-X)^3 - 4(Z-X)^2 + 2(Z-X) + \frac{\beta}{(\beta+1)\sqrt{\pi}} e^{-(Z-X)^2} + 2Z = 0 \quad (2.1-27a)$$

and

$$q \left(\frac{1}{Z-X} + 2 \right) e^{+Z^2} + (q - 1)K \left[\frac{2X + 1}{Z-X} \right] + \frac{(q - 1)K}{2\sqrt{\pi}} \left[\frac{-2Z}{(Z-X)^2} \right] e^{-(Z-X)^2} = 0 \quad (2.1-27b)$$

Once X_{opt} and Z_{opt} have been found

$$SNR_{ED opt} = X_{opt}^2 \quad (2.1-28)$$

$$\tau_D opt = \frac{SNR_{ED opt}}{\alpha} \quad (2.1-29)$$

and

$$P_{FA opt} = e^{-Z_{opt}^2} \quad (2.1-30)$$

This procedure does not seem to be sufficiently simple to be useful as a design tool. In addition, it is noted from the previous examples (Figures 2.1-2 and 2.1-3) that the optimum value of P_{FA} is greater than 0.1 (for a false alarm penalty of $K=5$) which is probably unacceptable from other system considerations.

REFERENCES

1. Holmes, J. K. and C. C. Chen, "Acquisition Time Performance of PN Spread-Spectrum Systems," IEEE Trans. on Comm., Vol COM-25, No. 8, Aug. 1977, pp 778-784.
2. Carlson, A. B., Communication Systems, 2nd Ed., McGraw-Hill, 1975, p 393.
3. Wozencraft, J. M. and J. M. Jacobs, Principles of Communication Engineering, Wiley, 1965, p 83.

SECTION 3.0
SERIAL SEARCH TECHNIQUES

3.0 SERIAL SEARCH TECHNIQUES

One technique used to obtain coarse code synchronization is the serial search, fixed dwell time acquisition system. This model assumes there are q cells to be searched, where q is related to the code length. If the code search is done in $\frac{1}{2}$ chip steps, which is normally the case, then q will equal twice the code length. It is assumed that the correct code phase is equally likely to be found at any given position. If the threshold is exceeded at any location, a verify mode is entered where the dwell time is increased to gain confidence that the correct code phase has been located. For each threshold crossing there is the probability that the true code phase has not been found which is given by the probability of false alarm (PFA). This increases the average acquisition time and is modeled as a constant times the fixed dwell time ($K_T D$). If it is determined that the correct code phase has been found then the tracking process can begin.

One method of characterizing the "goodness" of an acquisition technique is the time it takes to search the time uncertainty and locate the true code phase. This is complicated by the fact that this time is a random variable and the statistics required to fully characterize it are very difficult to generate. A partial characterization, however, can be had, by determining the mean time to acquire and variance associated with this time.

3.1 Single Integration

Figure 3.1-1 is a block diagram of the single integration model being considered. The input PN signal plus noise is multiplied by the receiver's best guess as to what the transmitter's PN code phase actually is. The resultant output signal is then bandpass filtered (BPF) and applied to a square law device. The bandwidth of the BPF will be determined by whether or not it has to pass data during the acquisition process. Also a different filter may be switched in once acquisition has taken place. The squared signal is then integrated for a period of time determined by the probability of detection requirement, PFA and the IF signal to noise ratio. This value is then compared to a threshold to determine if possibly the correct code phase has been found. If the threshold is exceeded, the integration process is continued for a time determined by just how much confidence is needed to initiate the tracking process. If the threshold is not exceeded, then a signal is sent to the PN

generator to cause it to change its phase by some amount, typically $\frac{1}{2}$ chip. The process is repeated until the correct code phase is found.

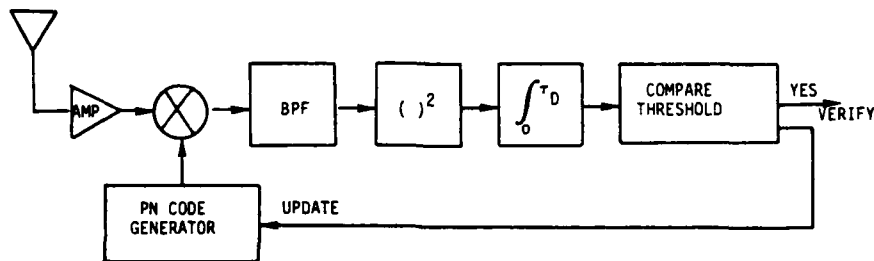


Figure 3.1-1.
Noncoherent Fixed Dwell Time Acquisition Model

The mean acquisition time and variance for this system is given by the equations: ^[1]

$$T = \frac{(2-P_D)(1+KP_{FA})}{2P_D} (q\tau_D) \quad (3.1-1)$$

$$\sigma^2 = \tau_D^2 (1+KP_{FA})^2 q^2 \left(\frac{1}{12} - \frac{1}{P_D} + \frac{1}{P_D^2} \right) \quad (3.1-2)$$

These equations assume

- No doppler
- Correlation error fixed at $\frac{1}{2}$ the update size (P_D is time invariant)

P_D = probability of a detection

P_{FA} = probability of a false alarm

K = penalty paid for false alarm

q = number of cells to search (q will equal twice the code length for one-half chip updates)

τ_D = dwell time

If doppler is present the following equations can be used.

$$T \approx \frac{(2 - P_D) (1 + KP_{FA}) (N\tau_D)}{2P_D \left| \frac{\Delta T_C}{T_C} + \tau_D \Delta fc + K\tau_D \Delta fc P_{FA} \right|} \quad (3.1-3)$$

$$\sigma^2 \approx \frac{(1 + KP_{FA})^2 N^2 \left(\frac{1}{12} - \frac{1}{P_D} + \frac{1}{P_D^2} \right) \tau_D^2}{\left(\frac{\Delta T_C}{T_C} + \tau_D \Delta fc + K\tau_D \Delta fc P_{FA} \right)^2} \quad (3.1-4)$$

N = number of chips to be searched

$\frac{\Delta T_C}{T_C}$ = step size of search in fractions of a chip (typically $\frac{1}{2}$)

Δfc = code doppler in chips

$\Delta fc \tau_D$ = PN code phase timing shift due to code doppler during dwell time

$\Delta fc K \tau_D$ = code phase shift during hit verification

P_{FA} = probability of a false alarm

P_D = probability of a detection

Note: The algebraic sign of the code doppler must be assigned so that when the search is speeded up by the code doppler, Δfc , is positive and vice versa.

For a fixed dwell perfect integrator system, the probability of detection and false alarm are given by:^[2]

$$P_D = \operatorname{erfc} \left[\frac{B - \operatorname{SNR} \sqrt{B_{if} \tau_D}}{\sqrt{2 \operatorname{SNR} + 1}} \right] \quad (3.1-5)$$

$$B = \operatorname{erfc}^{-1} (P_{FA})$$

where

$$\operatorname{erfc}(x) = \int_x^{\infty} \frac{1}{\sqrt{2}} \exp(-y^2/2) dy \quad (3.1-6)$$

SNR = pre-detection signal-to-noise ratio

B_{if} = pre-detection bandwidth

The SNR can be computed from the equation:

$$\operatorname{SNR} = 10 \log \frac{C}{N_0} + 10 \log \left[\frac{1}{B_{if} T_s} \right] - 10 \log R_s \quad (3.1-7)$$

C/N_0 = carrier-to-noise ratio

T_s = $1/R_s$ symbol time

R_s = coded symbol rate

The following is an example of the single integration calculations. The data used in this calculation will also be used in future calculations for different acquisition architectures so that a relative comparison can be made between their performances. The parameters were chosen arbitrarily.

Assume: $B_{if} = 200 \text{ KHz}$
 $\text{SNR} = -9.5 \text{ dB}$
 $P_D = .26$
 $P_{FA} = .0015$

Code = 2047 chips
 Search in $\frac{1}{2}$ chip steps
 Assume no doppler
 $K = 5$

From the relation $\beta = \text{erfc}^{-1}(P_{FA})$

$$\text{erfc}(x) = \frac{1}{\sqrt{2\pi}} \int_x^{\infty} \exp\left(-\frac{y^2}{2}\right) dy$$

$$\beta = 2.96$$

Now using the equation

$$P_D = \text{erfc} \left[\frac{\beta - \text{SNR} \sqrt{B_{if} \tau_D}}{\sqrt{1 + 2\text{SNR}}} \right]$$

For $P_D = .26$ the argument of the erfc equals .65.

$$\therefore .65 = \left[\frac{2.96 - .112 \sqrt{200 \times 10^3} \tau_D}{\sqrt{1 + 2(.112)}} \right]$$

Solving for $\tau_D = 2 \text{ ms}$

$$\text{Acquisition time } T = \frac{(2 - P_D)(1 + KP_{FA})}{2P_D} q \tau_D$$

$$T = \frac{(2 - .26)(1 + 5(.0015))}{2(.26)} (4094) (2 \times 10^{-3})$$

$$T = 27.6 \text{ s mean acquisition time for SNR} = -9.5 \text{ dB}$$

Figures 3.1-2, 3.1-3 and 3.1-4 were plotted assuming Gaussian statistics. The probability density at the output of a square law detector is "XI SQUARED." If the detector is followed by a filter whose bandwidth is much smaller than the predetection bandwidth then the output is usually assumed to be Gaussian.

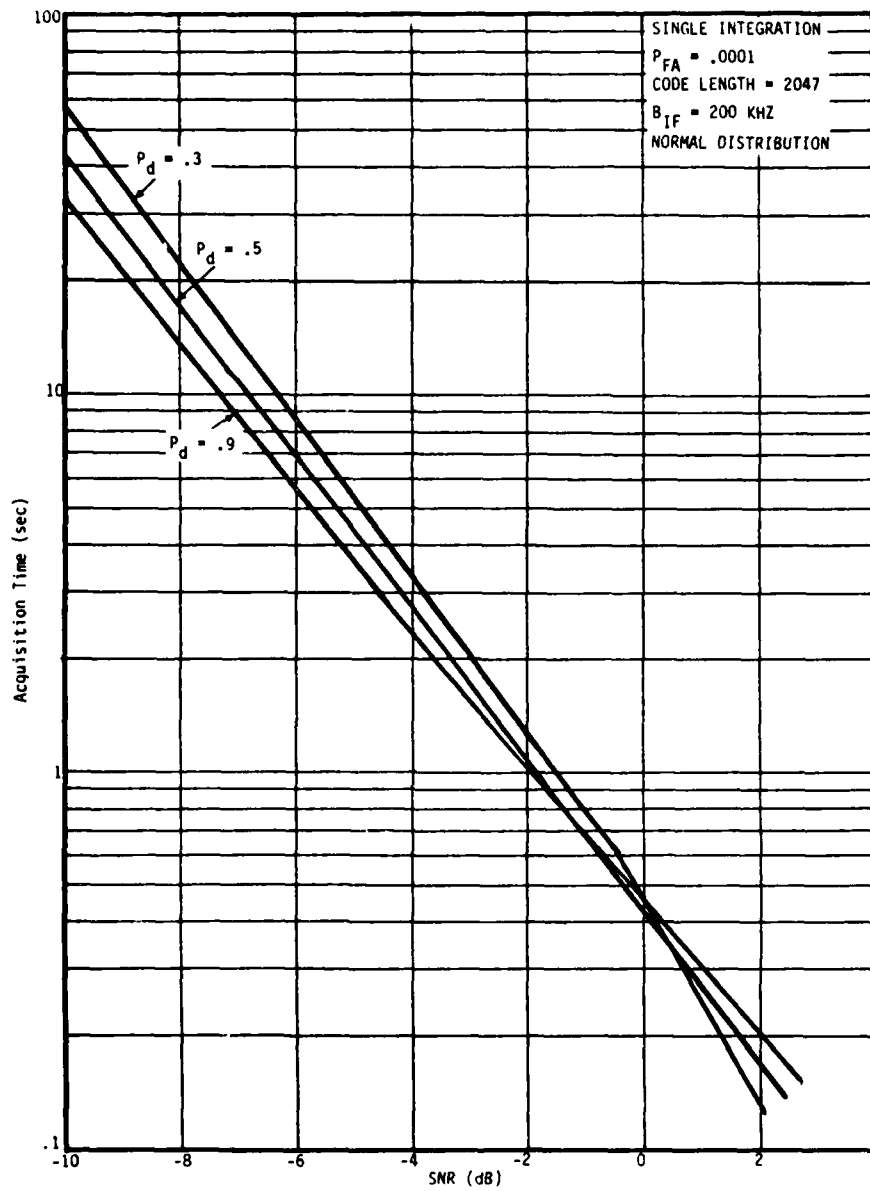


Figure 3.1-2.
Acquisition Performance

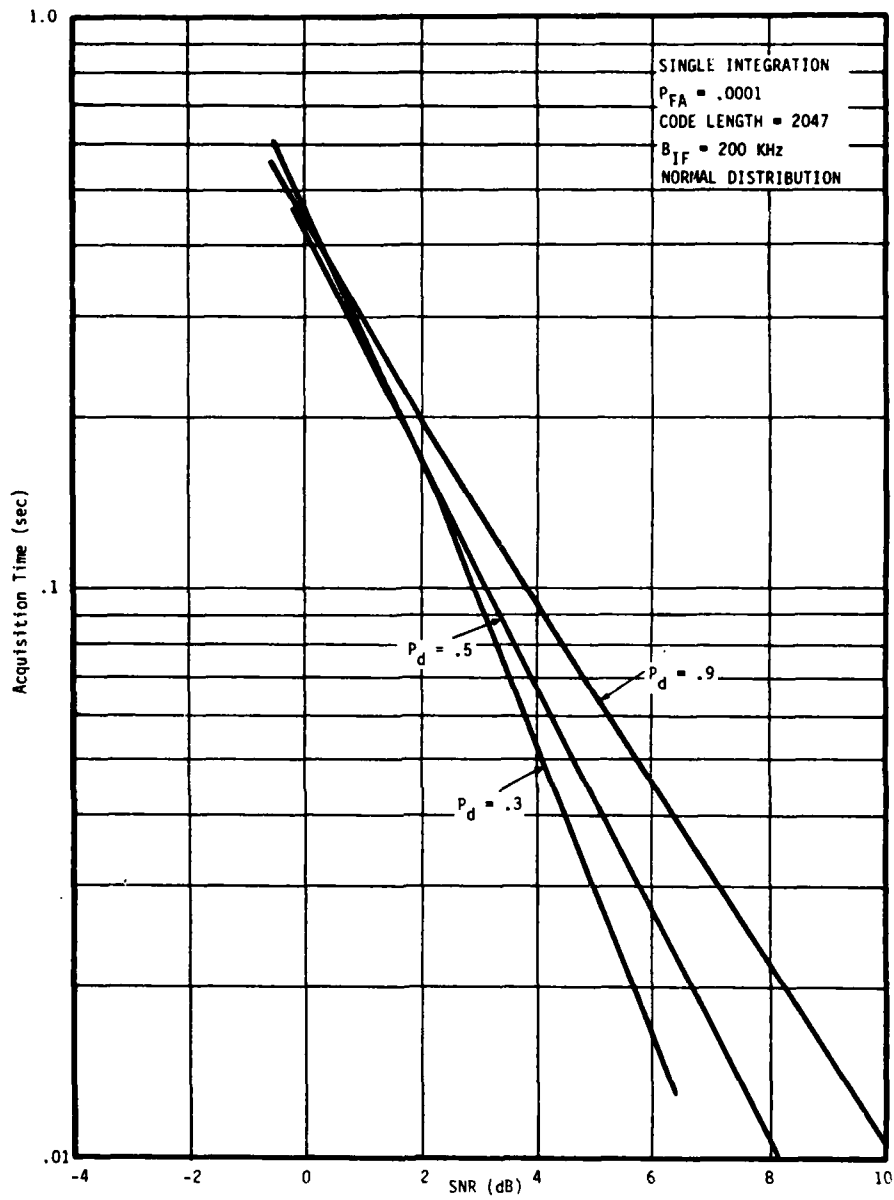


Figure 3.1-3.
Acquisition Performance

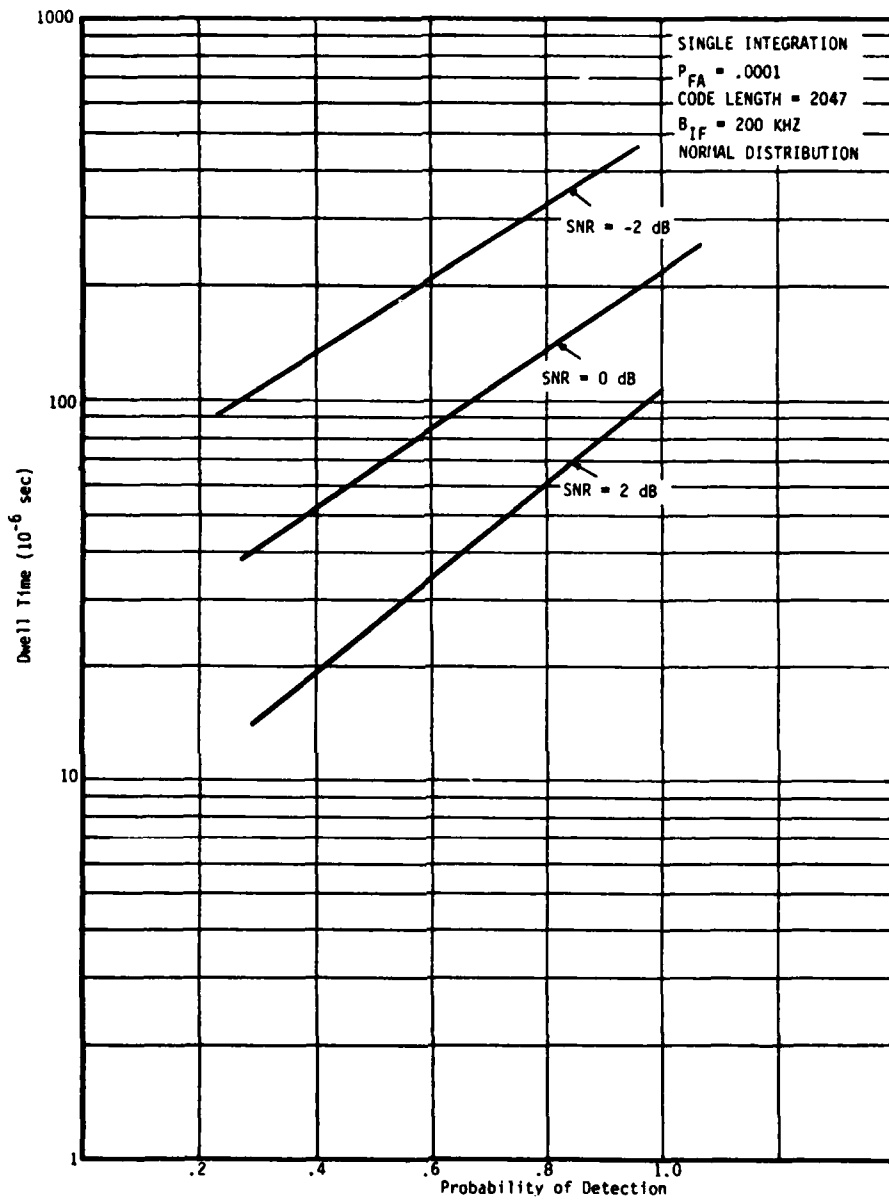


Figure 3.1-4.
Acquisition Performance

Figures 3.1-2 and 3.1-3 show how acquisition time varies with signal to noise ratio. These curves were plotted keeping probability of detection and probability of false alarm constant. A new dwell time was calculated each time the SNR was changed. Notice that the curves cross over around a SNR of 0 dB. This shows that at high SNR the acquisition time actually decreases with increasing probability of detection and is due to the fact that the probability of detection on the first pass increases significantly. For low SNR values the probability of detection on the first pass is quite low and to achieve a high probability of detection requires several pulses to be added together to increase the SNR to a value where detection can occur.

Figure 3.1-4 shows how the dwell time increases for increasing probability of detection and decreasing SNR.

In the derivation of the equation for acquisition time, the total time was shown to consist of two components; one due to the time required to search the time uncertainty to build up the SNR to a value where detection can be declared and one due to false alarms. Figure 3.1-5 is a plot of the false alarm contribution to the acquisition time. For the probabilities of false alarm assumed, the contribution is very small.

REFERENCES

1. J. K. Holmes, C. C. Chen, "Acquisition Time Performance of PN Spread-Spectrum Systems," IEEE Transactions on Communication Technology, Vol. COM-25, pp 778-783, August 1977.
2. Waddah K. Alem, Gaylord K. Huth, Jack K. Holmes, Sergei Udalov, "Spread Spectrum Acquisition and Tracking Performance for Shuttle Communications Links," IEEE Transactions on Communications Technology, Vol. COM-26, pp 1689-1703, November 1978.

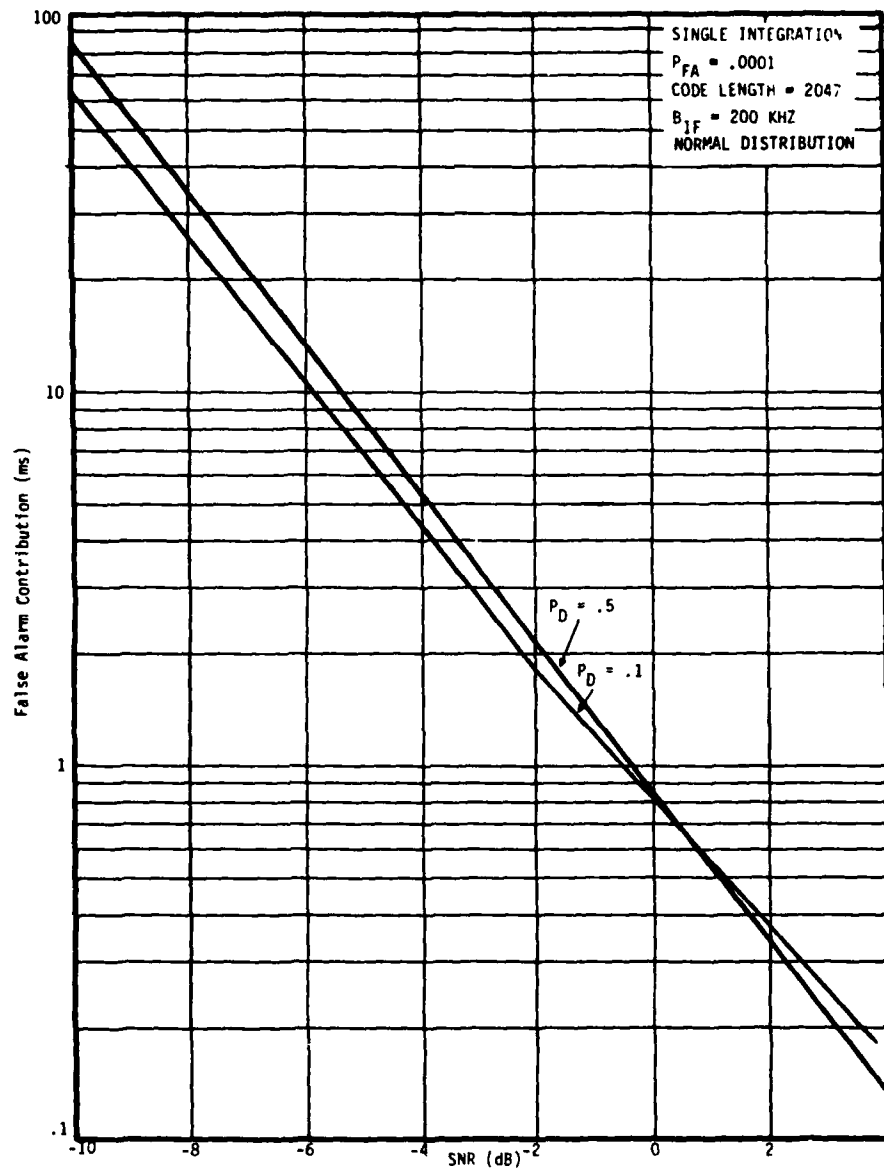


Figure 3.1-5.
Acquisition Performance

3.2 Double Integration

One disadvantage of the single integration method is that the dwell time is fixed so that just as much time is spent evaluating a noise only position as is spent for a potential alignment position. The double integration method, which will be considered next, cuts down on the time spent evaluating a noise only position. This is achieved by setting the threshold and integration time such that each phase is looked at for a smaller period of time and the number of false alarms increases. The noise only positions are then dismissed quicker. When a "hit" is detected, a second, longer, integration is started to determine if the code phase has been found or is it just a false alarm. If the second threshold is exceeded, then tracking may be initiated or a third integration may be attempted to verify further that the true code phase has been found. The basic idea in the above strategy is to apportion some of the false alarm protection in the first integration and place the remaining (usually greater) protection in the second integration. It will be seen that this double integration method reduces acquisition time over the single integration technique.

The noncoherent double dwell time block diagram is shown in Figure 3.2-1. The following are the equations and definitions for this configuration. [1]

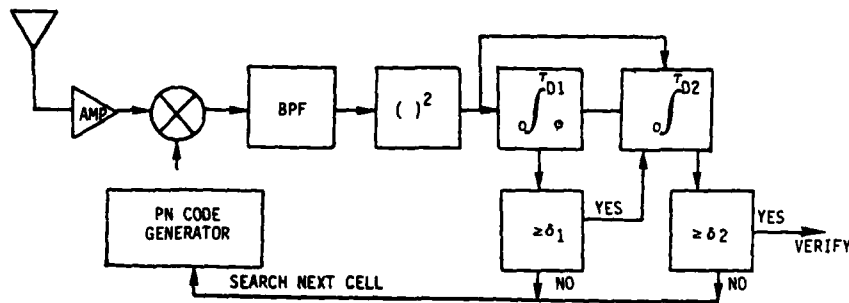


Figure 3.2-1.
Noncoherent Double Dwell Time Acquisition Model

$$T = \frac{2-P_D}{2P_D} [\tau_{D1} + \tau_{D2} P_{FA1}(1+KP_{FA2})]q \quad (3.2-1)$$

$$\sigma^2 = \tau_{D1}^2 + \tau_{D2}^2 P_{FA1}^2 (1+KP_{FA2})^2 q^2 \left(\frac{1}{12} - \frac{1}{P_D} + \frac{1}{P_D^2} \right) \quad (3.2-2)$$

$$q \gg P_{FA2}^{K(K+1)}$$

τ_{D1} = first dwell time

τ_{D2} = second dwell time

P_D = $P_{D1}P_{D2}$ product of detection probabilities at dwell one and two

P_{FA1} = false alarm probability of the first dwell

P_{FA2} = false alarm probability of the second dwell

q = number of cells to search

K = penalty of a false alarm at the second detector (number of τ_{D2} units of time)

If doppler is present the following equations can be used:

$$T \approx \frac{2-P_D}{2P_D} \left[\frac{N(\tau_{D1} + \tau_{D2} P_{FA1}(1+KP_{FA2}))}{\frac{\Delta T_c}{T_c} + \tau_{D1} \Delta f_c + P_{FA1} \tau_{D2} \Delta f_c + K \tau_{D2} \Delta f_c P_{FA1} P_{FA2}} \right] \quad (3.2-3)$$

$$\sigma^2 \approx \frac{N^2 [\tau_{D1} + \tau_{D2} P_{FA1}(1+KP_{FA2})]^2 \left(\frac{1}{12} - \frac{1}{P_D} + \frac{1}{P_D^2} \right)}{\left(\frac{\Delta T_c}{T_c} + \tau_{D1} \Delta f_c + \tau_{D2} \Delta f_c P_{FA1} + K \tau_{D2} \Delta f_c P_{FA1} P_{FA2} \right)^2} \quad (3.2-4)$$

For fixed dwell perfect integrator system, the probability of detection and false alarm are given by: [2]

$$P_D = \operatorname{erfc} \left[\frac{B - \operatorname{SNR} \sqrt{B_{if} \tau_{D1}}}{\sqrt{2\operatorname{SNR} + 1}} \right] \quad (3.2-5)$$

$$B = \operatorname{erfc}^{-1}(P_{FA})$$

Where

$$\operatorname{erfc}(x) = \int_x^{\infty} \frac{1}{\sqrt{2\pi}} \exp(-y^2/2) dy \quad (3.2-6)$$

SNR = pre-detection signal-to-noise ratio

B_{if} = pre-detection bandwidth

The SNR can be computed from the equation:

$$\operatorname{SNR} = 10 \log \frac{C}{N_0} + 10 \log \left(\frac{1}{B_{if} T_s} \right) - 10 \log R_s \quad (3.2-7)$$

The following is an example of the double integration calculations.

Assume:	$B_{if} = 200 \text{ KHz}$	Code = 2047 chips
	SNR = -9.5 dB	Search in $\frac{1}{2}$ chip steps
	$PD_1 = .28$	Assume no doppler
	$PD_2 = .9$	K = 5
	$P_{FA1} = .03$	
	$P_{FA2} = .05$	

From the relation $\beta_1 = \operatorname{erfc}^{-1}(P_{FA1})$

$$\beta_1 = 1.88$$

Solve for τ_{D1} from $P_{D1} = \text{erfc} \left[\frac{\beta - \text{SNR} \sqrt{B_{if}} \tau_{D1}}{\sqrt{1+2 \text{SNR}}} \right]$

For $P_{D1} = .28$ the argument of the erfc = .58

$$.58 = \left[\frac{1.88 - .112 \sqrt{200 \times 10^3} \tau_{D1}}{\sqrt{1+2(.112)}} \right]$$

Solving for $\tau_{D1} = 615 \mu\text{s}$

Solving for β_2 from $\beta_2 = \text{erfc}^{-1}(P_{FA2})$

$$\beta_2 = 1.65$$

Solve for τ_{D2} as above

For $P_{D2} = .9$ the argument of the erfc = -1.29

$$-1.29 = \left[\frac{1.65 - .112 \sqrt{200 \times 10^3} \tau_{D2}}{\sqrt{1+2(.112)}} \right]$$

$$\tau_{D2} = 3.75 \text{ ms}$$

$$T = \frac{2-P_D}{2P_D} \left[\tau_{D1} + \tau_{D2} P_{FA1} (1 + K P_{FA2}) \right] q = \frac{2-.26}{.52} \left[.615 \times 10^{-3} + 3.75 \times 10^{-3} (.03)(1+5(.05)) \right] 4094$$

$T = 10.4\text{s}$ mean acquisition time SNR = -9.5

The same basic data that was used to evaluate single integration was used to determine the performance of the double integration system. Figures 3.2-2 and 3.2-3 are plots of acquisition time versus SNR for various probabilities of detection. They show that acquisition time is not very sensitive to overall

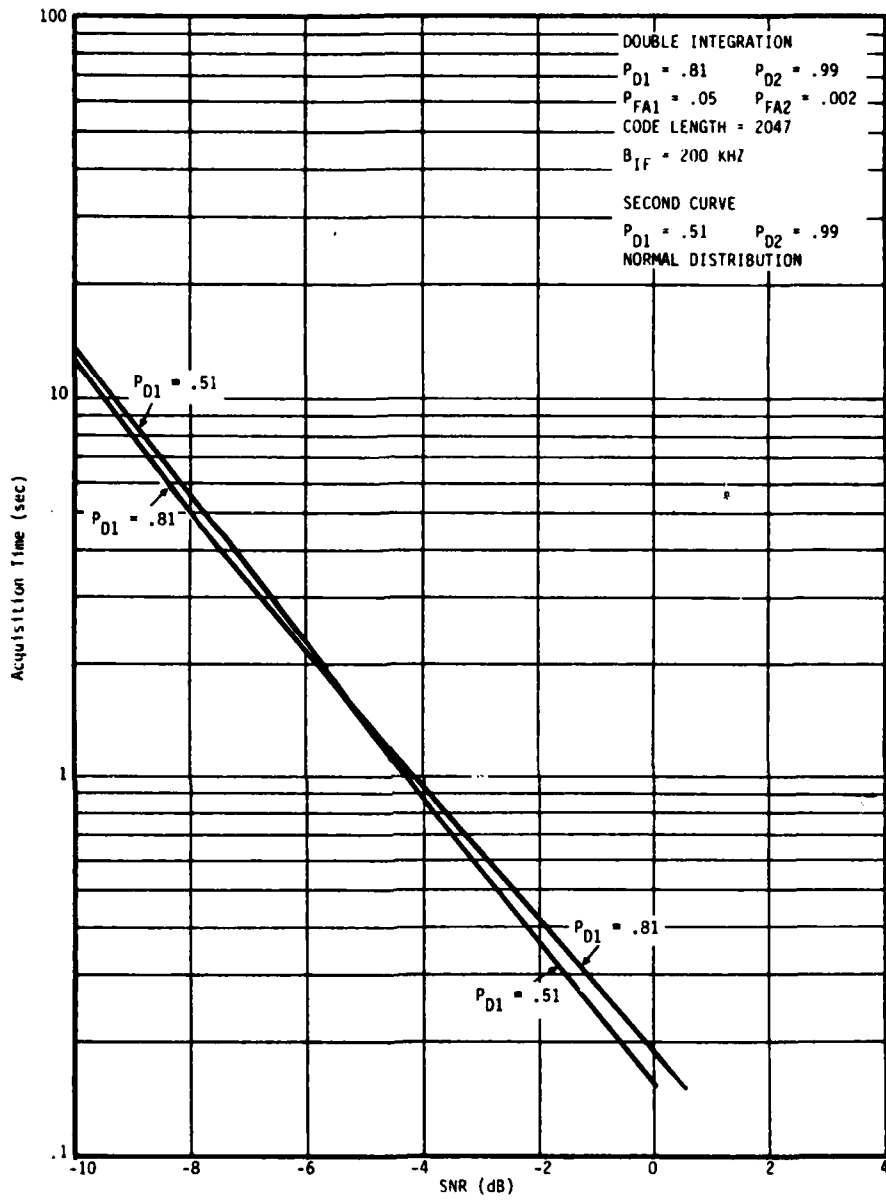


Figure 3.2-2.
 Acquisition Performance

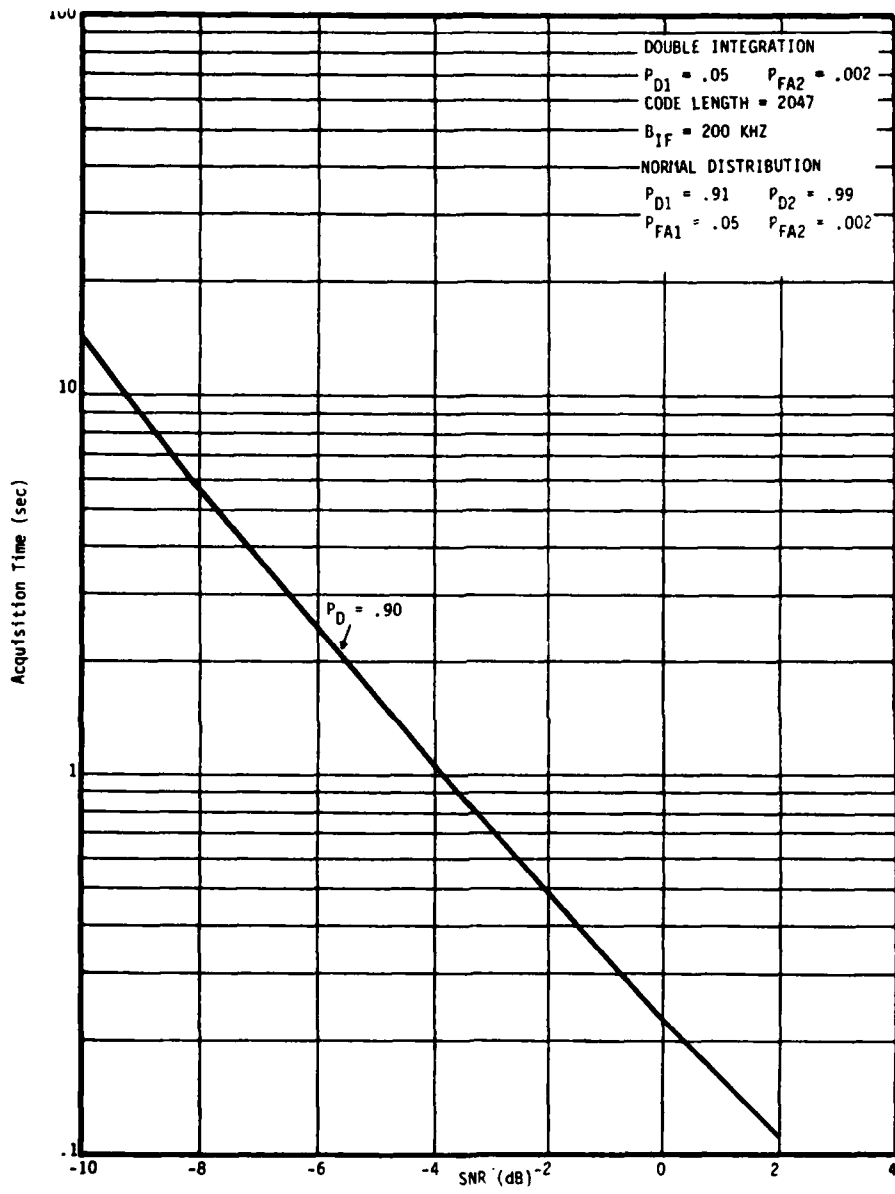


Figure 3.2-3.
 Acquisition Performance

probability of detection when the second probability of detection is very high. Notice the increase in acquisition time for the case of P_{D1} and P_{D2} equals .71. The total probability of detection is .5 but the acquisition time is 35% higher than the acquisition time for the P_{D1} equal .51 and P_{D2} equal .99. This is plotted in Figure 3.2-2.

REFERENCES

1. J. K. Holmes, C. C. Chen, "Acquisition Time Performance of PN Spread-Spectrum Systems," IEEE Transactions on Communication Technology, Vol. Com-25, pp 778-783, August 1977.
2. Waddah K. Alem, Gaylord K. Huth, Jack K. Holmes, Sengi Udalov, "Spread Spectrum Acquisition and Tracking Performance for Shuttle Communications Links," IEEE Transactions on Communications Technology, Vol. COM-26, pp 1689-1703, November 1978.

3.3 Sequential Detection

Since double integration decreased the acquisition time, with the short-term integrator dismissing the low noise values rapidly and the long integrator cleaning up the false alarms on high noise values, it would seem that maybe three integrators would improve acquisition time even more. One would be very short, rapidly dismissing the lowest noise values, the next would be a little longer and clean up the false alarms due to moderate noise values, and the third would do the final resolving of the highest noise samples. In fact, why stop at three -- Why not four or five? Better yet, the best system would be one which would automatically adjust its integration length to just long enough to make a satisfactory decision on whatever set of noise samples it happened to be getting. This, in effect, is what sequential detection does.

The sequential probability ratio test was discovered by Abraham Wald in the early 1940's while working on radar detection. If one is sampling a random variable and attempting to decide between two single hypotheses, then the sequential probability ratio test is the optimum test in the sense that for a given P_{FA} and P_D it requires the minimum average number of samples of the random variable to produce a decision. In our case minimizing the average number of samples required is equivalent to minimizing the average dwell time per code phase position, i.e., the sequential detector is an optimum correlation detector in the sense that it produces the minimum average dwell time for a given level of performance.

We will formulate the test procedure for the case of interest and then evaluate its performance. Let r_i be the independent samples of a random variable and consider that we are testing the hypothesis of signal plus noise present versus the hypothesis of noise only present. Under these conditions, the sequential test can be stated mathematically by,

$$\lambda_n = \frac{\prod_{i=1}^n P(r_i/S+N)}{\prod_{i=1}^n P(r_i/N)} \quad (3.3-1)$$

If $\lambda_n \geq V_u$ decide signal present

$\lambda_n \leq V_L$ decide noise only present

$V_L \leq \lambda_n \leq V_u$ compute λ_{n+1} using Equation 3.3-1 and repeat test

where $P(r_i/S+N)$ is the probability density function of the random variable r_i given signal plus noise, and λ_n is the familiar likelihood ratio.

For the case of interest, r_i is a sample of the envelope of a sine wave plus narrowband Gaussian noise. The density function for r_i under these conditions is the Rice density, i.e.,

$$P(r_i/S+N) = \frac{r_i}{\sigma^2} e^{-\frac{(r_i^2 + A^2)}{2\sigma^2}} I_0\left(\frac{r_i A}{\sigma^2}\right) \quad (3.3-2)$$

where A is the peak amplitude of the sine wave signal and σ^2 is the noise power in the narrowband filter.

The density of r_i given noise is found by letting A go to zero in Equation (3.3-2). Using Equation (3.3-2) in Equation (3.3-1) we formulate the test of interest as,

$$\lambda_n = \frac{\prod_{i=1}^n \frac{r_i}{\sigma^2} e^{-\frac{(r_i^2 + A^2)}{2\sigma^2}} I_0\left(\frac{r_i A}{\sigma^2}\right)}{\prod_{i=1}^n \frac{r_i}{\sigma^2} e^{-r_i^2/2\sigma^2}} \quad (3.3-3)$$

Simplifying Equation (3.3-3) and taking the log of both sides we have, [1]

$$\ln \lambda_n = \sum_{t=1}^n \ln I_0\left[\frac{r_t A}{\sigma^2}\right] - A^2/2\sigma^2 \quad (3.3-4)$$

Equation (3.3-4) defines the sequential test. In Equation (3.3-4), for convenience, we have compared the log of λ to the log of the thresholds. A block diagram of the sequential detector is shown in Figure 3.3-1. It is perhaps of interest to note that if one performs this derivation starting with a square law detector and computes the likelihood ratio for samples taken at the output of a square law detector he will find that the processor shown in Figure 3.3-1 is still optimum. The likelihood ratio processor for samples taken at the output of a square law detector contains a square root device before the multiplication by A/σ^2 , i.e., it computes the envelope first.

In Figure 3.3-1, $A^2/2\sigma^2$ is the SNR in the narrowband filter and represents a design parameter, i.e., it is the design value of SNR. The performance of the sequential detector is characterized by the probability of detection, probability of false alarm and average number of samples required for a decision. Wald has shown that for any sequential test

$$\frac{P_D}{P_{FA}} = e^{T_U} \quad (3.3-5)$$

and

$$\frac{1-P_D}{1-P_{FA}} = e^{T_L} \quad (3.3-6)$$

where P_D is probability of detection at the design value of SNR and P_{FA} is probability of false alarm. [2]

For cases of interest to us P_D is near 1 and P_{FA} is very small and under these conditions we have

$$P_{FA} = e^{-T_U} \quad (3.3-7)$$

$$P_D = 1 - e^{T_L}$$

where T_L is a negative number.

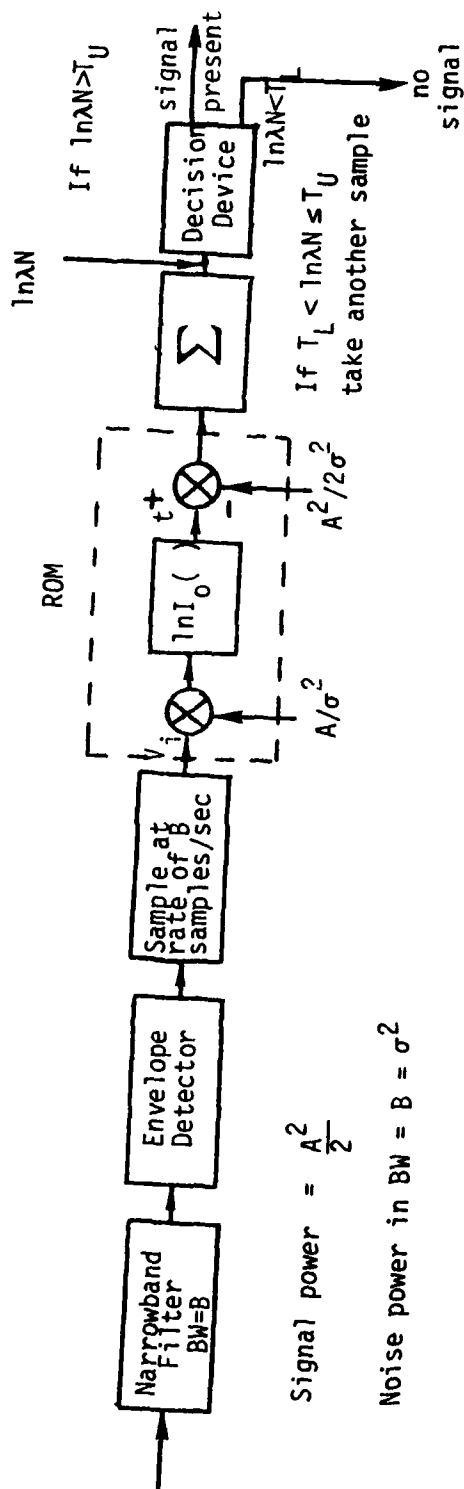


Figure 3.3-1. Block Diagram of Sequential Detector

Equation (3.3-7) defines the detection performance of the circuit, however, the average number of samples required (dwell time) must also be known if we are to evaluate the acquisition performance. The average number of samples required to dismiss with noise only at the input can be expressed as (again from Rubin),

$$\bar{M}(0) = \frac{(1-P_{FA}) \ln \left(\frac{1-P_D}{1-P_F} \right) + P_F \ln (P_D/P_F)}{E(z/\text{noise only})} \quad (3.3-8)$$

where

$$z = -A^2/2\sigma^2 + \ln I_0 \frac{r_i A}{\sigma^2}$$

Evaluation of Equation (3.3-8) is difficult because of the requirement to compute the average value of $\ln I_0(x)$. There are three approaches which can be taken for finding $M(0)$. First one can expand $\ln I_0(r_i A/\sigma^2)$ in a power series and compute the average value of z by computing the moments of the Rice random variable r . Figure 3.3-2 is a plot of $\ln I_0(x)$ versus x . From this figure it is apparent that for the square law approximation to be accurate the SNR must be less than 0 dB.

The second approach to computing the expected value in Equation (3.3-8) is by numerical integration. This is time consuming on a computer. In addition, this technique gives us no clue as to the P_D at values of SNR other than the design value.

The third approach is to simulate the sequential detector directly on the computer. This approach also uses considerable computer time, but it allows the evaluation of a wide range of parameters such as thresholds, design SNR, actual SNR, gain errors, and external accumulator steps.

This simulation has been run for a wide range of parameters. Figures 3.3-3, 3.3-4, and 3.3-5 summarize some of the data. Figure 3.3-3 is a plot of probability of miss versus SNR for a Design SNR of 0 dB. The curves are given for various lower thresholds. Figure 3.3-4 shows the mean-time-to-dismiss with no signal versus lower threshold for various Design SNR's. Figure 3.3-5 illustrates the effect of the external accumulator on the mean-time-to-dismiss with no signal.

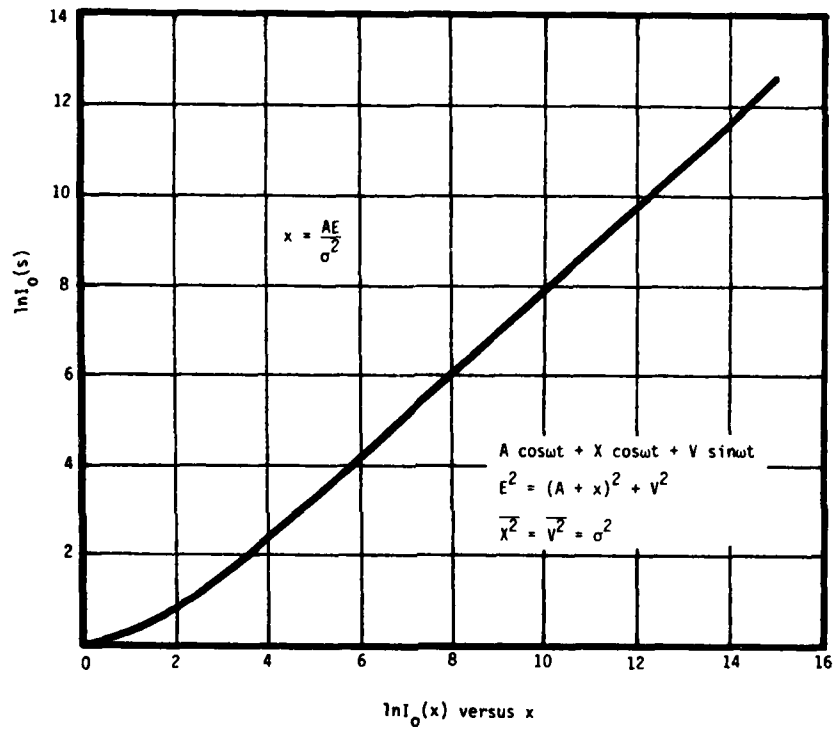


Figure 3.3-2.
Acquisition Performance

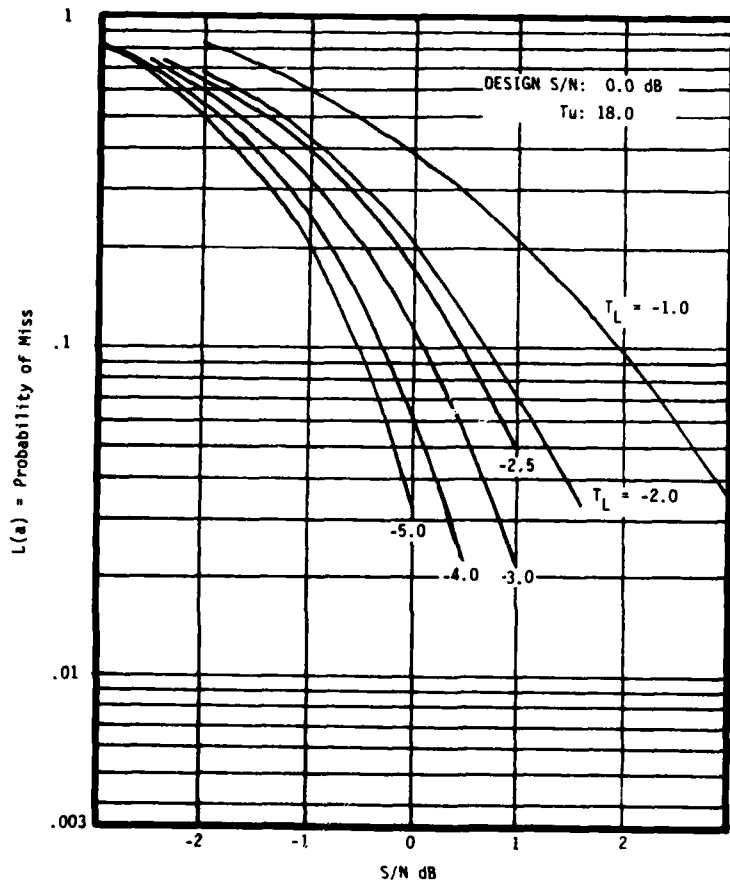


Figure 3.3-3.
 Miss Probability Versus S/N with Random Start Phase

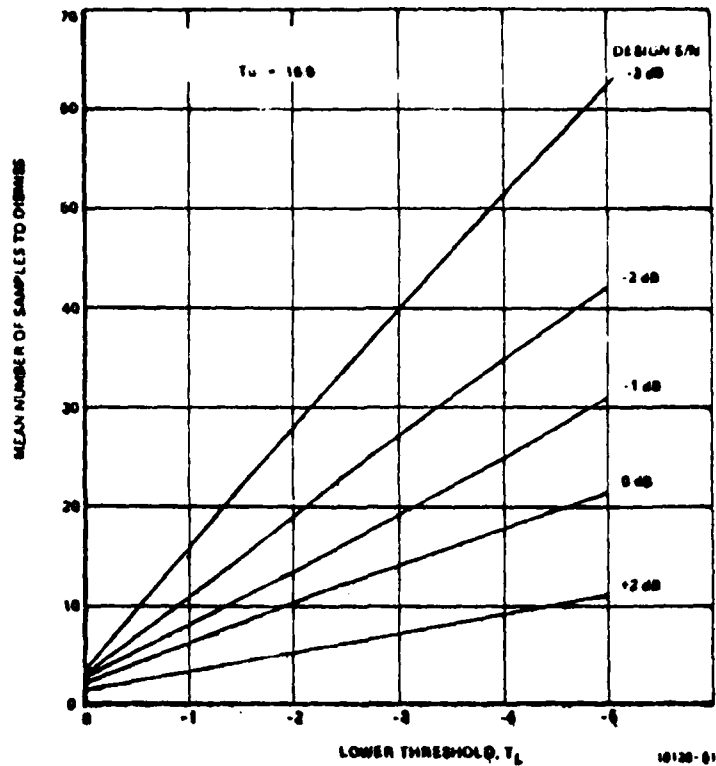


Figure 3.3-4.
Effect of Lower Threshold on Mean-Time-to-Dismiss (No Signal)

Choice of Parameters

The key design parameters are Design SNR, T_L , T_U , and number of external accumulator steps. The Design SNR determines the parameter A in Figure 3.3-1. This parameter is chosen to be equal to the minimum SNR for which acquisition is to take place. In this case, the chosen Design SNR is 0 dB.

After Design SNR has been chosen, T_L and mean-time-to-dismiss are linearly related. (See Figure 3.3-4.) T_L also governs probability of miss (Figure 3.3-3). T_L is chosen through a trade-off between mean-time-to-dismiss and probability of miss.

The parameter T_U is independent of the other parameters when T_U is chosen to give a low probability of false alarm (PFA). Increasing T_U decreases

PFA, but it also increases the mean time to declare a hit. However, this time is usually small when compared to the time spent dismissing samples during code search.

The number of external accumulator steps is determined by the speed of the sequential detector hardware. This number is made as small as possible because it tends to increase mean-time-to-dismiss. (Figure 3.3-5). An external accumulator is used only when the sequential detector is not fast enough to test the accumulator contents on every detector sample.

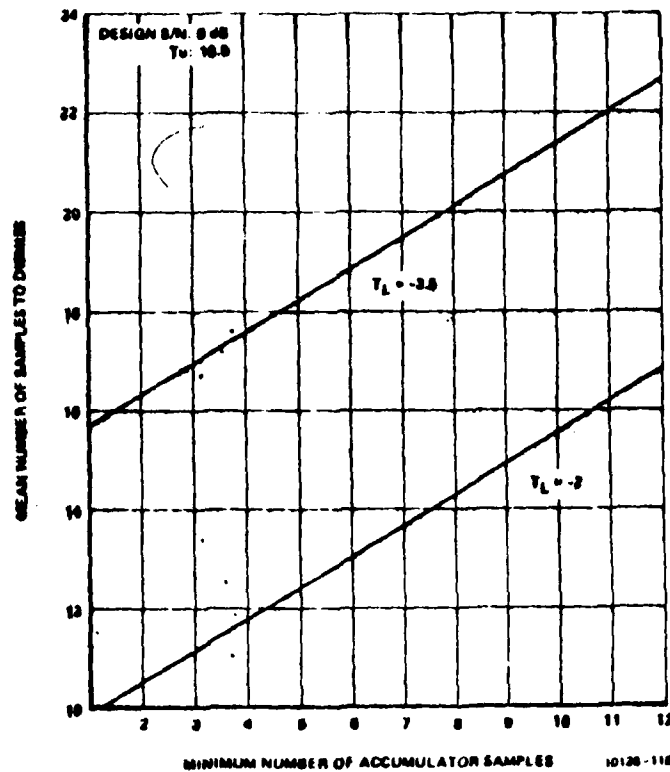


Figure 3.3-5.
Effect of External Accumulator on Dismissal Time

The data just presented was generated on a computer and is quite accurate. It is not feasible to date to get this degree of accuracy by using analytical models. Sometimes, however, it is desirable to get an estimate of

system performance without having to use the computer. The following equations can be used to calculate the approximate performance of a sequential detector. Calculations are included for the same system parameters used in the simulation so the approximate data can be compared to the simulated data to see how well they compare.

$$\begin{aligned} \text{Upper threshold } T_U &\cong \frac{1-B}{\alpha} & B &= \text{probability of a miss} \\ & & \alpha &= \text{probability of a false alarm} \\ \text{Lower threshold } T_L &\cong \frac{B}{1-\alpha} & 1-B &= P_D \text{ (probability of detection)} \end{aligned}$$

$$\text{Operating characteristic function} = L(a) = \frac{T_U^h - 1}{T_U^h - T_L^h} \quad (3.3-9)$$

h is approximated by $h = 1 - 2 \frac{a^2}{a_d^2}$ where a^2 is the actual SNR in the IF bandwidth and a_d^2 is the design SNR.

The average number of samples required for a given set of parameters is given by the equation^[2]

$$\text{ASN} = \frac{L(a) \log_e B + [1-L(a)] \log_e \frac{1-B}{\alpha}}{\frac{-a_d^2}{4} \left[\frac{1}{2} - \left(\frac{a}{a_d} \right)^2 \right]} \quad (3.3-10)$$

This equation was used to plot Figure 3.3-6. Comparing this to Figure 3.3-4 which was generated by the computer simulation model it is seen that the two compare quite well for $T_L = -1$ but they diverge quite rapidly for lower threshold values.

Figure 3.3-7 which shows probability of miss versus SNR was plotted using the equation:

$$L(a) = \frac{A^h - 1}{A^h - B^h} \quad (3.3-11)$$

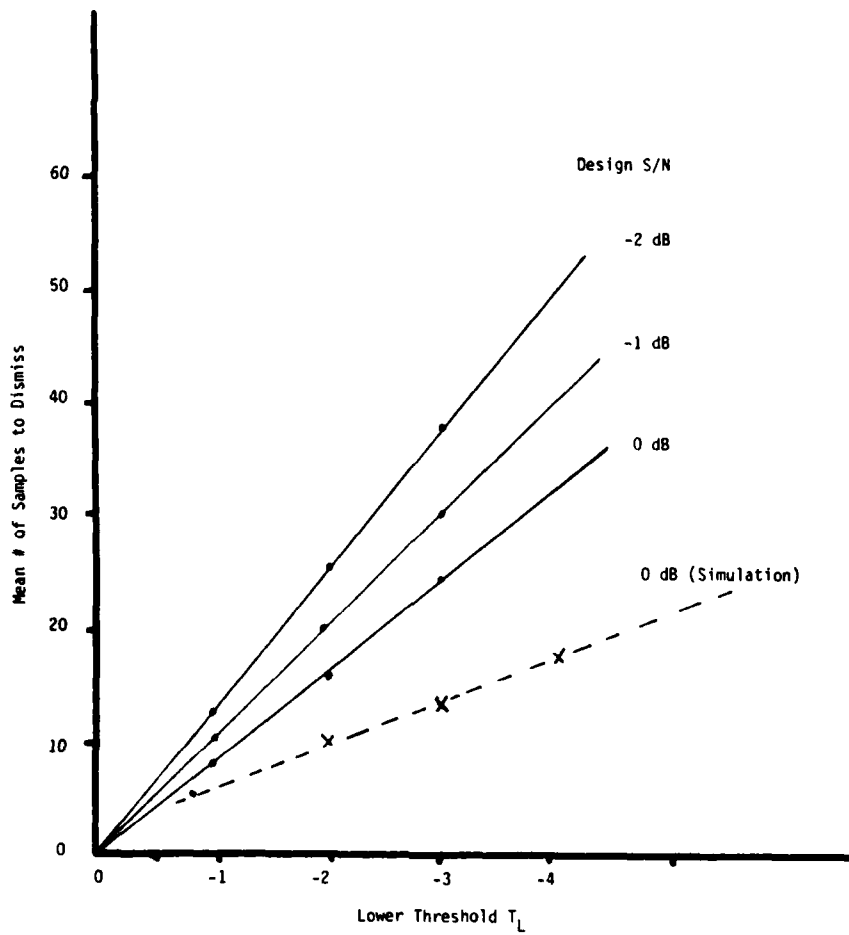


Figure 3.3-6.
 Effect of Lower Threshold on Mean-Time-to-Dismiss
 (No Signal) (Approximation)

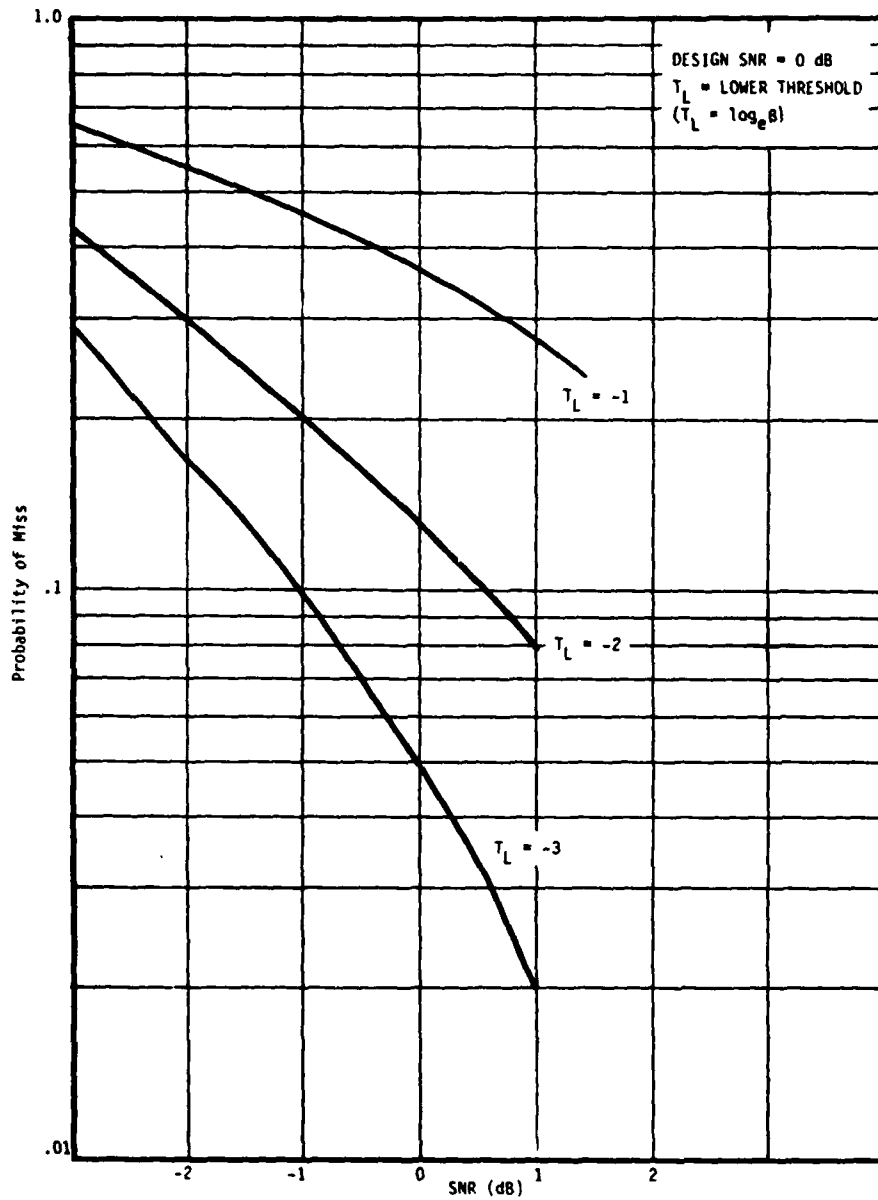


Figure 3.3-7.
 Acquisition Performance

Again, this is only an approximation and can be compared with the computer model data in Figure 3.3-3.

Figure 3.3-8 is another plot of ASN versus SNR. Note that the number of samples required decreases very rapidly for decreasing SNR, i.e., it dismisses the no signal condition quite rapidly. Notice that at signal levels where the ratio of the actual SNR to the design SNR equal .5 there is a peak in the ASN. At values of SNR around this point sequential detection is not much better than the fixed length test. This points out the fact that the design SNR should be chosen at the lowest SNR expected in operation.

Figure 3.3-9 is a plot of acquisition time versus SNR for the same parameters used in the single and double integration examples. This will allow a comparison of the acquisition times for the different techniques. This equation was plotted by determining the ASN for the no signal condition as shown previously. The design SNR was assumed to be the actual value as SNR was varied. The dwell time was then calculated using the ASN values. These dwell time values were then used in the same equation used to calculate the acquisition time for single integration. The equation is repeated below for convenience.

$$T = \frac{(2-P_D)(1+KP_{FA})}{2P_D} q\tau$$

where q = number of uncertainty positions
 τ = dwell time

From the derivation in Section 2.0 it can be seen that the terms

$$\frac{(2-P_D)(1+KP_{FA})}{2P_D} q$$

relate to the probability of detection on a particular pass through the code and to the time penalty paid for false alarms and has nothing to do with the detection technique used. The desirable feature about sequential detection is that the dwell time can vary depending on the SNR. Once this dwell time is chosen then it is necessary to determine how many passes through the code is required and what the penalties are for the false alarms that occur. The above equation takes these factors into account.

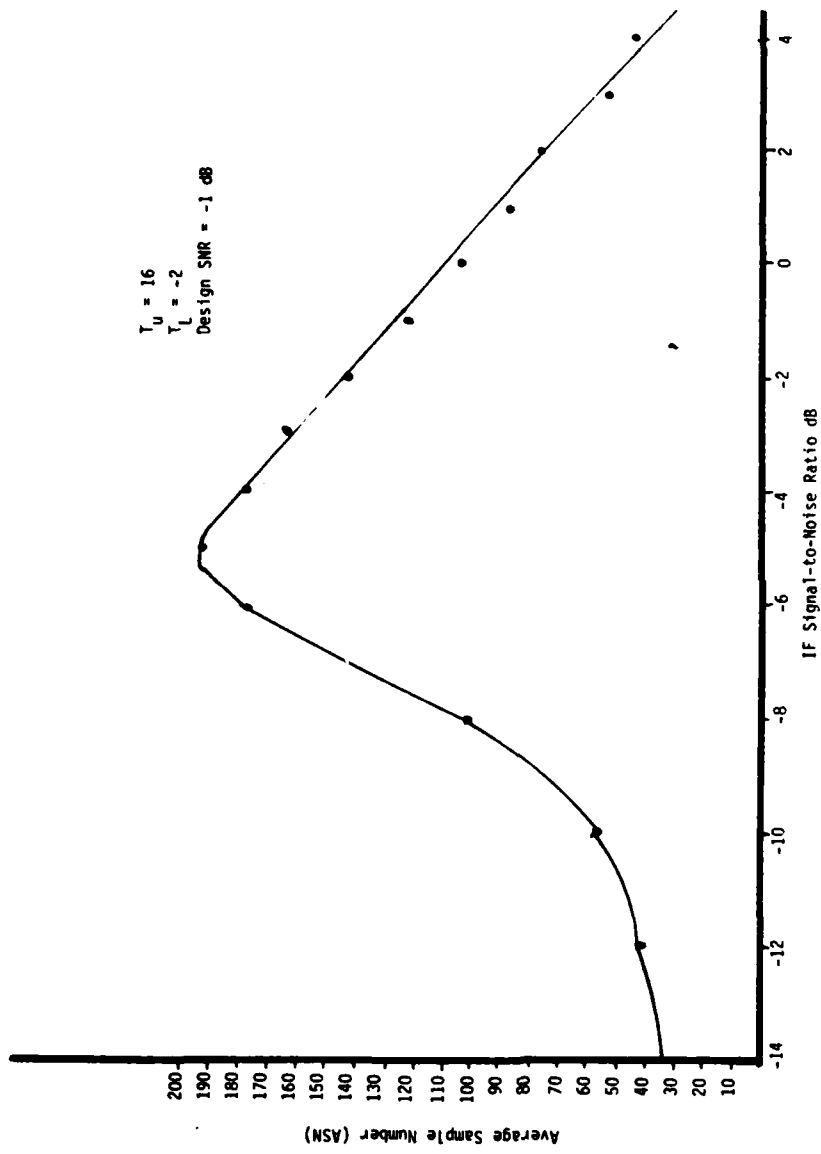


Figure 3.3-8.
Acquisition Performance

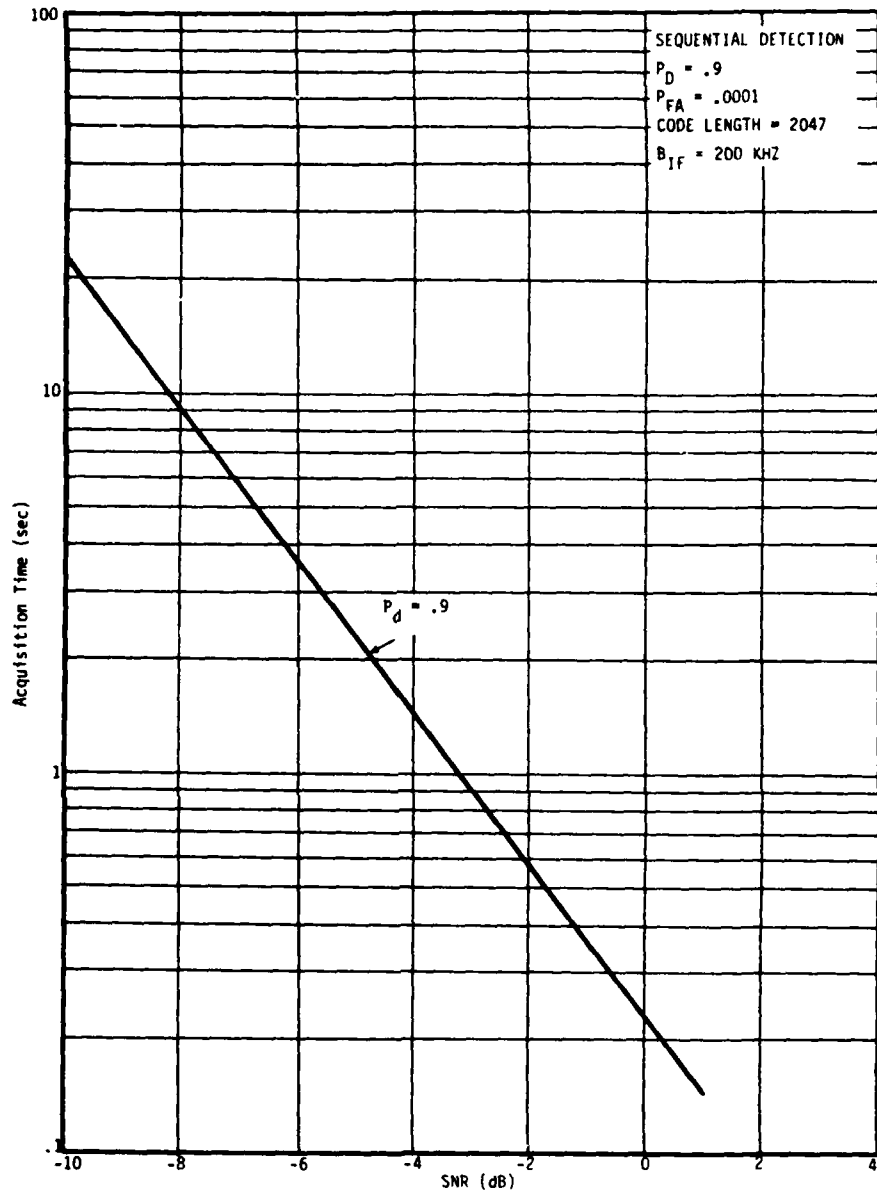


Figure 3.3-9.
 Acquisition Performance

Sequential Detection Example Calculations

$$P_D = .26 \quad \text{Design SNR} = -2 \text{ dB} = .63$$

$$P_{FA} = .0015$$

$$T_U = \frac{1-\beta}{\alpha} = \frac{.26}{.0015} = 173 \quad \ln 173 = 5.2$$

$$T_L = \frac{\beta}{1-\alpha} = \frac{.74}{.9985} = .74 \quad \ln .74 = -.3$$

For noise only

$$\text{ASN} = \frac{8 \log \beta}{-(a_d^2)^2} = \frac{(8)(-.3)}{-(.63)^2} = \frac{2.4}{.3969} = 6 \text{ samples}$$

Assume sampling at $B_{if} = 200 \times 10^3$

$$T_s = \frac{NM}{B}$$

N samples per position
M number of positions
B = samples/sec

$$T_s = \frac{(6)(4094)}{200 \times 10^3} = .122 \text{ s}$$

For signal + noise

$$T_U = 173 (5.2) \quad a_d^2 = -2 \text{ dB} = .63 \quad \frac{a^2}{a_d^2} = -6.5 + 2 = 4.50 (.35)$$

$$T_L = .74 (-.3) \quad a^2 = -6.5 \text{ dB} = .224$$

$$h = 1 - 2 \frac{a^2}{a_d^2} = 1 - .7 = .3$$

$$L(a) = \frac{(173)^3 - 1}{(173)^3 - (.74)^3} = \frac{4.69 - 1}{4.69 - .91} = \frac{3.69}{3.78} = .98$$

$$ASN = \frac{(.98)(-.3) + [1-.98][5.2]}{-1[.5-.35]} = \frac{-.294 + .104}{-.015} = 13 \text{ samples}$$

$$T_s = \frac{(13)(4094)}{200 \times 10^3} = \underline{\underline{.266s}}$$

REFERENCES

1. R. F. Cobb, A. D. Darby, "Acquisition Performance of Simplified Implementations of the Sequential Detection Algorithm," Presented at the 1978 International Telecommunications Conference, Birmingham, Alabama, 4-6 December, 1978.
2. DeFranco and Rubin, "Radar Detection," Prentice-Hall, Englewood Cliffs, New Jersey, 1968, Chapter 16.

3.4 Doppler Limitations

One potential problem that can degrade acquisition performance is doppler. In any system that includes RPVs and aircraft, this is definitely a consideration. It is both interesting and informative to evaluate the typical detection system investigated thus far in a doppler environment. The incoherent and coherent detectors will be investigated. Their performance will then be compared to that of the convolver in Section 5.3.1.

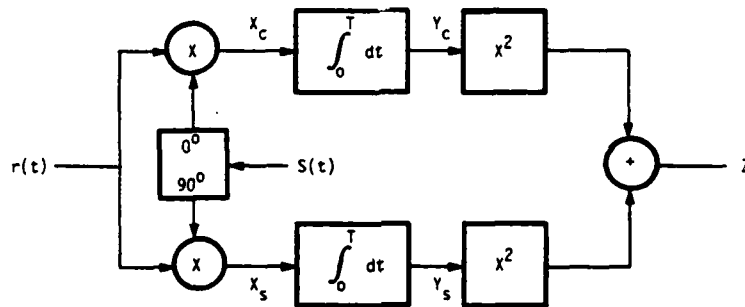


Figure 3.4-1.
Noncoherent Detector

The received signal, as shown in Figure 3.4-1, is

$$r(t) = \sqrt{2S} C(t) \cos([\omega + \omega_d]t) \quad (3.4-1)$$

where: S = signal power
 $C(t)$ = PN code $[\pm 1]$
 ω_d = doppler

and the receiver's replica signal is

$$S(t) = \sqrt{2S} C(t+\tau) \cos (\omega t + \phi) \quad (3.4-2)$$

where: τ = time offset of PN replica
 ϕ = carrier phase offset

It will be assumed that the data (if present) is at a rate low enough so that it may be neglected without consequence.

The question of concern is how ω_d effects the permissible value of integration time T. The outputs of the multipliers are given by

$$X_c = r(t) s(t) = \left\{ \sqrt{2S} C(t) \cos [(\omega + \omega_d)t] \right\} \left\{ \sqrt{2S} C(t+\tau) \cos (\omega t + \phi) \right\}$$

$$X_c = 2S C(t) C(t+\tau) \cos [(\omega + \omega_d)t] \cos [\omega t + \phi]$$

using the identity

$$\cos \alpha \cos \beta = \frac{1}{2} \cos(\alpha - \beta) + \frac{1}{2} \cos(\alpha + \beta) \quad (3.4-3)$$

$$X_c = 2S C(t) C(t+\tau) \left\{ \frac{1}{2} \cos [(\omega_d t - \phi)] + \frac{1}{2} \cos [(2\omega + \omega_d)t + \phi] \right\}$$

$$X_c = S C(t) C(t+\tau) \left[\cos [(\omega_d t - \phi)] + \cos [(2\omega + \omega_d)t + \phi] \right] \quad (3.4-4)$$

The output of the second multiplier is given by

$$X_s = r(t) S(t + \frac{\pi}{2})$$

$$X_s = \left\{ \sqrt{2S} C(t) \cos [(\omega + \omega_d)t] \right\} \left\{ \sqrt{2S} C(t+\tau) \sin (\omega t + \phi) \right\}$$

$$X_s = 2S C(t) C(t+\tau) \cos [(\omega + \omega_d)t] \sin (\omega t + \phi)$$

using the identity

$$\cos\alpha \sin\beta = \frac{1}{2} \sin(\alpha+\beta) - \frac{1}{2} \sin(\alpha-\beta)$$

$$\begin{aligned} X_s &= 2S C(t) C(t+\tau) \left\{ \frac{1}{2} \sin[(2\omega+\omega_d)t+\phi] - \frac{1}{2} \sin[\omega_d t-\phi] \right\} \\ X_s &= S C(t) C(t+\tau) \left\{ \sin[(2\omega+\omega_d)t + \phi] - \sin[\omega_d t-\phi] \right\} \end{aligned} \quad (3.4-5)$$

If $\omega \gg 1/T$ we can invoke the Riemann-Lebesgue Lemma to neglect the integrals with 2ω terms so that

$$Y_c = S \int_{-T/2}^{T/2} C(t) C(t+\tau) \cos(\omega_d t - \phi) dt \quad (3.4-6)$$

$$\begin{aligned} &= S \cos(\phi) \int_{-T/2}^{T/2} C(t) C(t+\tau) \cos(\omega_d t) dt \\ &+ S \sin(\phi) \int_{-T/2}^{T/2} C(t) C(t+\tau) \sin(\omega_d t) dt \end{aligned}$$

$$Y_s = -S \int_{-T/2}^{T/2} C(t) C(t+\tau) \sin(\omega_d t - \phi) dt \quad (3.4-7)$$

$$\begin{aligned} &= -S \sin(\phi) \int_{-T/2}^{T/2} C(t) C(t+\tau) \cos(\omega_d t) dt \\ &+ S \cos(\phi) \int_{-T/2}^{T/2} C(t) C(t+\tau) \sin(\omega_d t) dt \end{aligned}$$

While it is not possible to evaluate the two integrals in general, the results are certainly just two constants α and β where

$$\alpha \triangleq \int_{-T/2}^{T/2} C(t) C(t+\tau) \cos(\omega_d t) dt \quad (3.4-8)$$

$$\beta \triangleq \int_{-T/2}^{T/2} C(t) C(t+\tau) \sin(\omega_d t) dt \quad (3.4-9)$$

For this assumption, the outputs of the two integrators can be represented by

$$Y_C = S \alpha \cos \phi + S \beta \sin \phi \quad (3.4-10)$$

$$Y_S = S \beta \cos \phi - S \alpha \sin \phi \quad (3.4-11)$$

The outputs of the two channels are then summed yielding the following results

$$Z = Y_C^2 + Y_S^2 \quad (3.4-12)$$

$$Z = [S \alpha \cos \phi + S \beta \sin \phi]^2 + [S \beta \cos \phi - S \alpha \sin \phi]^2$$

$$Z = S^2 [\alpha^2 \cos^2 \phi + 2\alpha\beta \sin \phi \cos \phi + \beta^2 \sin^2 \phi] \\ + S^2 [\beta^2 \cos^2 \phi - 2\alpha\beta \sin \phi \cos \phi + \alpha^2 \sin^2 \phi]$$

$$Z = S^2 \left\{ \alpha^2 [\cos^2 \phi + \sin^2 \phi] + \beta^2 [\cos^2 \phi + \sin^2 \phi] \right\}$$

$$Z = S^2 [\alpha^2 + \beta^2] \quad \text{since } \cos^2 \phi + \sin^2 \phi = 1 \quad (3.4-13)$$

If we now assume that the doppler, ω_d , is zero and the PN code period is T then

$$\alpha \triangleq \int_{-T/2}^{T/2} C(t) C(t+\tau) \cos \omega_d t dt = \int_{-T/2}^{T/2} C(t) C(t+\tau) dt$$

This is immediately recognized as the autocorrelation function $R_C(\tau)$.

$$\alpha = R_C(\tau) \tag{3.4-14}$$

$$\beta \equiv 0$$

Therefore the output can be written as

$$Z = S^2 [\alpha^2 + \beta^2]$$

$$Z = S^2 R_C^2(\tau) \quad \text{output for no doppler} \tag{3.4-15}$$

If it is now assumed that there is doppler but the codes are in alignment then the output can be written,

$$\alpha \triangleq \int_{-T/2}^{T/2} C(t) C(t+\tau) \cos \omega_d t dt$$

for code alignment $\tau=0$

$$\alpha = \int_{-T/2}^{T/2} C^2(t) \cos \omega_d t dt \quad \text{but } C^2(t) = 1$$

$$\therefore \alpha = \int_{-T/2}^{T/2} \cos \omega_d t \, dt = \frac{\sin \omega_d t}{\omega_d} \Bigg|_{-T/2}^{T/2}$$

$$\alpha = \frac{1}{\omega_d} \left[\sin \frac{\omega_d T}{2} - \sin \left(-\frac{\omega_d T}{2} \right) \right]$$

$$\alpha = \frac{2 \sin \frac{\omega_d T}{2}}{\omega_d} = \frac{\sin \pi f_d T}{\pi f_d}$$

$$\alpha = T \operatorname{sinc} f_d T \quad (3.4-16)$$

$$\beta \triangleq \int_{-T/2}^{T/2} C(t) C(t+\tau) \sin \omega_d t \, dt$$

for $\tau=0$

$$\beta = \int_{-T/2}^{T/2} \sin \omega_d t \, dt$$

since $\sin \omega_d t$ is an odd function and the limits of integration are symmetrical then $\beta=0$. Now the output can be written as follows,

$$Z = S^2 \left[\alpha^2 + \beta^2 \right]$$

$$Z = S^2 T^2 \operatorname{sinc}^2 f_d T \quad (3.4-17)$$

This equation shows how the output is affected by doppler. Note that the output goes to zero for $f_d T=1$, which is the same results achieved with the convolver. Therefore the convolver has no advantage over the conventional quadrature method of incoherent detection.

SECTION 4.0

PARALLEL SEARCH OPERATION

4.0 PARALLEL SEARCH OPERATION

Thus far all of the techniques investigated have been serial search techniques where one code phase at a time is checked for alignment. A natural extension would seem to be to use two or more paths to search more than one code phase at a time. Hopefully the acquisition time would decrease in direct relation to the number of parallel paths used. This section investigates the possibilities of N parallel searches and looks at what the limitations are.

Rayleigh Assumption

Assume that the probability of dismissing an individual false alignment results in a Rayleigh distribution in time

$$P_{t_d}(t) = \frac{t}{\lambda} e^{-t^2/2\lambda} \quad t \geq 0 \quad (4.0-1)$$

The mean time to dismissal is $\bar{t}_d = \sqrt{\frac{\pi\lambda}{2}}$ and the variance is $\sigma_{t_d}^2 = \lambda(2 - \frac{\pi}{2})$.

The cumulative distribution function for t_d is given by

$$P\{t_d \leq t\} = \int_0^t \frac{x}{\lambda} e^{-x^2/2\lambda} dx \quad (4.0-2)$$

$$= \int_0^{t^2/2\lambda} e^{-\xi} d\xi = 1 - e^{-t^2/2\lambda}$$

where $\xi \triangleq x^2/2\lambda$ so that $d\xi = 2xdx/2\lambda = xdx/\lambda$.

If we have N searches progressing in parallel with a common control, then all N alignments must be dismissed before any can be dismissed. Assuming all searches have independent noise the probability of dismissing all N searches by time t is the N-fold product of dismissing each by time t, or

$$\begin{aligned}
 P[t_N \leq t] &= \prod_{i=1}^N \left[1 - e^{-t^2/2\lambda} \right] \\
 &= \left[1 - e^{-t^2/2\lambda} \right]^N
 \end{aligned}
 \tag{4.0-3}$$

The probability density function for t_N is given by the derivative of the cumulative distribution function as

$$\begin{aligned}
 P_{t_N}(t) &= \frac{d}{dt} \left\{ \left[1 - e^{-t^2/2\lambda} \right]^N \right\} \\
 &= \frac{Nt}{\lambda} e^{-t^2/2\lambda} \left[1 - e^{-t^2/2\lambda} \right]^{N-1} \quad t \geq 0
 \end{aligned}
 \tag{4.0-4}$$

Solving for the expected value of t_N gives

$$\bar{t}_N = \int_0^{\infty} \frac{Nt^2}{\lambda} e^{-t^2/2\lambda} \left[1 - e^{-t^2/2\lambda} \right]^{N-1} dt$$

Defining $\xi \triangleq t^2/2\lambda$ so that $d\xi = 2tdt/2\lambda$ gives

$$\begin{aligned}
 \bar{t}_N &= N\sqrt{2\lambda} \int_0^{\infty} \xi^{1/2} e^{-\xi} \left[1 - e^{-\xi} \right]^{N-1} d\xi \\
 &= N\sqrt{2\lambda} \sum_{k=0}^{N-1} (-1)^k \binom{N-1}{k} \int_0^{\infty} \xi^{1/2} e^{-(k+1)\xi} d\xi
 \end{aligned}
 \tag{4.0-5}$$

From Gradshteyn and Ryzhik, page 317, equation 317

$$\int_0^{\infty} x^{\frac{1}{2}} e^{-\mu x} dx = \frac{\sqrt{\pi}}{2\mu^{3/2}} \quad [\text{Re } \mu > 0] \quad (4.0-6)$$

Hence

$$\bar{t}_N = N \sqrt{\frac{\pi\lambda}{2}} \sum_{k=0}^{N-1} (-1)^k \binom{N-1}{k} \frac{1}{(k+1)^{3/2}} \quad (4.0-7)$$

Recognizing that $\sqrt{\frac{\pi\lambda}{2}} = \bar{t}_d$ and rewriting gives

$$\bar{t}_N = \bar{t}_d N \sum_{k=1}^N (-1)^{k-1} \binom{N-1}{k-1} \frac{1}{k^{3/2}} \quad (4.0-8)$$

$$= \bar{t}_d \sum_{k=1}^N (-1)^{k-1} \frac{N(N-1)!}{(N-k)! k(k-1)!} \frac{1}{\sqrt{k}}$$

$$= \bar{t}_d \sum_{k=1}^N \frac{(-1)^{k-1}}{\sqrt{k}} \binom{N}{k}$$

Exponential Assumption

Assume that the time required to dismiss a false position is an exponentially distributed random variable

$$P_t(\alpha) = \frac{1}{\beta} e^{-\alpha/\beta} \quad \alpha \geq 0 \quad (4.0-9)$$

with mean

$$\begin{aligned} \mu &= \int_0^{\infty} \frac{\alpha}{\beta} e^{-\alpha/\beta} d\alpha \\ &= \beta \int_0^{\infty} \xi e^{-\xi} d\xi = \beta \quad \xi \triangleq \frac{\alpha}{\beta} \end{aligned} \quad (4.0-10)$$

The probability that the position will be dismissed by time t is

$$\begin{aligned} P[t_d < t_0] &= \int_0^{t_0} \frac{1}{\beta} e^{-\alpha/\beta} d\alpha \\ &= \left[-e^{-\alpha/\beta} \right]_0^{t_0} = (1 - e^{-t_0/\beta}) \end{aligned} \quad (4.0-11)$$

If there are N searches going on in parallel, the probability that they will all be dismissed by time t_0 is

$$P[\text{all dismissed}] = (1 - e^{-t_0/\beta})^N \quad (4.0-12)$$

Thus the distribution of t_0 is

$$P_{t_p}(t) = \frac{d}{dt} \left\{ (1 - e^{-t/\beta})^N \right\} \quad (4.0-13)$$

$$= N (1 - e^{-t/\beta})^{N-1} \left(\frac{1}{\beta} e^{-t/\beta} \right)$$

$$= \frac{N}{\beta} e^{-t/\beta} [1 - e^{-t/\beta}]^{N-1} \quad (4.0-13)$$

Hence the mean time to dismiss N positions is

$$\begin{aligned}
 & \int_0^{\infty} \frac{Nt}{\beta} e^{-t/\beta} [1 - e^{-t/\beta}]^{N-1} dt \\
 &= (-1)^{N-1} N\beta \int_0^{\infty} \frac{t}{\beta} e^{-t/\beta} [e^{-t/\beta} - 1]^{N-1} \frac{dt}{\beta} \\
 &= (-1)^{N-1} N\beta \int_0^{\infty} x e^{-x} [e^{-x} - 1]^{N-1} dx \quad \begin{array}{l} V=2 \\ M=1 \\ N=N-1 \end{array} \\
 &= (-1)^{N-1} N\beta \Gamma(2) \sum_{k=0}^{N-1} (-1)^k \binom{N-1}{k} \frac{1}{(N-k)^2} \quad (4.0-14)
 \end{aligned}$$

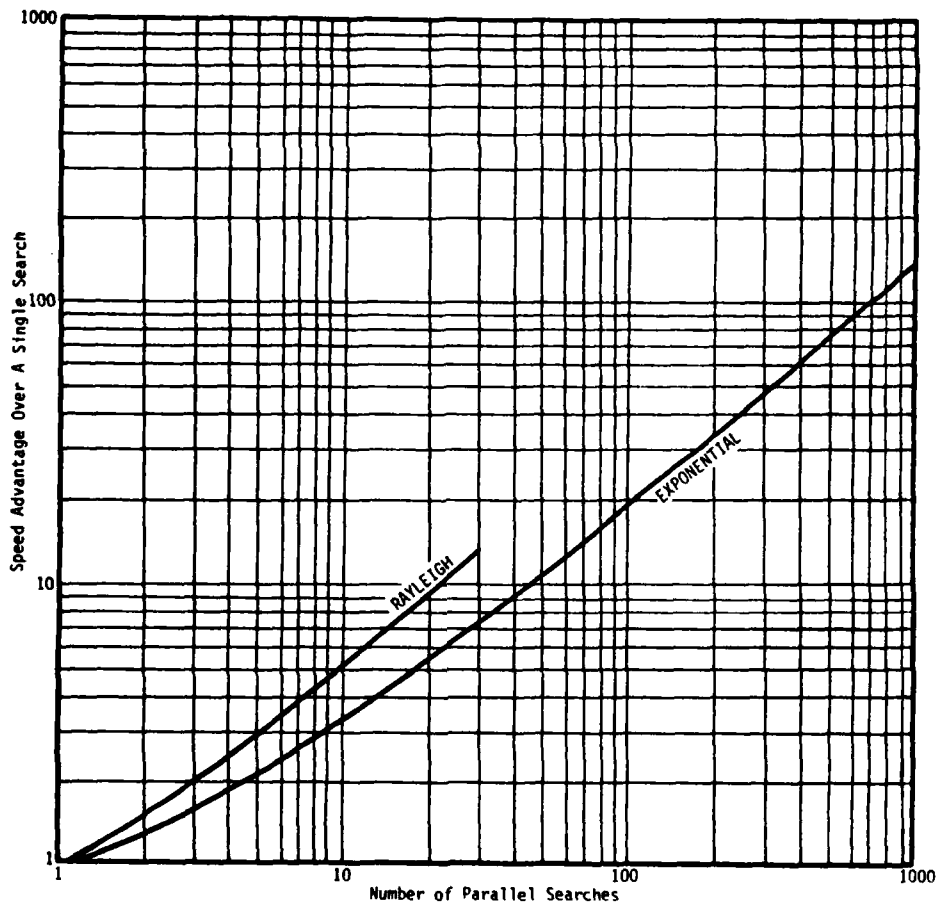


Figure 4.0-1.
Acquisition Performance

SECTION 5.0
MATCHED FILTER TECHNOLOGY

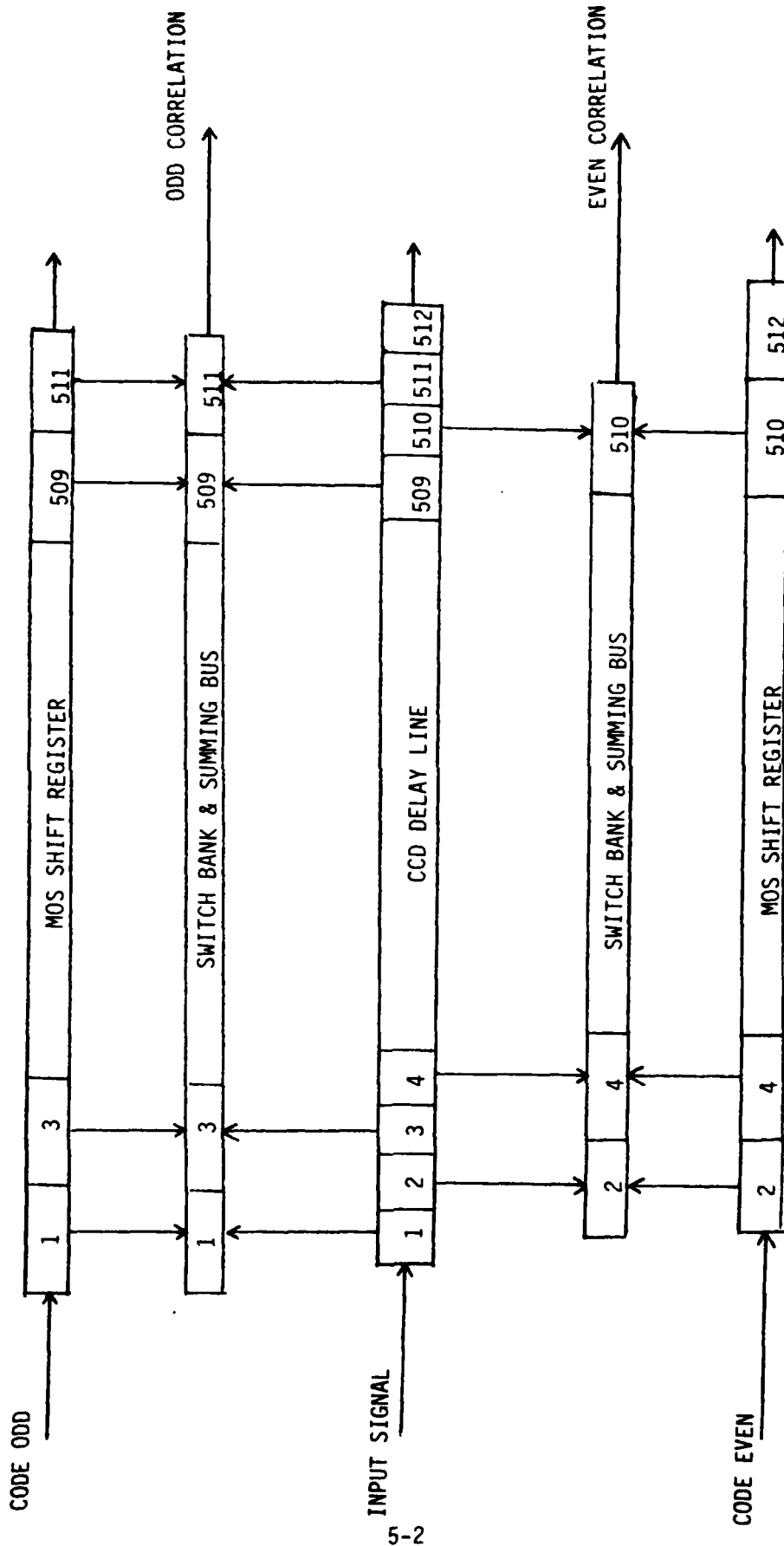
5.0 MATCHED FILTER TECHNOLOGY

The key implementation consideration for future AJ modems will be the type of matched filter technology employed for acquisition and data demodulation. Due to the increasing drive towards greater AJ data link flexibility (wider range of data ranges and vehicle dynamics, etc.) versatility of the matched filter will be a consideration as well as the obvious issues of process gain, cost, size, etc. The candidate matched filter technologies are CCD, digital correlators and SAW convolvers. In addition, a correlator device presently under development at Harris, consisting of parallel correlators performing both analog and digital functions, offers considerable promise.

The digital correlators, CCDs and SAW convolvers are generally considered to satisfy the low, medium and high PN rate requirements, respectively. However, CCDs seem to be losing out since demonstrated performance to date has not lived up to expectations and the digital correlators are moving up into the medium PN rate range. The utilization of convolvers imposes some additional hardware requirements in that: (1) the reference PN code must be reversed in time since correlation, not convolution, is the required operation; (2) the output of the convolver is at twice the frequency of the input and hence the correlation pulse is compressed to half the normal width. This compression requires that post-convolver processing be at twice the normal speed, at least for a portion of the circuitry.

5.1 CCD

An example of the CCD implementation of a PN matched filter is the Fairchild PTF-2. It is a 512-stage CCD delay line with taps on 511 of the stages. Basically, the device generates the correlation value by modifying the sign of the analog signal sample at each tap by the sign of the corresponding PN chip and summing the resulting values. This is accomplished by using the polarity of each PN chip to switch the corresponding signal value onto either a positive or negative summing bus and then subtracting the two bus values. The device actually contains dual banks of PN shift registers, switch banks and summing buses as shown in Figure 5.1-1. The CCD delay line taps are interleaved into the two banks so that BPSK, QPSK or OQPSK signal formats can be accommodated. The CCD delay line can operate at sampling rates of up to 10 MHz and the MOS shift registers at up to 2.5 MHz each, rates which are comparable to those of the SAW convolvers. The primary advantage of the CCD is the relatively long



5-2

Figure 5.1-1. 511-Stage CCD Matched Filter

length available. In fact the PTF-2 provides the delayed analog samples and PN reference signals as outputs so that two or more devices may be cascaded to form an even longer matched filter. However, charge leakage places a limitation on the maximum length achievable.

5.2 Digital Correlator

The state-of-the-art in digital correlators is exemplified by the TRW TDC1023J, a 64-bit monolithic correlator whose functional block diagram is presented in Figure 5.2-1. In this device the signal, after one bit quantization, is serially loaded into the "A" register and the PN reference is serially loaded into the "B" register. Contents of the "B" register are then parallel dumped into the "R" holding register and the correlation between the "A" and "R" registers calculated. The effective length of the correlator is adjusted by loading "0"s into the "M" register at locations which are to be unused. The bit-for-bit results of the active exclusive-OR operations are digitally summed to produce a 7-bit word indicating the number of positions which are matched. This 7-bit word is compared to the user-set threshold value. Whenever the correlation sum equals or exceeds the threshold, the threshold flag goes high.

Each of the three shift registers may be independently clocked at shift speeds up to 40 MHz but the maximum rate of correlation between the "A" and "R" registers is 20 MHz.

5.3 SAW Convolver

Considerable development efforts have been devoted in recent years to the utilization of SAW devices as matched filters for spread spectrum signals. Current state-of-the-art SAW convolvers exhibit time-bandwidth products ranging from 100 to 2000 depending on the material and fabrication technology employed. Basically, the convolution operation is obtained from the non-linear parameters of the piezoelectric substrate. The degree of non-linearity and the efficiency of the interaction between the two acoustic waves can be enhanced through several methods. The air gap convolver employs a semiconductor device, separated a small distance from the piezoelectric substrate, to enhance the non-linearity. This approach results in the highest performance to date but requires a complex and costly fabrication process and exhibits serious mechanical and temperature instabilities. At this point in time it appears that the SAW convolvers which

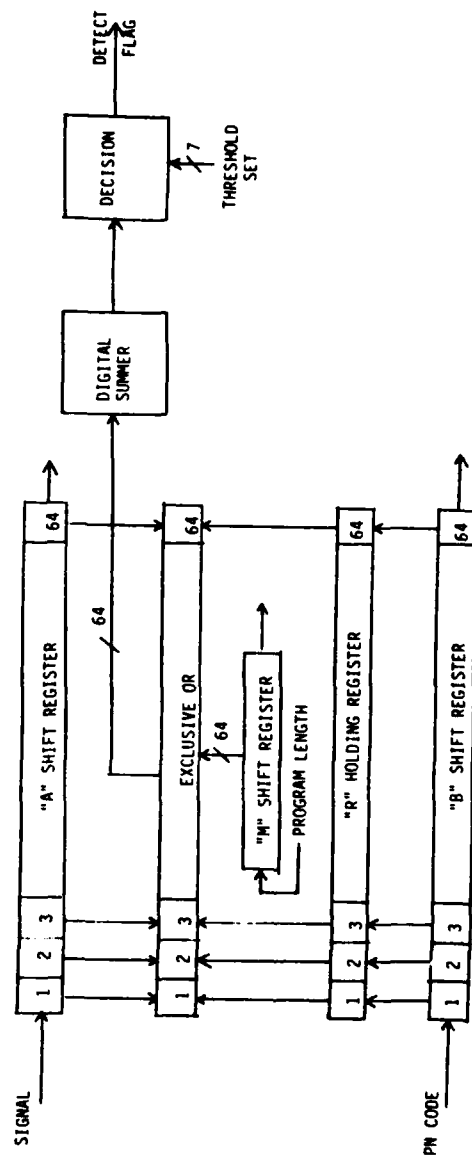


Figure 5.2-1. 64-Bit Digital Correlator

rely solely on the non-linear piezoelectric elastic parameters of the substrate for the non-linear interaction (the so-called elastic convolvers) are better suited to military applications.

The performance of the basic elastic convolver can be improved by compressing the acoustic waves prior to their reaching the convolution region. A simplified diagram of such a SAW-Beam Width Compression Convolver (SAW-BWCC) is shown in Figure 5.3-1. Beam width compression of 15:1 has been achieved with significant resulting improvement in efficiency and dynamic range. The efficiency of the non-linear interaction is a function of the ratio of length L to width W of the convolution region. More importantly from a spread spectrum processing gain viewpoint is that the integration time is directly proportional to the length L, with a current maximum of about 10 microseconds. Two techniques presently used for beam width compression are parabolic horn focusing with aluminum metal film on the substrate and multiple strip couplers (MSC) parallel to the input transducers. The parabolic horn approach results in somewhat better bandwidth and center frequency characteristics but also typically requires about ten times greater overall physical length. Table 5.3-1 summarizes performance characteristics of the current SAW convolvers. SAWTECH claims the capability of fabricating a SAW-BWCC using MSC beam compression with 300 MHz center frequency, 100 MHz bandwidth and 10 microseconds integration time.

5.3.1 Effects of Doppler and Random Phase Variations

The input to the convolver is represented by $f(t)e^{j\omega_1 t}$, while $g(t)e^{j\omega_2 t}$ represents the locally generated reference signal, as shown in Figure 5.3.1-1. The waveform at any time t and position x can be represented by [1]

$$\bar{dV} = (\bar{E}_1 + \bar{E}_2)(\bar{E}_1 + \bar{E}_2)^* \quad (5.3.1-1)$$

assuming a second order nonlinearity. \bar{E}_1 and \bar{E}_2 are given by the real parts of the following:

$$\bar{E}_1 = f\left(t - \frac{x}{v}\right)e^{j(\omega_1 t - k_1 x)} \quad \bar{E}_2 = g\left(t + \frac{x}{v}\right)e^{j(\omega_2 t + k_2 x)}$$

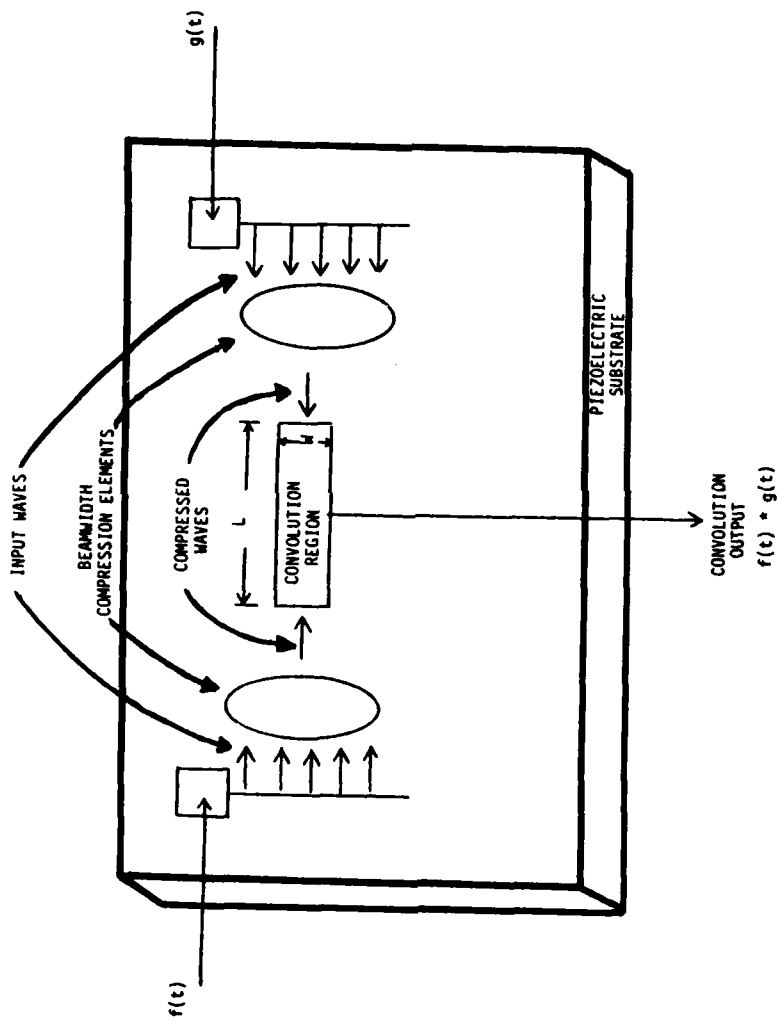


Figure 5.3-1. SAW Beamwidth Compression Convolver

TABLE 5.3-1. CURRENT MATCHED FILTER TECHNOLOGY

Device	Construction	Bandwidth (MHz)	Time Delay (μ seconds)	F_o (MHz)	Dynamic Range (dB)	Efficiency (dBm)	Comments
Si/LiNbO ₃	Air Gap	100	20	300	50	-65	<ul style="list-style-type: none"> • State-of-the-Art • High Performance • Currently Developed in Industry • Very High Cost • Mechanical/Temperature Instability • Complex Fabrication
LiNbO ₃	Monolithic	9	12	105	50	-84	<ul style="list-style-type: none"> • Simple Fabrication • Monolithic • Low Performance
LiNbO ₃	Monolithic MSC	50	12	156	65	-71	<ul style="list-style-type: none"> • Easy Fabrication • Monolithic • Low Cost • Mechanically Stable • Medium Performance
BMCC	Monolithic Horn	95	10	300	50	-80	<ul style="list-style-type: none"> • Mechanically Stable • Medium Performance
Si/ZnO	Monolithic	50	3	120	-	-58	<ul style="list-style-type: none"> • Multi-Level Fabrication • Monolithic • Low Cost • Still in Early Development • It is not Clear that it Can Compete with LiNbO₃ - BMCC

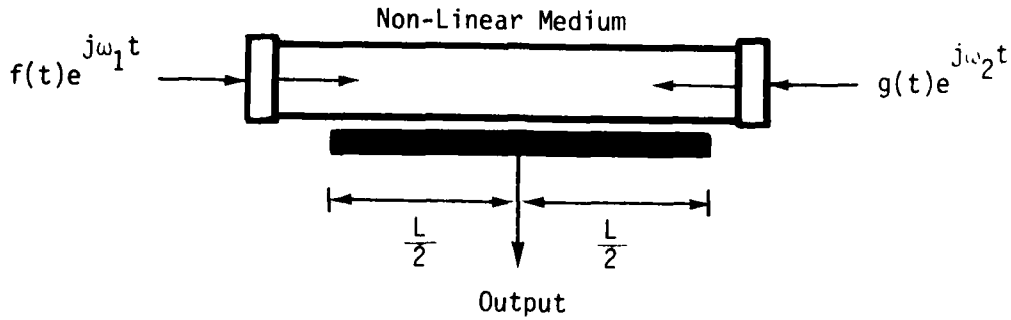


Figure 5.3.1-1.
SAW Convolver

In these two equations, k_1 and k_2 represent propagation constants given by:

$$k_1 = \frac{\omega_1}{v} \quad k_2 = \frac{\omega_2}{v}$$

The quantities ω_1 and ω_2 represent the input and reference frequencies to the convolver respectively. The velocity of propagation in the acoustic material is given by v . Performing the indicated multiplication produces the following results

$$\begin{aligned} \overline{dV} &= \left\{ f\left(t-\frac{x}{v}\right) \left[\frac{e^{j(\omega_1 t - k_1 x)} + e^{-j(\omega_1 t - k_1 x)}}{2} \right] + g\left(t+\frac{x}{v}\right) \left[\frac{e^{j(\omega_2 t + k_2 x)} + e^{-j(\omega_2 t + k_2 x)}}{2} \right] \right\} \\ &\times \left\{ f\left(t-\frac{x}{v}\right) \left[\frac{e^{-j(\omega_1 t - k_1 x)} + e^{j(\omega_1 t - k_1 x)}}{2} \right] + g\left(t+\frac{x}{v}\right) \left[\frac{e^{-j(\omega_2 t + k_2 x)} + e^{j(\omega_2 t + k_2 x)}}{2} \right] \right\} \\ \overline{dV} &= \frac{\left[f\left(t-\frac{x}{v}\right) \right]^2}{2} + \frac{\left[g\left(t+\frac{x}{v}\right) \right]^2}{2} + \frac{f\left(t-\frac{x}{v}\right)^2}{2} \cos \left[2\omega_1 t - 2k_1 x \right] + \frac{g\left(t+\frac{x}{v}\right)^2}{2} \cos \left[2\omega_2 t + 2k_2 x \right] \\ &+ f\left(t-\frac{x}{v}\right) g\left(t+\frac{x}{v}\right) \cos \left[(\omega_1 - \omega_2)t - (k_1 + k_2)x \right] + f\left(t-\frac{x}{v}\right) g\left(t+\frac{x}{v}\right) \cos \left[(\omega_1 + \omega_2)t - (k_1 - k_2)x \right] \end{aligned} \tag{5.3.1-2}$$

In this expression, the only term of interest is the following:

$$f\left(t-\frac{x}{v}\right) g\left(t+\frac{x}{v}\right) \cos \left[(\omega_1+\omega_2)t - (k_1-k_2)x \right].$$

There are two methods that can be used to detect this sum frequency term. If ω_1 is not equal to ω_2 then an interdigital transducer with a finger pair spacing, d , is capable of responding to a signal with a propagation constant

$$k_d = \frac{\omega_1 - \omega_2}{v}$$

such that $k_d d = 2\pi$.

If on the other hand ω_1 equals ω_2 , then the waveform does not vary with x and can be detected between metal films laid down on the top surface and lower surface of the piezoelectric substrate. This is the configuration of most interest in the acquisition process, where a reference waveform is varied until it exactly matches the incoming signal.

The metal film laid down on the substrate performs a spatial integration of the resultant signals. This yields the following expression at the output of the convolver.

$$y(t) = \int_{-\frac{L}{2}}^{\frac{L}{2}} f\left(t-\frac{x}{v}\right) g\left(t+\frac{x}{v}\right) \cos \omega_s t \, dx \quad (5.3.1-3)$$

where

$$\omega_s = \omega_1 + \omega_2.$$

By making a change of variable the detected output can be represented by:

$$\text{Let } t - \frac{x}{v} = \tau$$

$$y(t) = v \int_{t-\frac{L}{2v}}^{t+\frac{L}{2v}} f(\tau) g(2t-\tau) \, d\tau \quad (5.3.1-4)$$

This represents the conventional convolutional integral.

Suppose now that the input signal is received having undergone a doppler shift. How is the output of the convolver affected? Since ω_1 is not equal to ω_2 then k_d is not equal to zero. The convolver output can now be expressed as:

$$y(t) = \int_{-\frac{L}{2}}^{\frac{L}{2}} f\left(t - \frac{x}{v}\right) g\left(t + \frac{x}{v}\right) \cos\left[\omega_s t - k_d x\right] dx \quad (5.3.1-5)$$

For purposes of illustration, assume $f(t)$ and $g(t)$ are 10 microsecond pulses that have undergone a doppler shift. The above integral reduces to the following.

$$\begin{aligned} y(t) &= \int_{tv - \frac{T_i v}{2}}^{\frac{T_i v}{2} - tv} \cos\left[\omega_s t - k_d x\right] dx \\ &= \cos \omega_s t \int_{tv - \frac{T_i v}{2}}^{\frac{T_i v}{2} - tv} \cos k_d x \, dx + \sin \omega_s t \int_{tv - \frac{T_i v}{2}}^{\frac{T_i v}{2} - tv} \sin k_d x \, dx \end{aligned}$$

Since the limits of integration are symmetrical and $\sin k_d x$ is an odd function, this term will integrate to zero, leaving only the $\cos k_d x$ term. Evaluating the resulting expression, the convolver output is given by:

$$y(t) = \frac{(T_i - 2t)v \sin \pi f_d (T_i - 2t)}{\pi f_d (T_i - 2t)} \cos \omega_s t \quad (5.3.1-6)$$

In this example the input signal is symmetrical so that the convolution integral also represents the autocorrelation function. This can be seen for the case of no doppler as shown in Figure 5.3.1-1A. The output is the familiar triangle function, which is the autocorrelation function for a square pulse. Figure 5.3.1-2 shows the output for a 10 kHz doppler. The output is normalized with the value at no doppler. The basic shape of the waveform does not change and the peak amplitude is reduced only slightly. Figure 5.3.1-3 shows the output for a 50 kHz doppler. The waveform is becoming rounded which makes it more difficult to determine when the two waveforms are in alignment. Note that there is also a significant decrease in the amplitude of the output. As the doppler is increased a point is reached where the peak is no longer at the origin. Figure 5.3.1-4 clearly shows this for a doppler of 80 kHz. Here the doppler causes the convolver output to peak at t equal to $2 \mu\text{s}$ giving a false indication of alignment.

The loss in convolver peak output versus doppler is plotted in Figure 5.3.1-5. The 3 dB point is about 60 kHz for this example.

Suppose now that in addition to doppler the input signal contains a random phase term. How is convolver performance affected? Going back to the original equations, the input vector E_1 is now represented as shown.

$$\bar{E}_1 = f\left(t - \frac{x}{v}\right) e^{j(\omega_1 t - \phi - k_1 x)} . \quad (5.3.1-7)$$

The reference input $g(t)$ is assumed to be a perfect replica of the input without the random phase term. If the same process is repeated as before with the new \bar{E}_1 then the sum frequency term of interest can be represented as follows:

$$y(t) = \int_{-\frac{L}{2}}^{\frac{L}{2}} f\left(t - \frac{x}{v}\right) g\left(t + \frac{x}{v}\right) \cos\left[\omega_s t + \phi - k_d x\right] dx . \quad (5.3.1-8)$$

The cosine term can be expanded to simplify the expression.

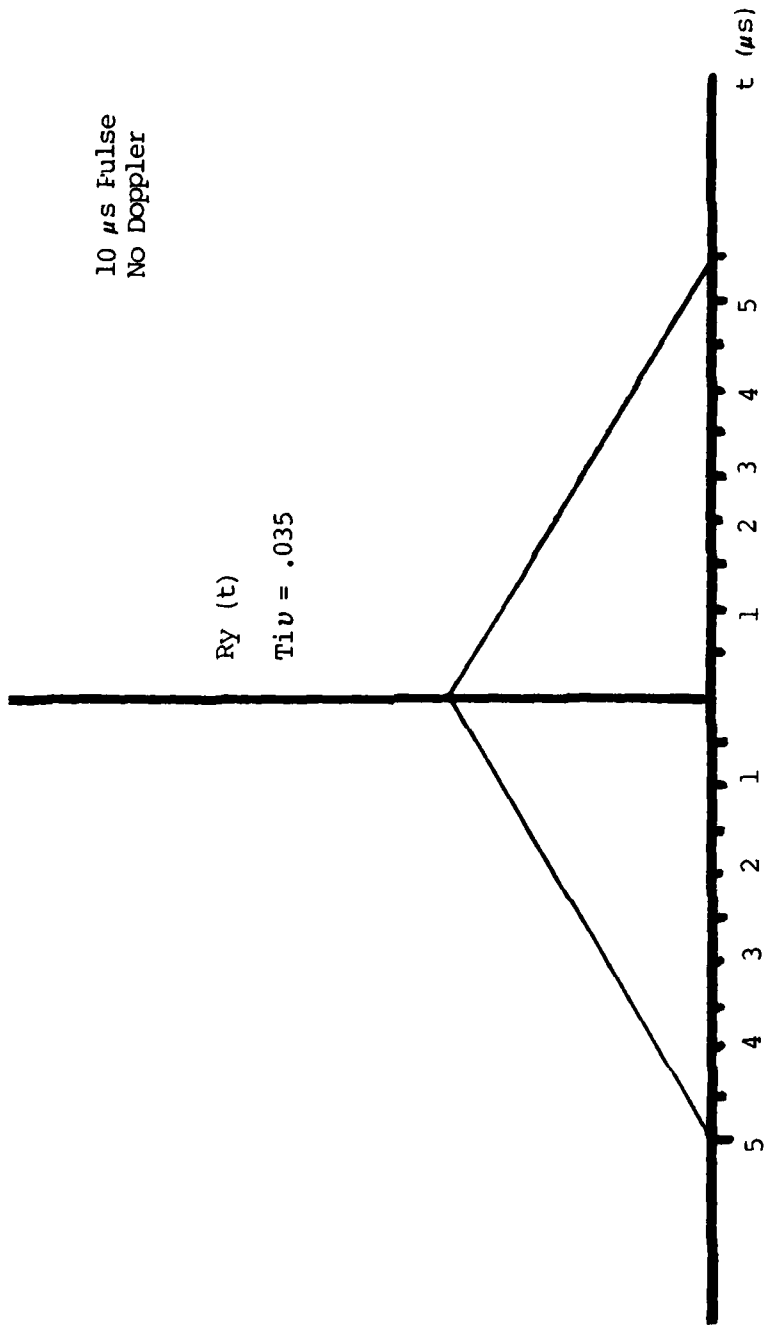


Figure 5.3.1-1A.
 Normalized Function for Output of Convolver with the Input
 and Reference Waveforms Being 10 μ s Pulses

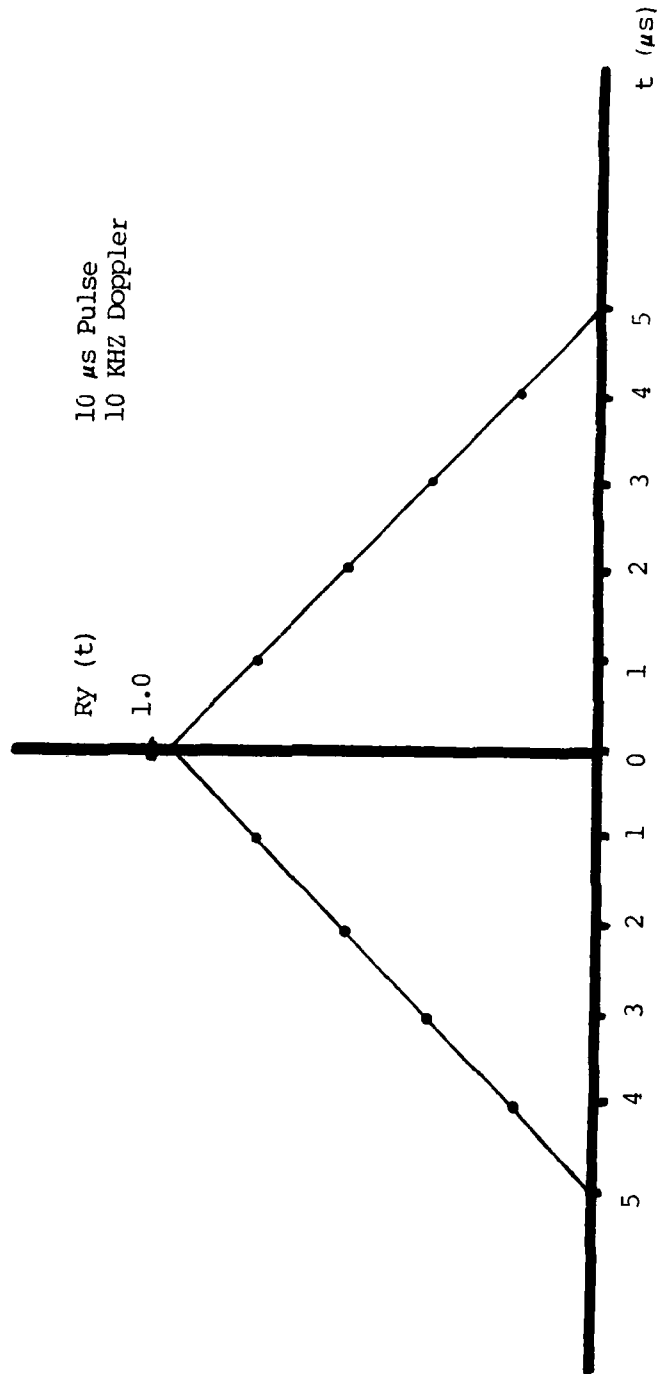


Figure 5.3.1-2.
Normalized Correlation Function for Output of Convolver with the Input
and Reference Waveforms Being 10 μ s Pulses with 10 KHZ of Doppler

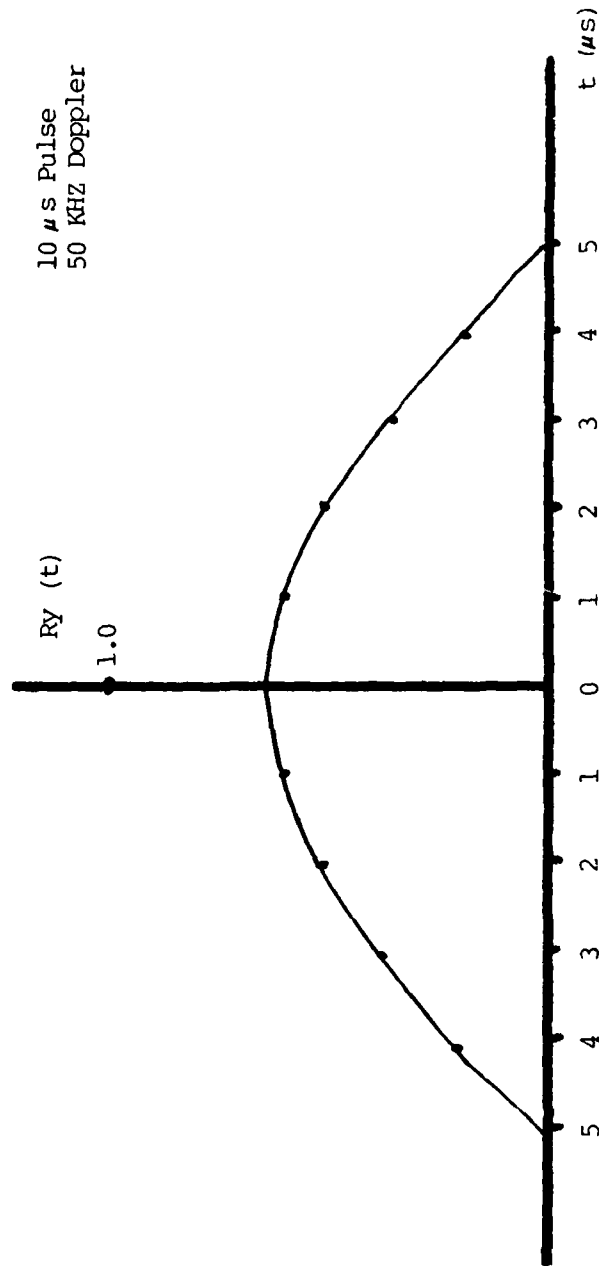


Figure 5.3.1-3.

Normalized Correlation Function for Output of Convolver with the Input
and Reference Waveforms Being 10 μ s Pulses with 50 KHz of Doppler

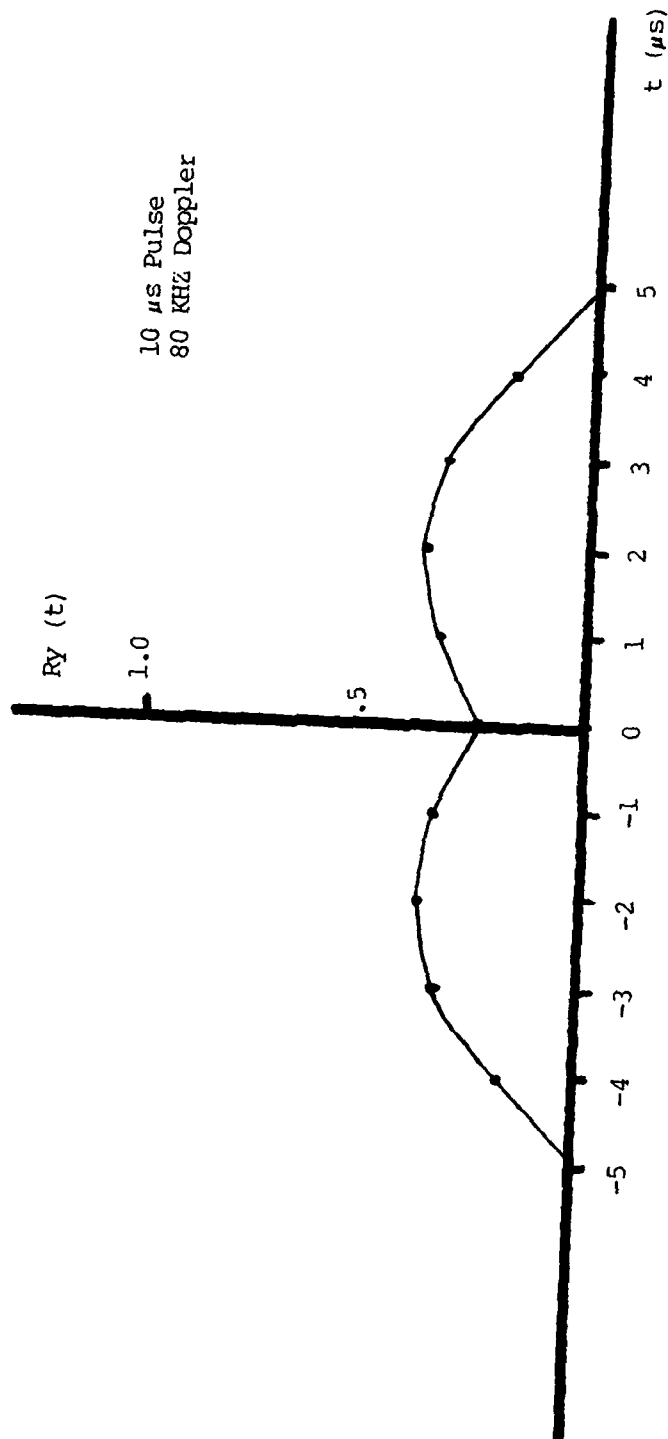


Figure 5.3.1-4,
Normalized Correlation Function for Output of Convolver with the Input
and Reference Waveforms Being 10 μ s Pulses with 50 KHz of Doppler

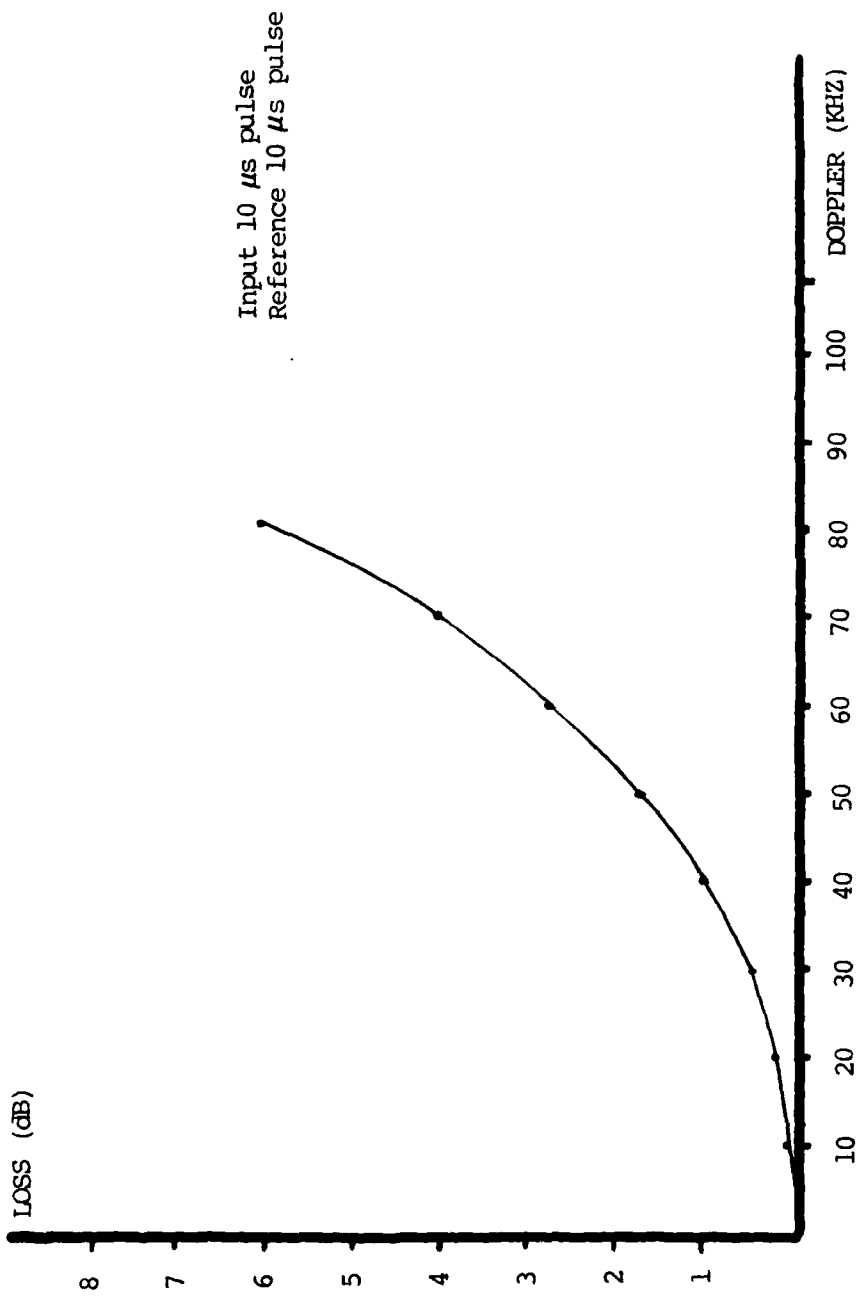


Figure 5.3.1-5.

Loss in Convolver Peak Output Due to Doppler for the Input and Reference Waveforms being 10 μ s Pulses.

$$y(t) = \int_{-\frac{L}{2}}^{\frac{L}{2}} f\left(t-\frac{x}{v}\right) g\left(t+\frac{x}{v}\right) \cos\left[\left(\omega_s t - k_d x\right) \cos \phi - \sin\left(\omega_s t - k_d x\right) \sin \phi\right] dx .$$

Since the limits of integration are symmetrical and $\sin(\omega_s t - k_d x)$ is an odd function, it will integrate to 0. This leaves the following expression for the output of the convolver.

$$y(t) = \cos \phi \int_{-\frac{L}{2}}^{\frac{L}{2}} f\left(t-\frac{x}{v}\right) g\left(t+\frac{x}{v}\right) \cos\left[\omega_s t - k_d x\right] dx . \quad (5.3.1-9)$$

This is recognized as the same expression that was developed previously multiplied by the cosine of the random variable. For the case of a square wave input with doppler and random phase, the output can be written immediately as:

$$y(t) = \frac{(T_i - 2t)v \sin \pi f_d (T_i - 2t)}{\pi f_d (T_i - 2t)} \cos \phi \cos \omega_s t \quad (5.3.1-10)$$

The expression for the output now contains a random variable. Therefore a meaningful description of the output is given by the mean and mean square value. The mean value is given as follows; assuming the random variable ϕ is uniformly distributed between 0 and 2π .

$$\begin{aligned} E[y(t)] &= E\left\{ \frac{(T_i - 2t)v \sin \pi f_d (T_i - 2t)}{\pi f_d (T_i - 2t)} \cos \phi \cos \omega_s t \right\} \\ &= \frac{(T_i - 2t)v \sin \pi f_d (T_i - 2t)}{\pi f_d (T_i - 2t)} \overline{\cos \phi} \cos \omega_s t \end{aligned}$$

$$= \frac{(T_i - 2t)v \sin \pi f_d (T_i - 2t) \cos \omega_s t}{\pi f_d (T_i - 2t)} \frac{1}{2\pi} \int_0^{2\pi} \cos \phi \, d\phi$$

(5.3.1-11)

$$E[y(t)] = 0.$$

The mean value of the output is zero. Now determine the mean square value. This is given as follows:

$$E[y^2(t)] = \left[\frac{(T_i - 2t)v \sin \pi f_d (T_i - 2t)}{\pi f_d (T_i - 2t)} \cos \omega_s t \right]^2 \frac{1}{2\pi} \int_0^{2\pi} \cos^2 \phi \, d\phi.$$

The $\cos^2 \phi$ term can be expressed as $\frac{1 - \cos 2\phi}{2}$.

The $\cos 2\phi$ term will integrate to zero leaving the following expression for the mean square value of the output.

$$E[y^2(t)] = \frac{\left[\frac{(T_i - 2t)v \sin \pi f_d (T_i - 2t)}{\pi f_d (T_i - 2t)} \right]^2}{2} \cos^2 \omega_s t \quad (5.3.1-12)$$

This expression is evaluated for various values of doppler as shown in Figure 5.3.1-6 thru Figure 5.3.1-9. The affects caused by doppler and random phase are similar to those caused by doppler alone. The peak output decreases and the waveform gradually changes shape until the peak is no longer at the origin but moves to t equals $2 \mu s$ as shown in Figure 5.3.1-9. Figure 5.3.1-10 is a plot of the loss in convolver mean square output due to doppler and random phase variations versus doppler. Notice the 3 dB loss now occurs at about 43 kHz where as for doppler alone it occurs at about 60 kHz.

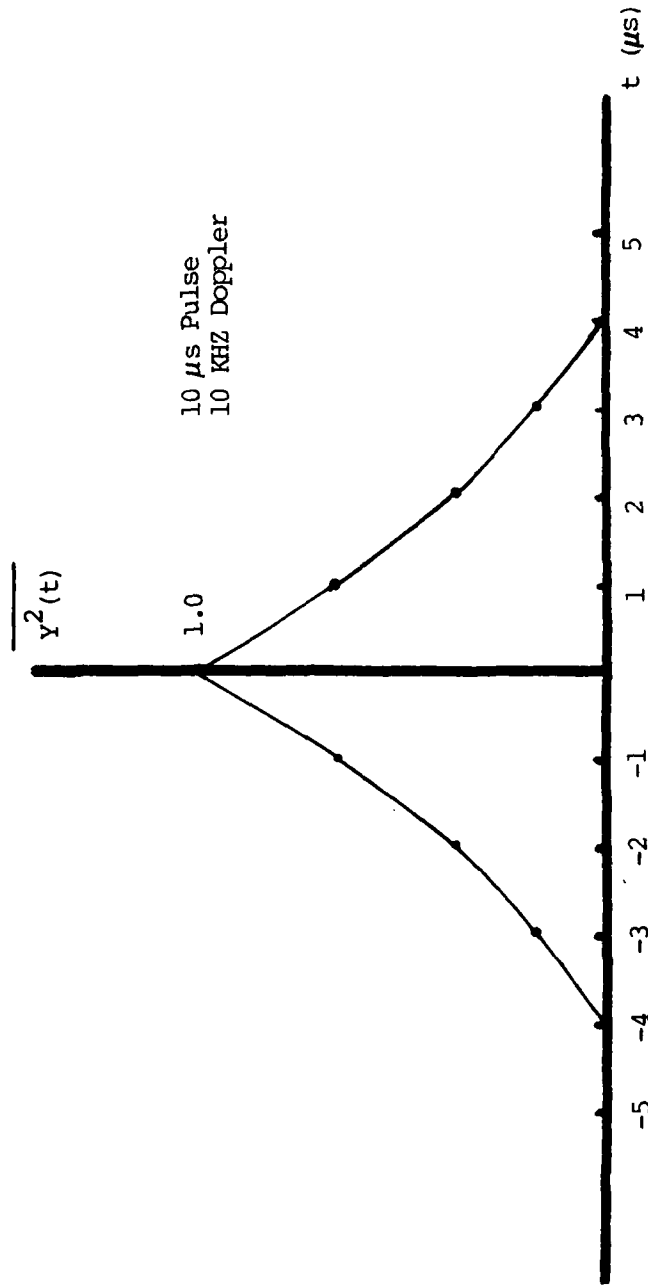


Figure 5.3.1-6.

Normalized Mean Square Value of Convolver Output with Random Phase Input

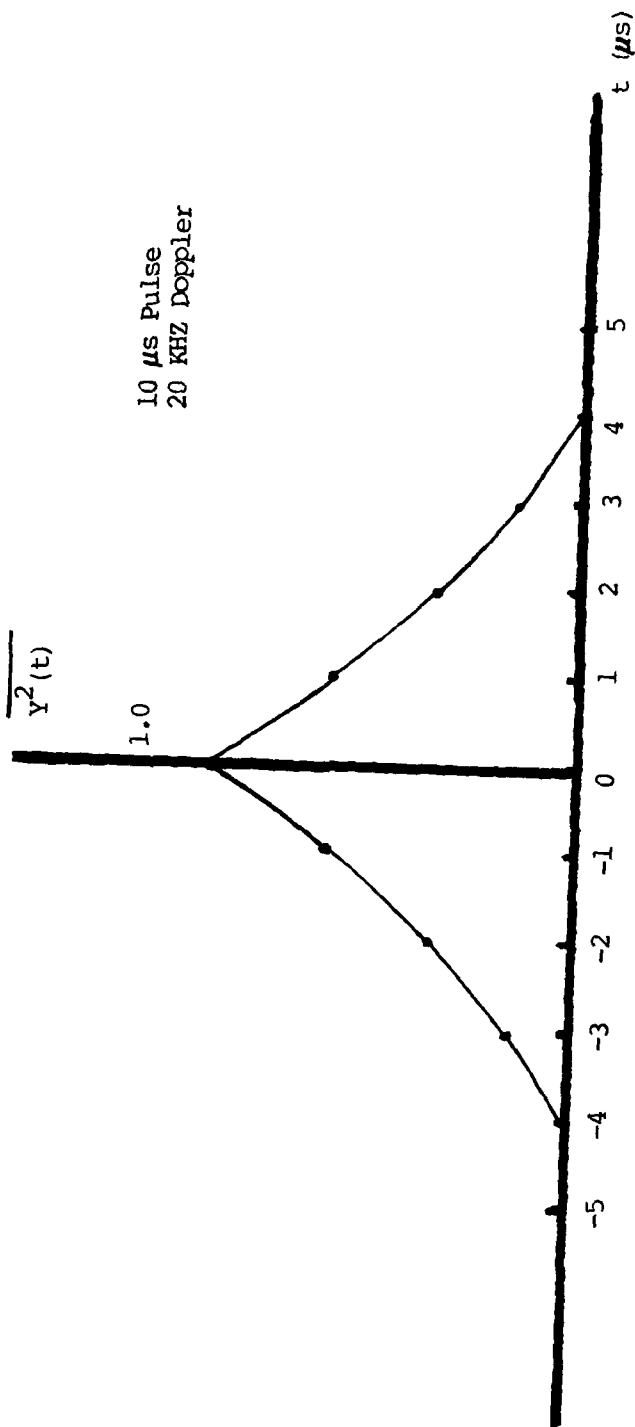


Figure 5.3.1-7.
Normalized Mean Square Value of Convolver Output with Random Phase Input

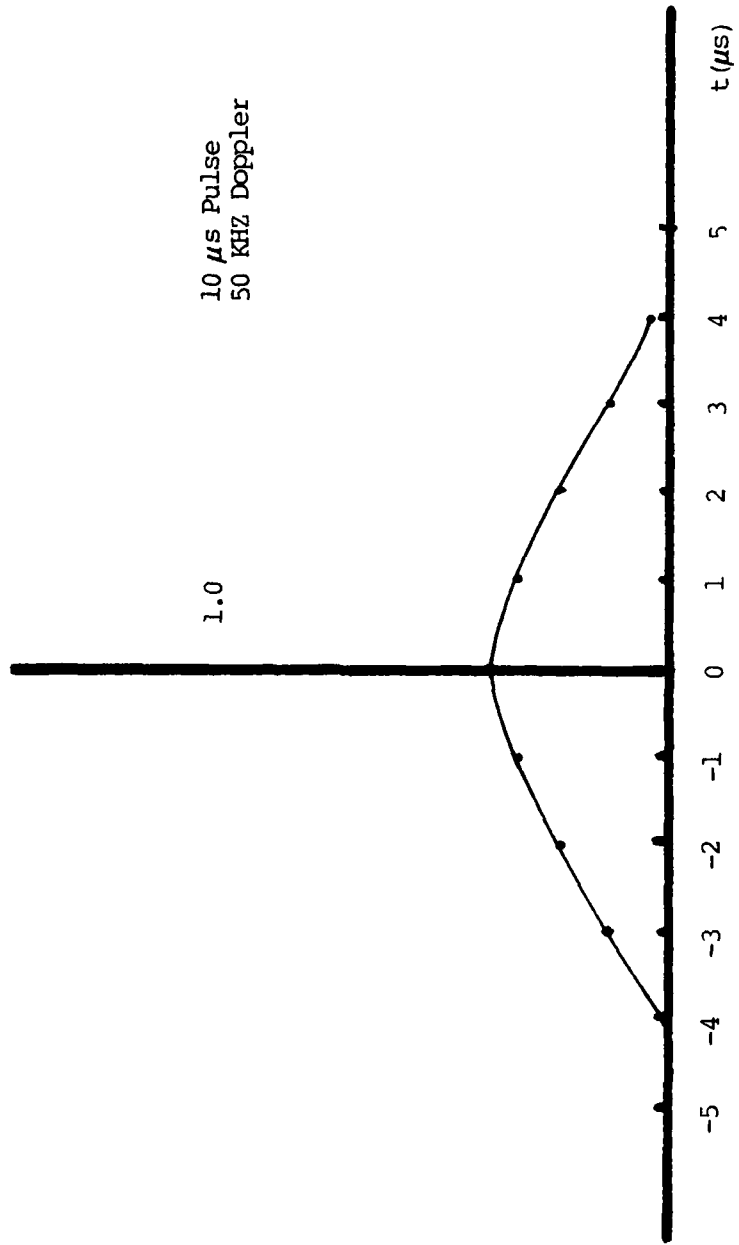


Figure 5.3.1-8.
Normalized Mean Square Value of Convolver Output with Random Phase Input

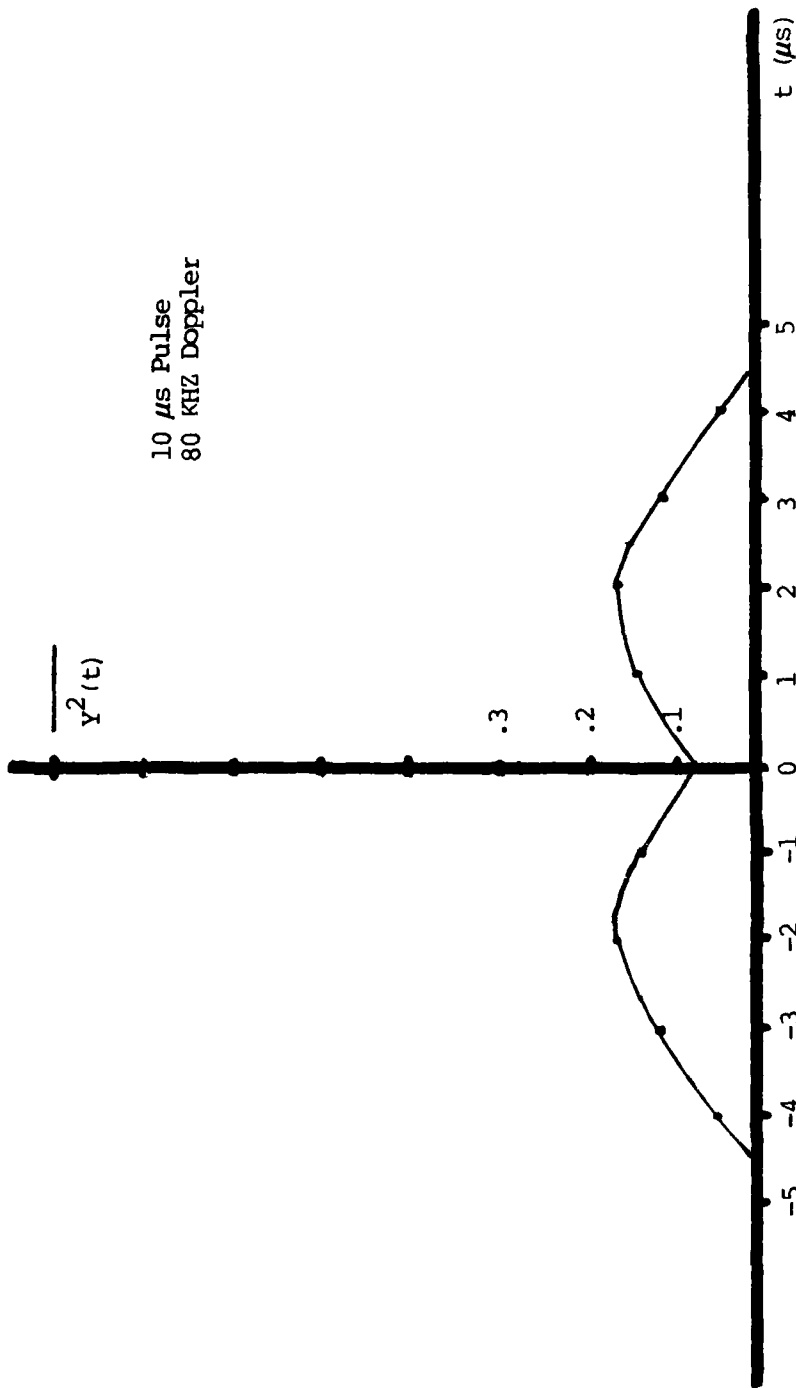


Figure 5.3.1-9.
Normalized Mean Square Value of Convolver Output with Random Phase Input

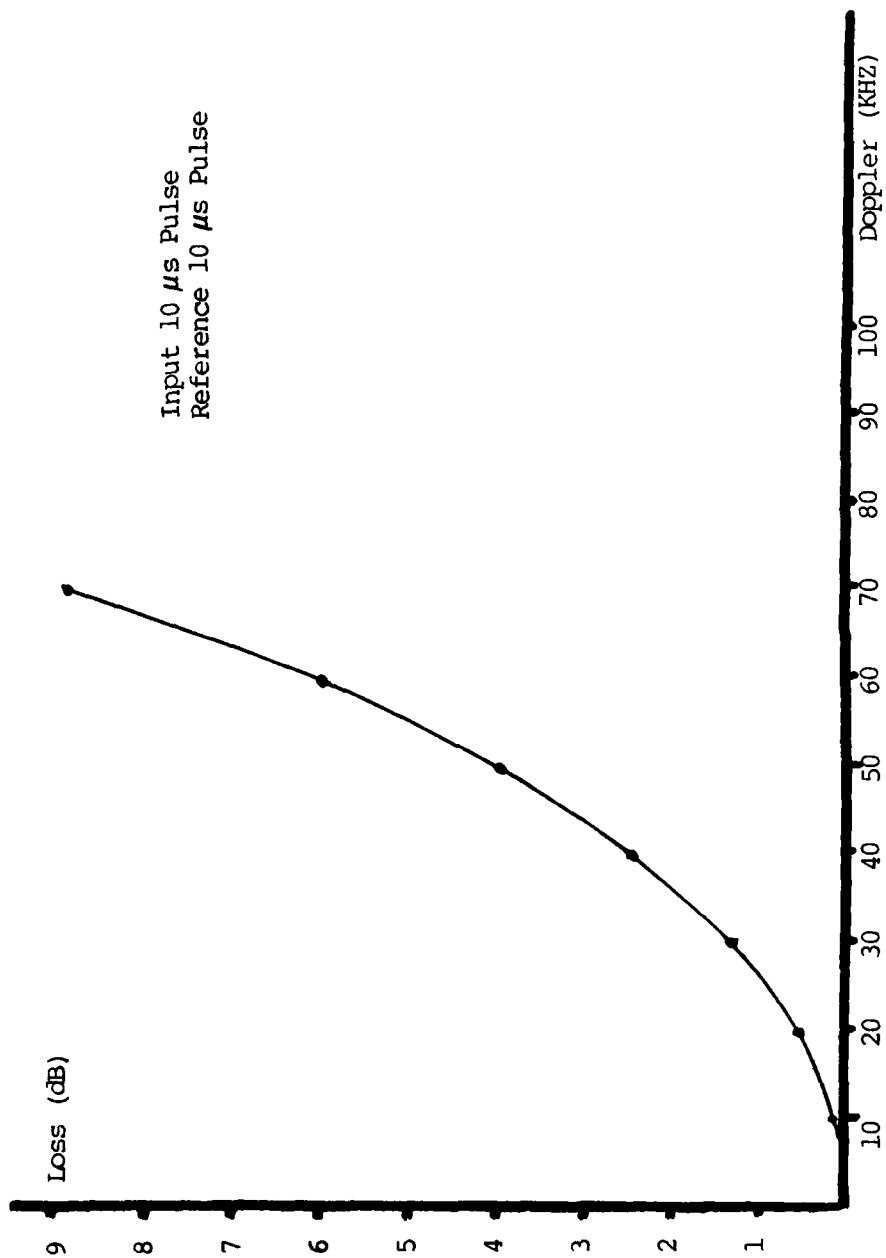


Figure 5.3.1-10.

Loss in Convolver Mean Square Output Due to Doppler and Random Phase Variations

5.4 Hybrid Array Correlator

A correlator device which provides two performance advantages over the standard digital correlator is presently being developed at Harris GISP. The first performance advantage accrues from the fact that the device operates on analog rather than digital signals so that the degradation associated with one bit quantization common to the digital correlator is avoided. The second performance advantage is that multiple correlators, operating in parallel, are implemented on a single LSI chip. The current design is capable of PN rates up to 20 megachips/second, with growth to 50 to 100 megachips/second anticipated, and contains 64 correlators. A simplified functional diagram of this Hybrid Array Correlator (HAC) is shown in Figure 5.4-1. As illustrated by this figure, the HAC is a bank of multiply-and-integrate correlators which forms, in parallel, the correlation between the baseband analog signal and each of the delayed versions of the PN reference. The delays are actually achieved by a 64 stage shift register which is shifting the PN reference at twice the chip rate. Thus, with the resulting $\frac{1}{2}$ chip offset between correlation cells the outputs of the 64 correlators represent the simultaneous search over 32 chip positions in $\frac{1}{2}$ chip steps. The multiplexed output is therefore the time sampled profile, over 32 chips in $\frac{1}{2}$ chip steps, of the correlation between the input signal and the PN reference. For initial acquisition the HAC can be operated as a time invariant matched filter by circulating an advanced 32 chip segment of the PN reference through the shift register. When the correlation peak appears in the 32 chip window the PN reference timing is adjusted to place the correlation peak in the center of the array and the shift register is then loaded with the continuous PN reference sequence. PN code tracking is accomplished by simply observing the location of the correlation peak within the array and adjusting the local timing to keep the peak centered. Timing need be adjusted only often enough to keep the peak within the array, that is, to within ± 16 chips of the center.

The HAC actually contains dual in-phase and quadrature paths for both the input and PN reference signals, with each correlator cell containing four mixers. With

$d_I(t), d_Q(t)$ = In-phase and quadrature data

$I(t), Q(t)$ = In-phase and quadrature PN sequences

\emptyset = Phase offset between signal carrier and local oscillator

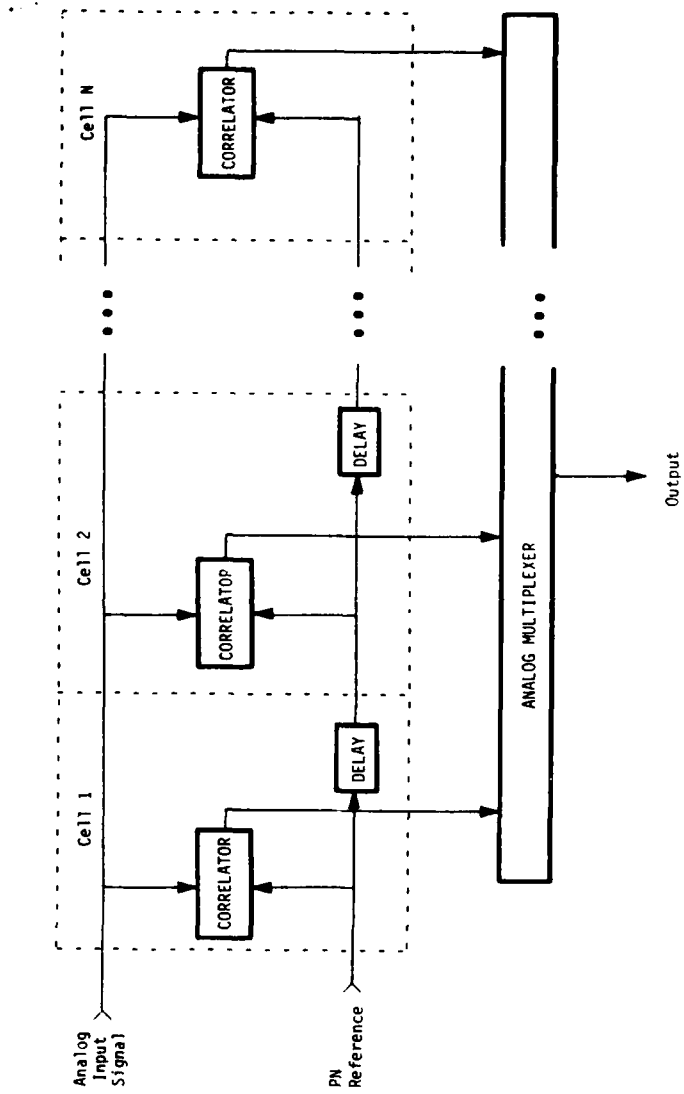


Figure 5.4-1. Hybrid Array Correlator Concept

the downconverted I and Q components are

$$S_I(t) = A d_I(t) I(t-\tau) \cos \theta + A d_Q(t) Q(t-\tau) \sin \theta$$

$$S_Q(t) = A d_Q(t) Q(t-\tau) \cos \theta - A d_I(t) I(t-\tau) \sin \theta$$

The four mixers multiply these signals by the local PN sequences to produce

$$\begin{aligned} X_1(t) &= S_I(t) I(t) \\ &= A d_I(t) I(t) I(t-\tau) \cos \theta + A d_Q(t) I(t) Q(t-\tau) \sin \theta \end{aligned}$$

$$\begin{aligned} X_2(t) &= S_Q(t) Q(t) \\ &= A d_Q(t) Q(t) Q(t-\tau) \cos \theta - A d_I(t) Q(t) I(t-\tau) \sin \theta \end{aligned}$$

$$\begin{aligned} X_3(t) &= S_Q(t) I(t) \\ &= A d_Q(t) I(t) Q(t-\tau) \cos \theta - A d_I(t) I(t) I(t-\tau) \sin \theta \end{aligned}$$

$$\begin{aligned} X_4(t) &= S_I(t) Q(t) \\ &= A d_I(t) Q(t) I(t-\tau) \cos \theta + A d_Q(t) Q(t) Q(t-\tau) \sin \theta \end{aligned}$$

These four signals are combined and integrated as appropriate to the signalling format. If the same data appears on both the I and Q channels, i.e.

$$d_I(t) = d_Q(t) = d(t)$$

then two integrators are used with inputs

$$X_1(t) + X_2(t)$$

and

$$X_4(t) - X_3(t)$$

with the resulting outputs

$$A = \int_0^T [X_1(t) + X_2(t)] dt$$

$$\cong 2 A d(t) R_{PN}(\tau) \cos \theta$$

and

$$B = \int_0^T [x_4(t) - x_3(t)] dt$$

$$\cong 2 A d(t) R_{PN}(\tau) \sin \theta$$

where $R_{PN}(\tau)$ is the common autocorrelation function of $I(t)$ and $Q(t)$. The configuration of each correlation cell for this case is illustrated in Figure 5.4-2. If the data on the I and Q channels are different then each cell can be configured with four integrators to produce

$$A = \int_0^T x_1(t) dt \cong A d_I(t) R_{PN}(\tau) \cos \theta$$

$$B = \int_0^T x_2(t) dt \cong A d_Q(t) R_{PN}(\tau) \cos \theta$$

$$C = - \int_0^T x_3(t) dt \cong A d_I(t) R_{PN}(\tau) \sin \theta$$

$$D = \int_0^T x_4(t) dt \cong A d_Q(t) R_{PN}(\tau) \sin \theta$$

Thus, the HAC approach is general enough to permit configuration to process BPSK, QPSK, OQPSK and MSK with either one or two data streams.

Although the underlying principle of the multiply-and-integrate correlator has been known and applied for many years, the design concepts incorporated in the HAC permit the implementation of many (i.e., 64) of these correlator cells on a single LSI chip. These design features include the use of on-off switches for mixers, the use of shift registers for obtaining the $\frac{1}{2}$ chip offset between the cells and the incorporation of analog multiplexer output circuits. The first two features are made possible by the use of binary reference signals. The use of binary references in the correlation operation

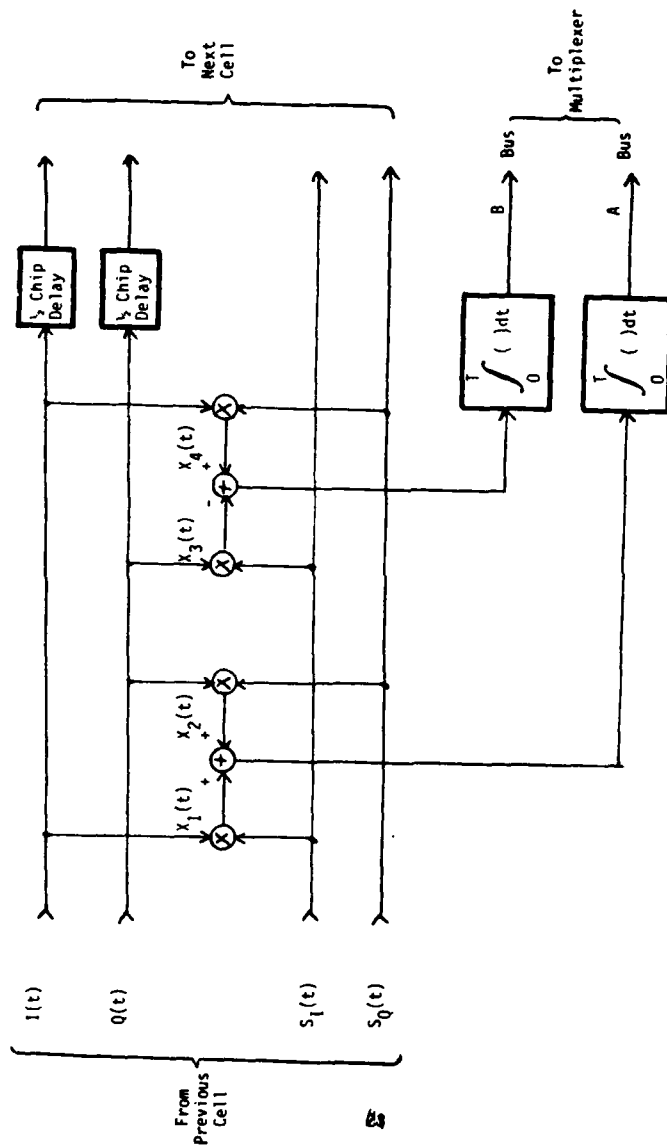


Figure 5.4-2. Correlator Cell of Hybrid Array Correlator

is appropriate for BPSK, QPSK and OQPSK since the data and PN sequences for these formats are transmitted as bipolar pulses. For other spreading forms, such as MSK, some correlation loss does occur by correlating with a two-level reference but generally this loss is on the order of a few tenths of a dB. The analog output multiplexer feature provides a convenient means of reducing the number of output pins to a practical number. As presently conceived the complete 64-cell HAC will be contained in a single 24-pin IC package.

SECTION 6.0

DIRECT SERIAL SEARCH VS. MATCHED FILTER SEARCH

6.0 DIRECT SERIAL SEARCH VS. MATCHED FILTER SEARCH

In this section direct serial search and matched filter search techniques are examined in such a manner as to highlight the procedural and performance differences between these two acquisition processes. DS spreading is assumed in order to minimize implementation complexities which would tend to obscure the key issues.

In a DS spread spectrum system the processing gain is generally defined as the ratio of the PN chip rate r_c to bit rate r_b , which is equal to the number of PN chips per bit, $N_{c/b}$.

$$P_{gDS} = \frac{r_c}{r_b} = N_{c/b} .$$

This processing gain is usually realized in the receiver by a multiply and integrate correlator as shown in Figure 6.0-1.

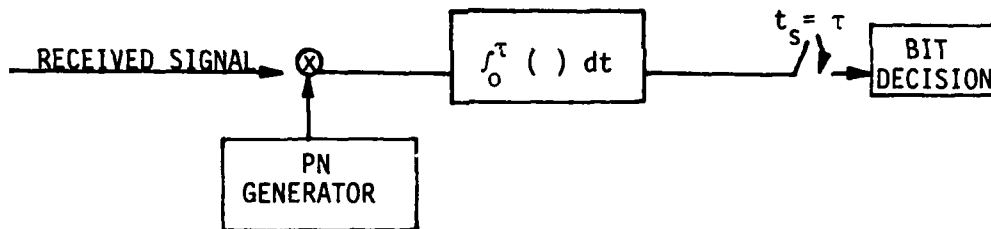


Figure 6.0-1. Multiply and Integrate Correlator Receiver

where the integration time τ is the bit length

$$\tau = T_b = 1/r_b .$$

Thus the processing gain is achieved by integrating over a length of time which contains $N_{c/b}$ chips.

A similar process is used in the direct serial search method of PN code acquisition illustrated in Figure 6.0-2.

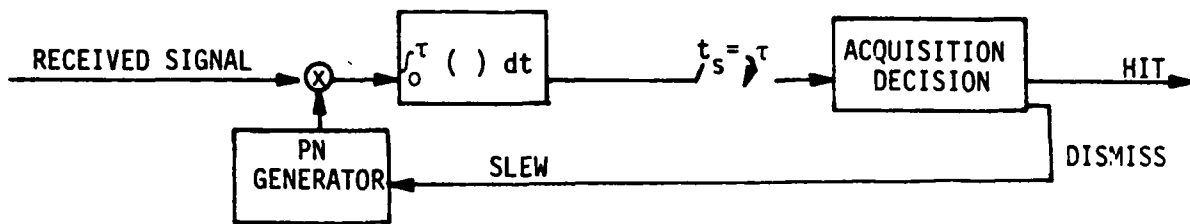


Figure 6.0-2. Direct Serial Search

If the same processing gain is required for acquisition as for data demodulation then the product of the received signal and local PN reference is integrated for τ seconds ($N_{c/b}$ chips) and the result used for making an acquisition decision, usually by a threshold device. If a "hit" occurs, a validation procedure is initiated; if a "no hit" decision occurs the PN reference is slewed $\frac{1}{2}$ -chip and the process repeated. The basic limitation to search speed is that the correlator integrates over a completely new set of $N_{c/b}$ chips of the received signal for each test. Thus the search rate is

$$\begin{array}{l} \text{Search Rate for} \\ \text{Direct} \\ \text{Serial Search} \end{array} = \frac{r_c}{N_{c/b}} = r_b, \frac{1}{2}\text{-chip positions per second.}$$

The search rate can be significantly increased by replacing the multiply and integrate correlator by an MF device. Acquisition of DS by an MF is best illustrated by considering a digital correlator of Figure 6.0-3. The received signal is sampled and digitized (to one bit) at twice the chip rate and serially loaded into a shift register. An advance segment of the PN reference is loaded into a holding register. The contents of the two registers are correlated by comparing the contents of the corresponding stages, generating a "+1" if the contents match and a "-1" if they do not, and summing the results. The correlation value is tested at the clock rate (which is twice the PN chip rate) so that the search rate for this method is

$$\begin{array}{l} \text{Search Rate for} \\ \text{MF} \end{array} = 2 r_c, \frac{1}{2}\text{-chip positions per second.}$$

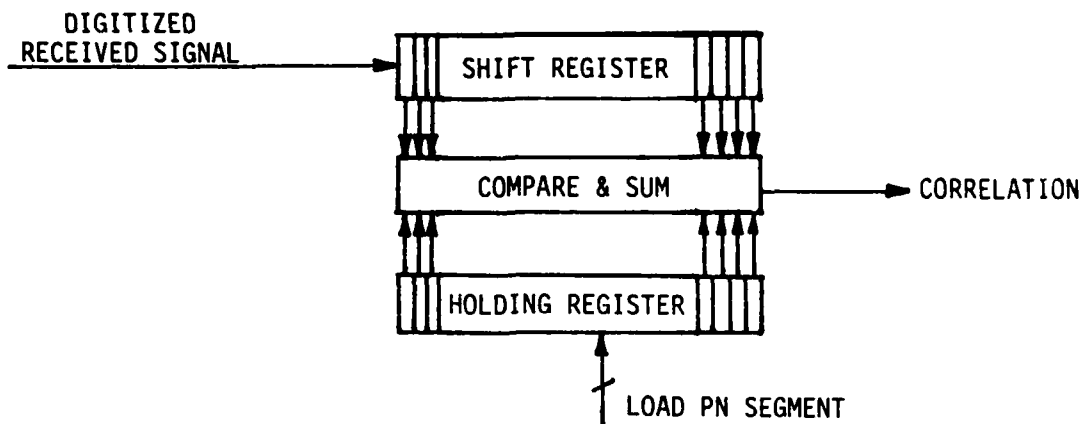


Figure 6.0-3. MF For DS Acquisition

This indicates a reduction in search time over the direct serial search method by

$$\begin{aligned} \frac{\text{Matched Filter Search Rate}}{\text{Direct Serial Search Rate}} &= \frac{2r_c}{r_b} \\ &= 2 N_{c/b} \\ &= 2 p_{gDS} \end{aligned}$$

Therefore if a processing gain of 30 dB is required during acquisition then the MF reduces the time to search over the total uncertainty region by a factor of 2000. The improvement in search time is a consequence of the fact that only a new $\frac{1}{2}$ -chip of received signal is required for each correlation test since prior samples are already stored in the shift register. (As a practical note, the processing gain of an MF is proportional to its length and at present no digital correlator is available which will provide 30 dB of processing gain in a single package.)

A basic difference in receiver operations for the multiply and integrate and MF methods is that in the multiply and integrate receiver the local PN generator is running continuously, whereas in the MF receiver the PN segment

in the holding register is fixed. The multiply and integrate acquisition process may be visualized as having both the received and local PN sequences moving together at the chip rate, with $\frac{1}{2}$ -chip shifts in the relative phase introduced every τ seconds. These $\frac{1}{2}$ -chip shifts are continued until alignment of the two sequences occurs. In the MF receiver the local PN reference is stationary and the received PN sequence slides past until alignment occurs, at which time the local PN generator is enabled. These processes are illustrated in Figure 6.0-4.

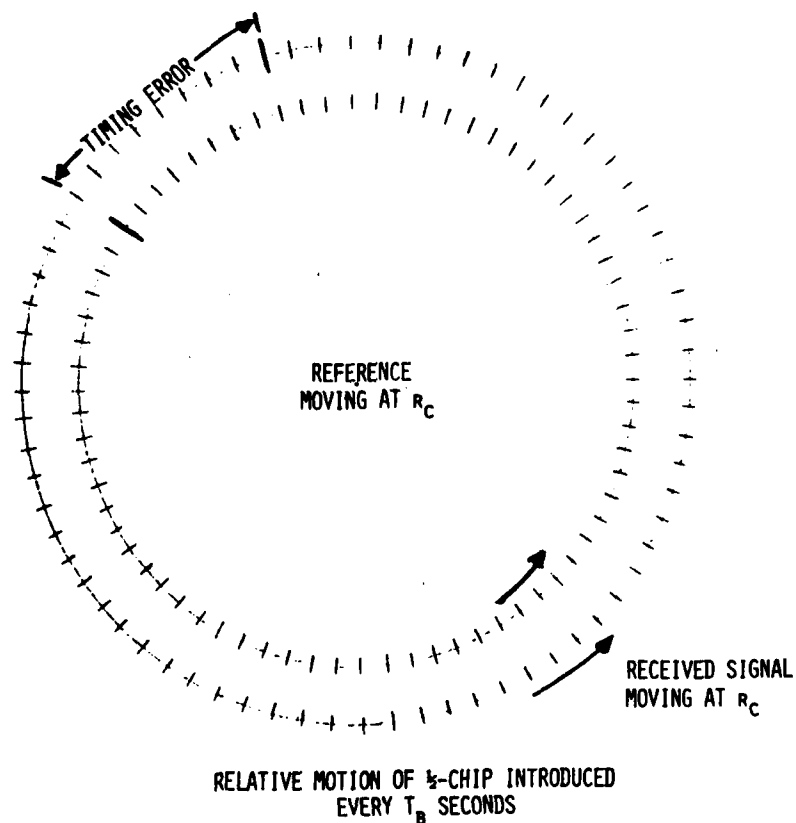


Figure 6.0-4(a). Direct Serial Search

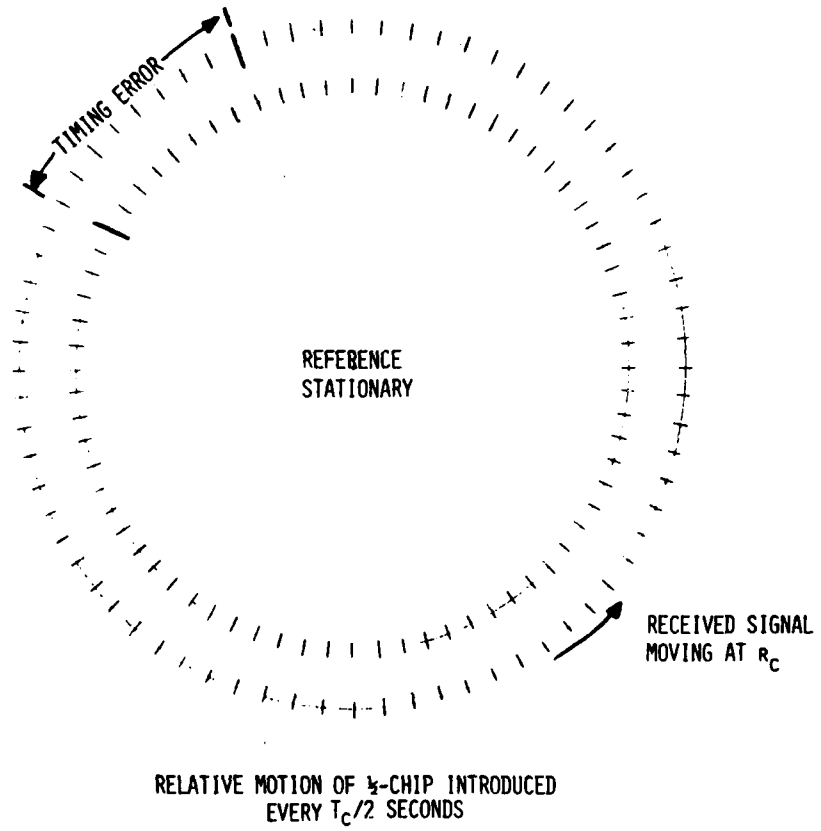


Figure 6.0-4(b). Matched Filter Search

FIGURE 7.0
COMPARISON OF DS, FH AND FH/DS

7.0 COMPARISON OF DS, FH AND FH/DS

In Section 6.0 acquisition performance was examined as a function of the structure of the receiver's acquisition system, i.e., direct search versus MF. In this section acquisition performance is examined as a function of the type of spreading function employed.

7.1 Direct Sequence

The results of Section 6.0 can be used directly in characterizing DS acquisition performance relative to the other forms. For the direct search method the search rate is the data rate,

$$\begin{array}{l} \text{Search Rate for} \\ \text{Direct Search} \end{array} = r_b, \frac{1}{2}\text{-chip position per second}$$

whereas for the MF method the search rate is twice the PN chip rate,

$$\begin{array}{l} \text{Search Rate} \\ \text{for MF} \end{array} = 2 r_c, \frac{1}{2}\text{-chip position per second.}$$

In both methods the search is normally conducted in $\frac{1}{2}$ -chip increments so that when synchronization is achieved timing uncertainty between the transmitter and receiver is resolved to within $\frac{1}{2}$ -chip.

7.2 Frequency Hop

In frequency hop (FH) systems processing gain is a function of the number of hop frequencies rather than the number of PN chips per bit. With

W_{SS} = Bandwidth of the FH spread spectrum signal

B_S = Bandwidth of each frequency slot

N_F = Number of hop frequencies

then the processing gain is

$$P_{gFH} = \frac{W_{SS}}{B_S} = N_F \cdot$$

The basic FH transmitter is as shown in Figure 7.2-1.

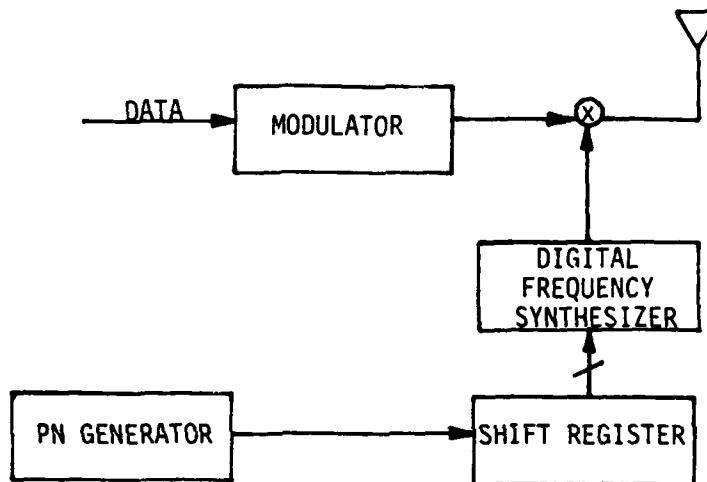


Figure 7.2-1. Basic FH Transmitter

The PN generator is used to generate the binary address of the hop frequency by providing one new chip to the shift register for each hop. If there are $N_{H/b}$ frequency hops per bit, then the rate of the PN generator, r_{cFH} , is related to the bit rate by

$$r_{cFH} = N_{H/b} r_b$$

The corresponding rate of the PN generator in a DS system is

$$r_{cDS} = N_{c/b} r_b$$

Since there are typically many orders of magnitude more chips per bit in a DS system than there are frequency hops per bit in a FH system, the ratio of the two PN rates,

$$\frac{r_{cDS}}{r_{cFH}} = \frac{N_c/b}{N_H/b}$$

is typically many orders of magnitude. Thus the width of a FH chip, T_{cFH} , is many orders of magnitude greater than the width of a DS chip, T_{cDS} .

7.2.1 Direct Search of FH

Direct search for FH is conducted in a manner analogous to DS direct search, as illustrated in Figure 7.2.1-1.

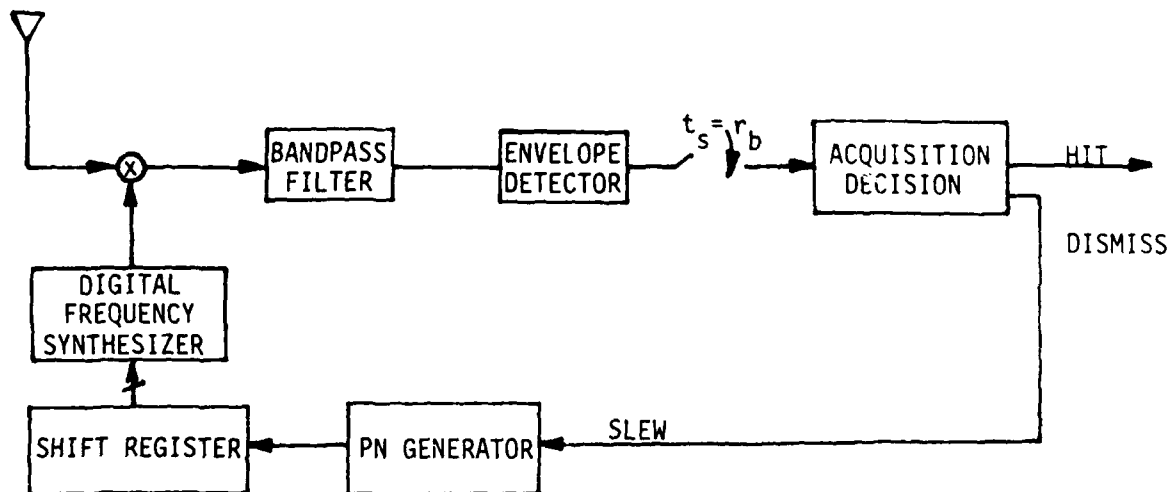


Figure 7.2.1-1. Direct Search for FH Acquisition

By searching at a rate equal to the bit rate, r_b , and slewing the PN generator in $\frac{1}{2}$ -chip steps this direct search progresses through the timing uncertainty region at the same basic rate and in the same manner as the DS direct search. But with the greater width of the FH chip a larger portion of the uncertainty region is covered in each step, by the factor

$$\frac{\frac{1}{2} T_{CFH}}{\frac{1}{2} T_{CDS}} = \frac{N_{C/b}}{N_{H/b}}$$

Therefore the time required to search through a given uncertainty range is reduced by the factor $N_{C/b}/N_{H/b}$. Of course we can't expect something for nothing --- the price is that when timing is resolved to within $\frac{1}{2}$ -chip in each of the two systems the resolution is coarser in the FH system by the same $N_{C/b}/N_{H/b}$ factor. This would seem to indicate that FH is an attractive acquisition aid, rapidly reducing a large initial timing uncertainty to a range which permits rapid acquisition of DS by a MF. However, it must be noted that when the frequency hop rate is one-half the bit rate, both FH acquisition and MF acquisition of DS show the same acquisition speed advantage over direct search of DS, and the MF acquisition of DS results in finer timing resolution. For lower FH rates FH does show a speed advantage over the MF acquisition of DS but an even greater reduction in resolution.

7.2.2 MF for FH

The obvious next step is to reduce the time required for acquisition of FH by utilizing a FH MF such as in Figure 7.2.2-1.

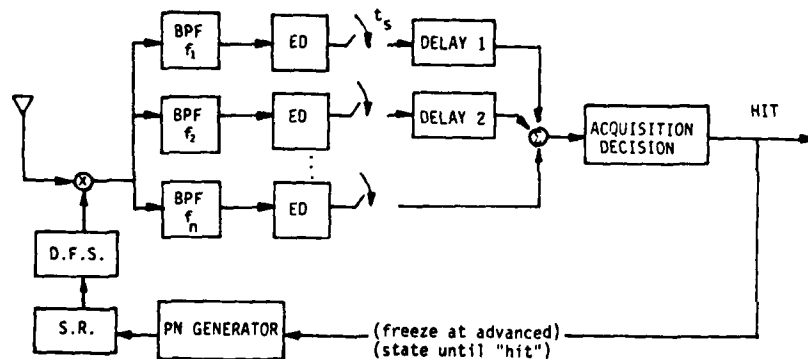


Figure 7.2.2-1. MF for FH Acquisition

In this receiver the PN generator is held at an advanced state so that the Discrete Frequency Synthesizer produces a constant frequency. The input to the N parallel channels is therefore a FH pattern which is simply offset in frequency from the received FH pattern. The output of a particular BPF is large when the frequency of the input pattern matches the frequency of the filter. The filter frequencies and the corresponding delays are selected to match the FH pattern which will be generated by the PN sequence prior to and including the PN segment held in the PN generator. A typical advanced FH pattern is shown in Figure 7.2.2-2.

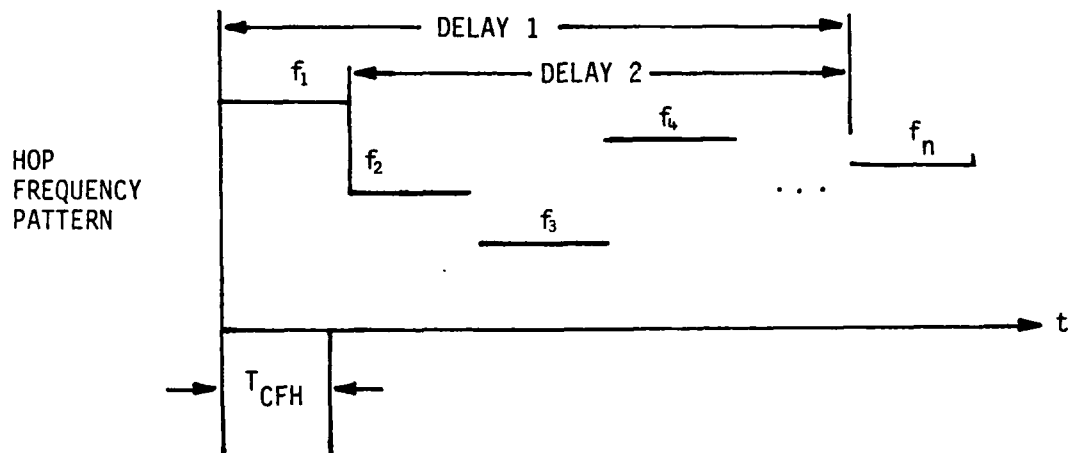


Figure 7.2.2-2. Advanced FH Pattern

With this arrangement the time-hopped pulses at the envelope detector outputs will be in alignment at the input to the summing network, providing a S/N advantage over and above the FH processing gain. Thus if the S/N at the acquisition detector in this system is to be maintained at the same level as in the conventional FH direct search system, the S/N ratio of each channel can be reduced. This permits the BPF bandwidths to be increased and the sampling rate to be increased. Ideally (ignoring non-coherent combining loss) these parameters are linearly related, that is, the S/N ratio into the acquisition detector is unchanged if the number of channels is increased from 1 to N , the bandwidths increased by N and the sampling rate increased by N . In general the number of parallel channels, N , will have to be somewhat larger than the number of samples

per frequency hop interval, N_S , to overcome the non-coherent combining loss. With N_S samples per FH interval, the undelayed samples in each channel will be as shown in Figure 7.2.2-3 and the delayed samples as in Figure 7.2.2-4. The acquisition detector will be triggered at the time of first coincidence of the signal which occurs no later than T_{CFH}/N_S seconds after the beginning of the N^{th} interval. Thus acquisition with this MF approach provides timing resolution of

$$\frac{\text{Resolution of MF}}{\text{Acquisition of FH}} = \frac{T_{CFH}}{N_S}$$

which for large N_S would indicate a considerable improvement over the $T_{CFH}/2$ resolution of direct search acquisition of FH. In fact, by noting that

$$\frac{T_{CFH}}{N_S} = \frac{\frac{N_{c/b}}{N_{H/b}} T_{cDS}}{N_S}$$

we see that MF acquisition of FH can achieve the $T_{cDS}/2$ resolution of DS by sampling at a rate of

$$N_S = \frac{2 N_{c/b}}{N_{H/b}}$$

samples per frequency hop. This is a surprising result since the MF approach was anticipated to produce an improvement in acquisition time, not timing resolution.

The question now is: Does the MF approach to FH acquisition provide any improvement in acquisition time? To answer this question recall that it was noted earlier that direct search of FH results in the same acquisition time performance as MF acquisition of DS when the frequency hopping rate is one-half the bit rate, and FH gains some advantage when the hop rate is reduced. Thus the question can be answered by comparing the search rates of MF acquisition of FH and MF acquisition of DS:

$$\frac{\text{Search Rate for MF}}{\text{Acquisition of FH}} = \frac{1 \text{ FH-chip of time searched}}{\text{per FH time interval.}}$$

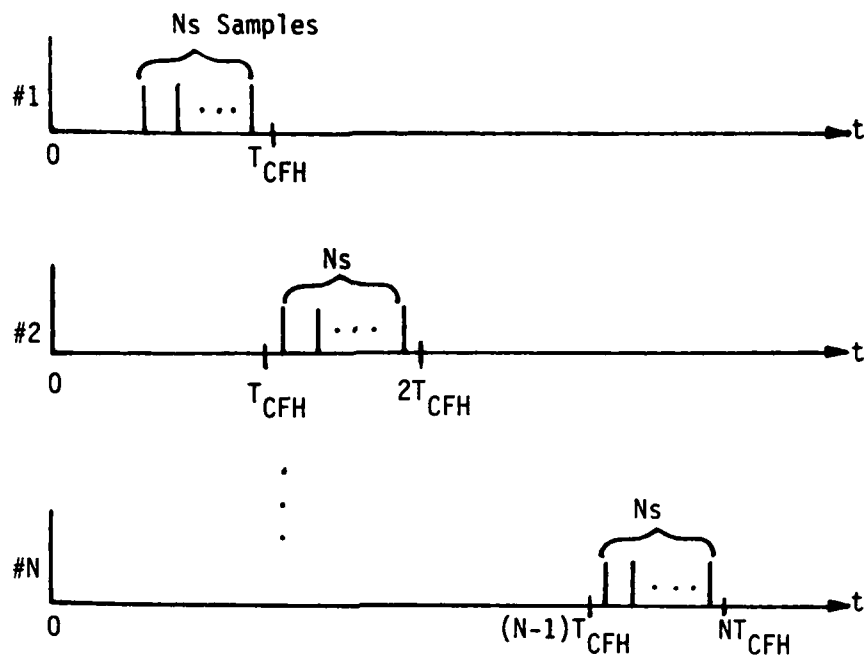


Figure 7.2.2-3. Undelayed Samples

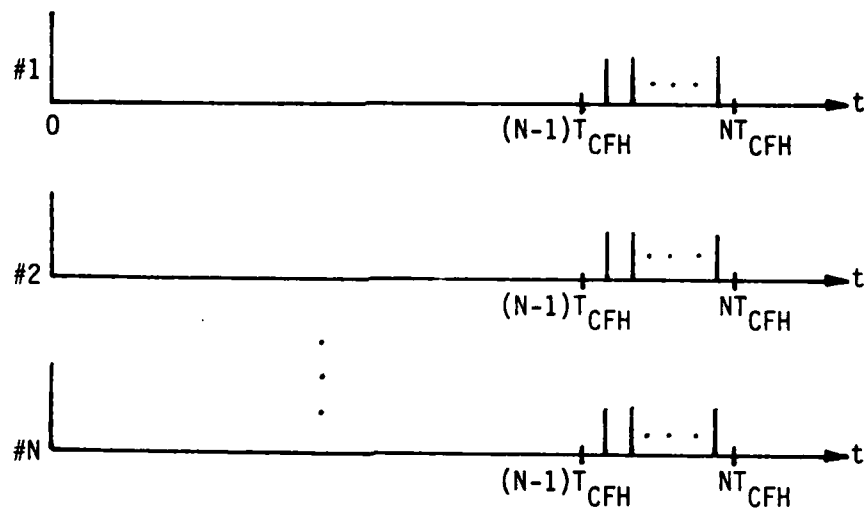


Figure 7.2.2-4. Delayed Samples

$$= \frac{1}{T_{cFH}} , \text{ FH-chips of time searched per second}$$

$$= \frac{N_{c/b}/N_{H/b}}{T_{cFH}} , \text{ DS-chips of time searched per second}$$

$$= \frac{N_{c/b}/N_{H/b}}{N_{c/b}/N_{H/B} T_{cDS}} , \text{ DS-chips of time searched per second}$$

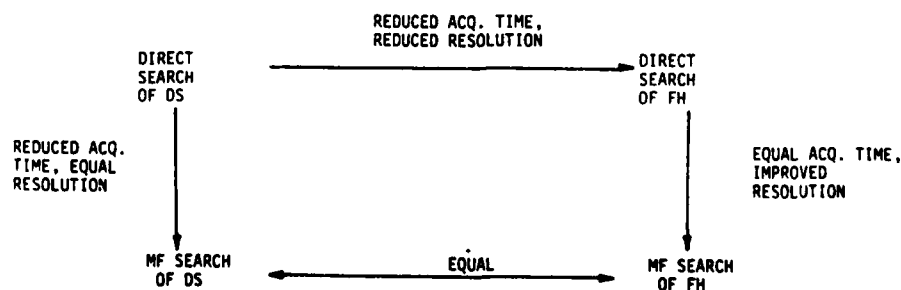
$$= \frac{1}{T_{cDS}} , \text{ DS-chips of time searched per second}$$

$$= r_{cDS} , \text{ DS-chips of time searched per second}$$

Search Rate for MF Acquisition of DS = $2 r_{cDS}$, $\frac{1}{2}$ DS-chips of time searched per second

$$= r_{cDS} , \text{ DS-chips of time searched per second}$$

Thus for any initial timing uncertainty the two MF approaches would achieve acquisition in the same time. In addition, if the sampling rate is high enough in the FH MF system the timing resolutions at acquisition are the same for the two systems. The relationship between the four acquisition methods can be summarized by:



7.3 Frequency Hop/Direct Sequence

In FH/DS systems the total processing gain (in dB) is approximately equal to the sum of the processing gains due to the FH spreading and the DS spreading,

$$P_{gFH/DS}(\text{dB}) \cong P_{gFH}(\text{dB}) + P_{gDS}(\text{dB}) .$$

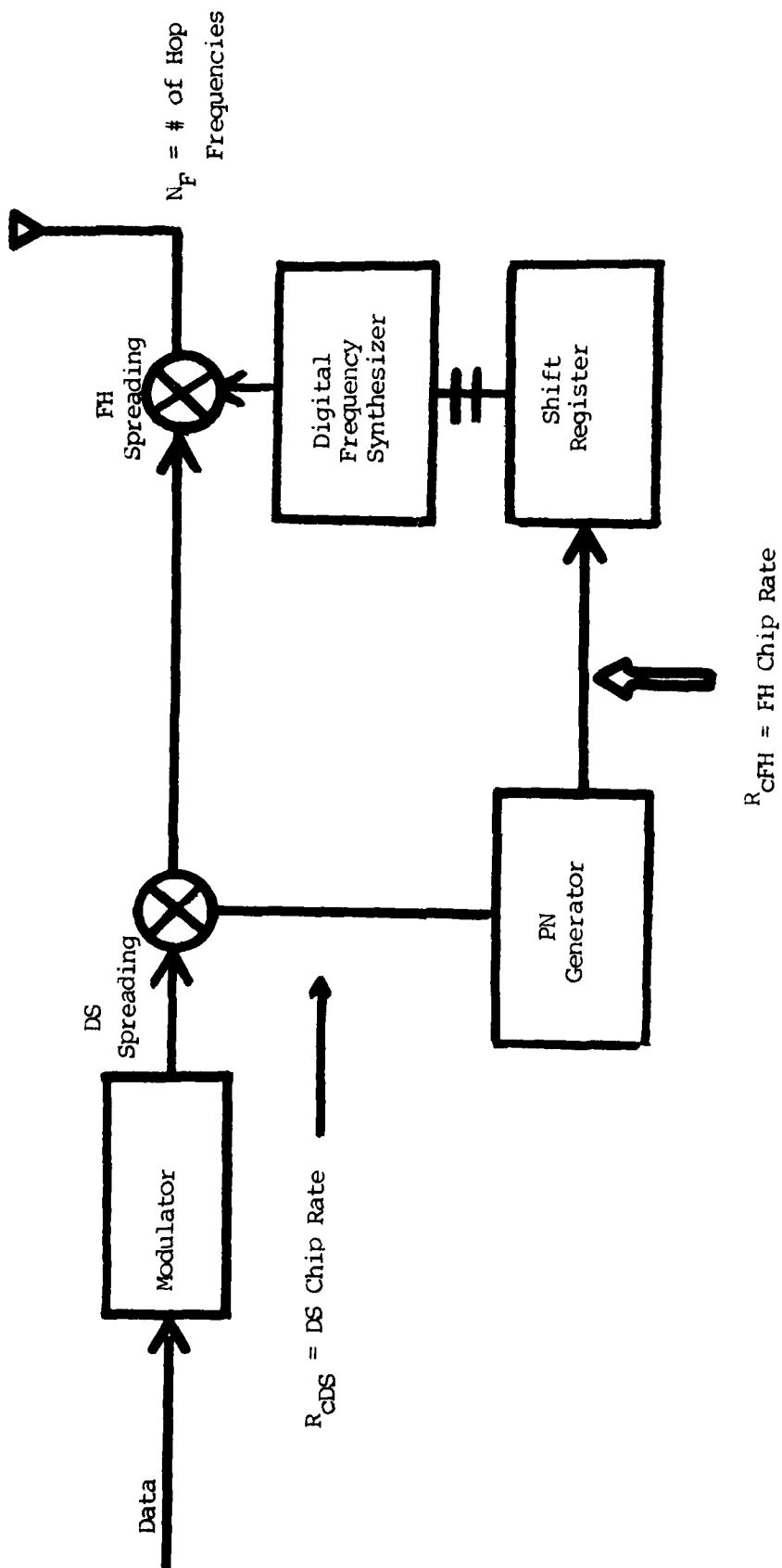
In terms of the nomenclature defined on the basic FH/DS transmitter block diagram of Figure 7.3-1, the processing gain is

$$P_{gFH/DS} \cong 10 \log N_F + 10 \log N_{c/b} . \quad (7.3-1)$$

This processing gain is essentially fixed by the bandwidth of the spread spectrum signal and may be divided between the two spreading functions as desired. The frequency hopping rate (number of frequency hops per bit, $N_{H/b}$) does not enter into the processing gain per se but rather is determined by considering the frequency-following capability of the jamming threat. Typically the number of DS chips per bit, $N_{c/b}$, is two or more orders of magnitude greater than the number of frequency hops per bit, $N_{H/b}$, so that the DS PN rate is correspondingly greater than the FH PN rate.

7.3.1 Direct Search

The receiver structure for direct search acquisition of FH/DS is shown in Figure 7.3.1-1. It is assumed, as before, that the multiply and integrate correlator for the DS despreading integrates over a bit interval so that the search rate is equal to the bit rate. The PN generator is stepped through the timing uncertainty region in increments equal to $\frac{1}{2}$ of the smaller chip width, i.e., either $\frac{1}{2}$ DS chip or $\frac{1}{2}$ FH chip depending on which is smaller. As noted earlier the DS PN rate is usually much greater than the FH PN rate so that the DS chip width is usually smaller and the timing uncertainty region is searched in increments of $\frac{1}{2}$ a DS chip. Consequently, once acquisition is achieved the timing uncertainty is resolved to within $\frac{1}{2}$ a DS chip. Note that for systems with the same processing gain pure FH typically has the lowest chip rate, pure DS has the highest and FH/DS is in-between. Therefore,



$$N_{c/b} = \# \text{ PN chips/bit for DS Spreading}$$

$$N_{H/b} = \# \text{ PN chips/bit for FH Spreading} \\ = \# \text{ Frequency Hops/bit}$$

$$R_{cFH} = \text{FH Chip Rate}$$

$$R_{cDS} = \text{DS Chip Rate}$$

$$N_F = \# \text{ of Hop Frequencies}$$

Figure 7.3-1. Basic FH/DS Transmitter

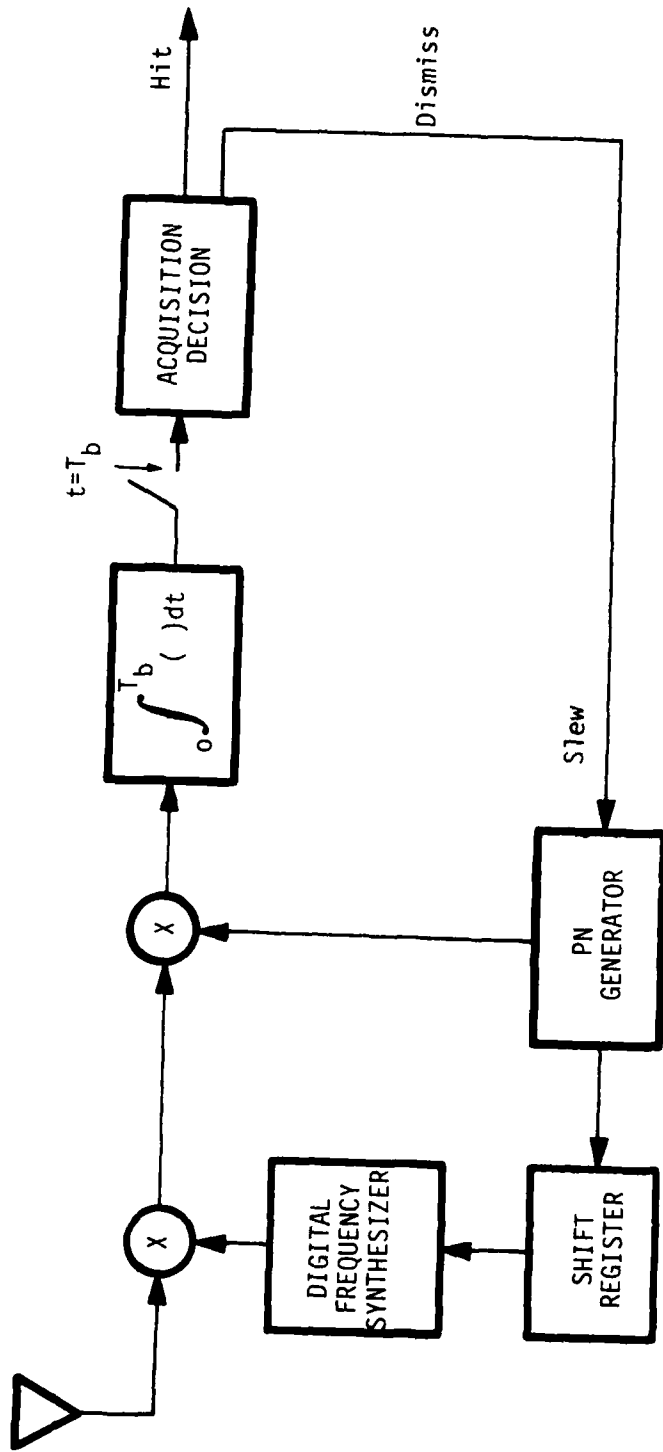


Figure 7.3.1-1.
Direct Search of FH/DS

FH has the largest search increment, fastest acquisition and coarsest timing resolution; DS has the smallest search increment, slowest acquisition and finest timing resolution; and FH/DS is in-between in all three respects. Thus FH/DS provides a means of compromising between acquisition time and timing resolution.

More quantitatively let ΔT be the timing uncertainty, assume the search is conducted in $\frac{1}{2}$ -chips increments at a rate equal to the data rate, R_b , and let R_c denote the chip rate appropriate to the type of spreading being considered. (There is no ambiguity regarding R_c in pure DS or pure FH systems, in FH/DS systems the appropriate R_c is the higher of the DS and FH chip rates.) Then the total number of $\frac{1}{2}$ -chip increments in the uncertainty region is

$$\begin{array}{l} \text{\#}\frac{1}{2}\text{-chip} \\ \text{Increments of} \\ \text{Uncertainty} \end{array} = 2 \Delta T R_c$$

and the acquisition time (or, more precisely, the time for one complete search) is

$$\text{Acquisition Time} = \frac{2 \Delta T}{R_b} R_c .$$

The timing uncertainty remaining at acquisition is $\frac{1}{2}$ -chip,

$$\begin{array}{l} \text{Timing Uncertainty} \\ \text{at Acquisition} \end{array} = \frac{1}{2} T_c = \frac{1}{2} \frac{1}{R_c} .$$

Typically R_c increases in going from FH to FH/DS to DS. In DS systems R_c is set by the required processing gain; in FH systems by the frequency hopping rate required to avoid a frequency-following jammer (with processing gain coming from the number of hop frequencies). FH/DS systems provide an additional degree of freedom in that the three parameters, DS chip rate, FH rate and number of hop frequencies, can be selected as a set to simultaneously provide the required AJ performance and reduced acquisition time. The performance comparisons for direct search can be summarized by:

<u>Spreading</u>	<u>Search Increment Size</u>	<u>Acquisition Time</u>	<u>Timing Resolution</u>
FH	↓	↓	↓
FH/DS	Decreasing	Increasing	Increasing
DS	↓	↓	↓

7.3.2 Matched Filter

In the MF method of acquiring FH/DS, as in the MF method for all types of spreading functions, the PN generator is fixed at some advanced state and the receiver simply awaits coincidence between the received and local spreading functions. The receiver structure, as shown in Figure 7.3.2-1, is the same as for direct search of FH/DS except that the integrate and multiple correlator for the DS despreading is replaced by a MF.

Comparing MF acquisition of FH/DS with MF acquisition of DS, the FH/DS system has:

- Lower DS Chip Rate
- Larger Search Increments
(i.e. Larger $\frac{1}{2}$ -Chip Width)
- Lower Search Rate
(i.e. Twice the DS Chip Rate)

The larger search increments dictate coarser timing resolution at acquisition. Since the increase in size of the search increment is exactly offset by the decrease in search rate the total search time, or acquisition time, remains unchanged from the DS case. Comparison of acquisition performances for the six possible combinations of spreading function and receiver techniques is summarized in Figure 7.3.2-2.

Intuitively it would seem that a parallel bank of channels at different frequencies (analogous to the FH system of Figure 7.2.2-1, not parallel search operations) would improve the timing resolution in the FH/DS system as it did in the FH system. However, the resolution in the FH/DS is limited by the fact that the received signal is sampled and correlated with the reference DS signal at twice the DS chip rate. Therefore timing resolution can be no

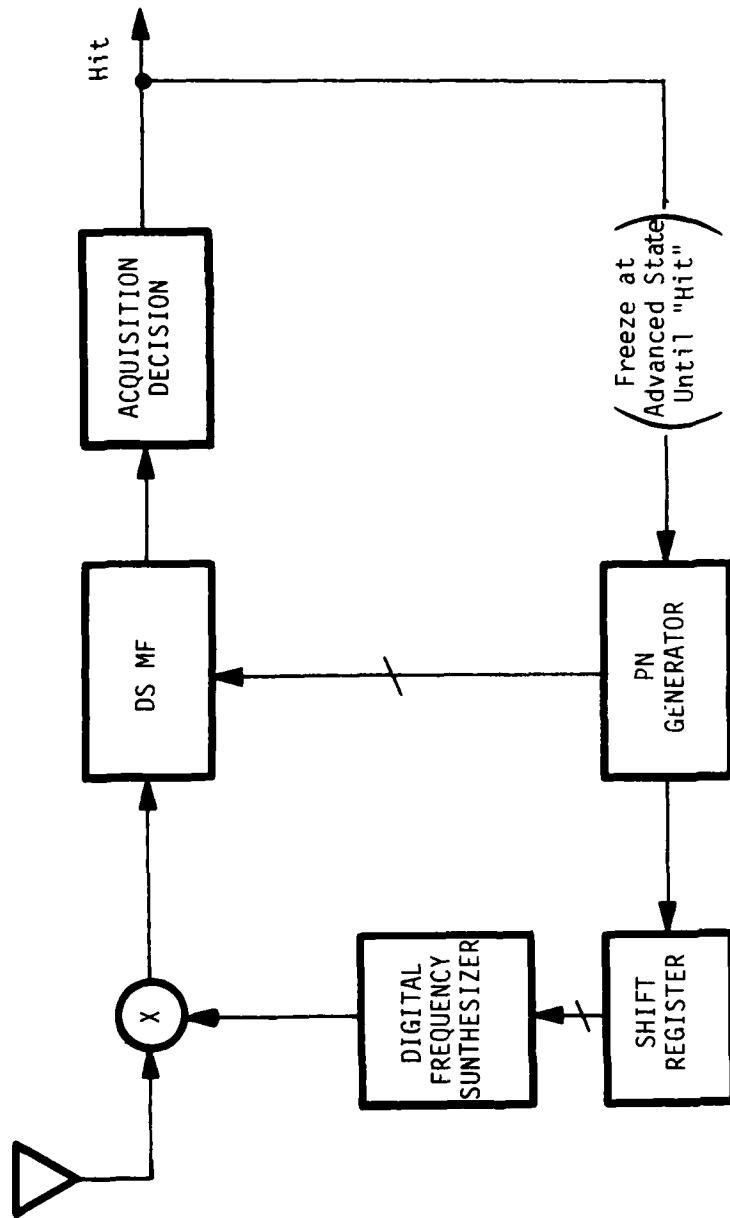
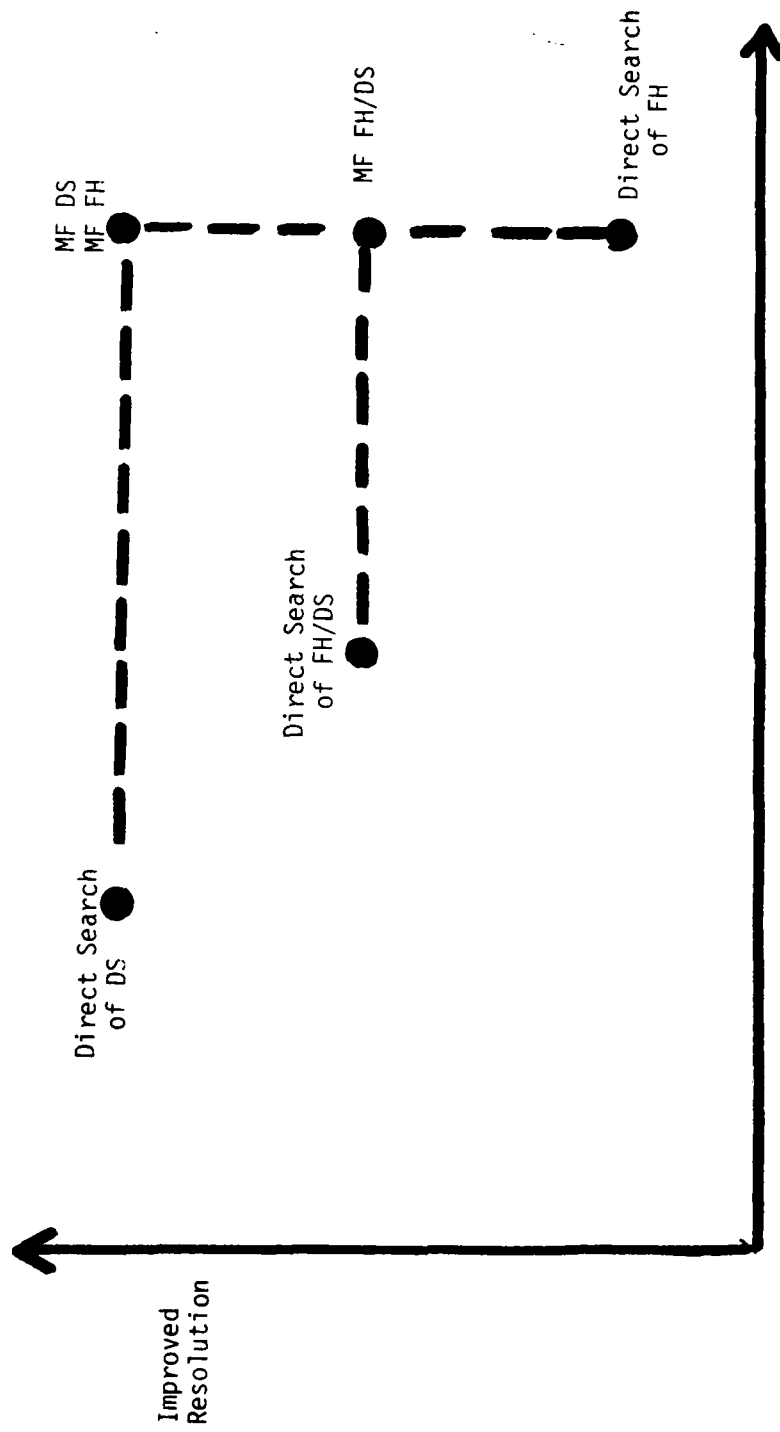


Figure 7.3.2-1. MF Receiver for FH/DS



Improved Acquisition Time

Figure 7.3.2-2.

Summary of Acquisition Performances

better than $\frac{1}{2}$ a DS chip. Likewise multiple channels can not improve the acquisition time since the search rate is set by the rate of the incoming signal. Multiple channels would provide a higher S/J at the input to the acquisition detector which would improve P_D and/or P_{FA} , parameters which have not been considered in the performance comparisons presented in this section.

SECTION 8.0
BASIC ACQUISITION STRATEGIES

8.0 BASIC ACQUISITION STRATEGIES

In this part we turn our attention to the basic strategies for transferring timing information from transmitter to receiver. The context is military spread spectrum applications which imposes the additional requirement that protection against intelligent jamming not be unduly compromised during the acquisition process. The intent is to characterize the basic acquisition strategies available, rather than specific acquisition techniques or implementations, in such a manner as to permit order-of-magnitude comparisons in potential acquisition time and to assess to some degree the potential vulnerability to intelligent jamming.

The "acquisition time" expressions developed are actually expressions for "time to complete one search of the timing uncertainty region" or "time to transmit timing information," etc. rather than more precise characterizations of acquisition time such as "mean time to acquire." Effects of false alarms and missed detections have been neglected so that the key parameters which dictate performance potential can readily be identified. Likewise, timing uncertainty is expressed in terms of the number of PN chips, L , of uncertainty which exists between the transmitter and receiver in order to minimize the number of parameters. L may be the total length of the PN code or some portion of it depending on the extent of timing uncertainty. Timing uncertainty in seconds, ΔT , is related to L by the PN chip rate, R_c ,

$$L = \Delta T R_c \quad (8.0-1)$$

For a given value of ΔT the corresponding value of L can vary greatly depending on the type of spreading employed; for example for the same ΔT , L would typically be several orders of magnitude greater for a direct sequence system than for a frequency hop system due to the typically large difference in PN rates. These are systems considerations which are implicitly accounted for in the acquisition models presented, but which are not explicitly shown in order that the key features of the basic strategies, not fundamental system concepts, be emphasized.

Basically with a PN code of length L chips timing information can be transferred from transmitter to receiver by either transmitting the PN code-driven spreading function and searching for the correct code phase in the receiver or by transmitting the code phase as an N -bit binary number using a fixed spreading function, where

$$L \leq 2^N$$

The first method has the advantage of full AJ protection during acquisition but results in excessively long acquisition times for typically long code lengths. The second method results in very rapid acquisition but is quite vulnerable to smart jammers since the spreading function remains fixed while transmitting the N bits of timing information. A third approach is to use a combination of these two, that is partially resolving the timing uncertainty by transmitting and searching over a short PN code-driven spreading function and then transmitting the remaining timing information as data on the short code-spread signal.

8.1 Search Methods

There are two basic search methods of acquisition, direct search (also commonly referred to as conventional serial search) and matched filter (MF) search. In direct search the receiver correlates the incoming signal with the local reference over a τ second time interval and makes a decision as to whether or not the two are synchronized. If not then the timing of the local reference is incremented one-half chip and tested again. This continues until synchronization is achieved. If there are S such search devices each independently searching 1/S of the uncertainty region, then the time required to search the entire $2L$ $\frac{1}{2}$ -chip element uncertainty region is

$$T_{DS} = \frac{2L}{S} \tau .$$

The search rate for this technique is

DS: $R_s = 1/\tau$, $\frac{1}{2}$ -chip positions/second so
that T_{DS} may be expressed as

$$T_{DS} = \frac{2L}{SR_s} \quad (8.1-1)$$

In the MF search method the reference section of an MF is loaded with an advanced segment of the incoming spreading waveform, checks the correlation between the incoming signal and the frozen reference at twice the chip

rate and signals synchronization when the correlation exceeds a threshold value. The search rate in this case is thus

$$\text{MF: } R_S = 2 R_C, \frac{1}{2}\text{-chip position/second}$$

With S MF's each MF is assigned $(2L/S)$ $\frac{1}{2}$ -chip positions. The time required to send over the complete uncertainty region is the time required to initially load the devices and obtain the first correlation test values, τ_0 , plus the time for each MF to search over the remaining $(2L/S)$ positions at a rate of R_S , i.e.,

$$T_{MFS} = \frac{1}{R_S} \left(\frac{2L}{S} - 1 \right) + \tau_0 \quad (8.1-2)$$

The initial response time, τ_0 , is a function of the length of the MF,

$$L_{MF} \triangleq \text{MF Length in chips}$$

and the input chip rate R_C ,

$$\begin{aligned} \tau_0 &= \frac{L_{MF}}{R_C} \\ &= \frac{2L_{MF}}{R_S} \end{aligned} \quad (8.1-3)$$

Note that the two expressions for search time are similar even though the actual search times may be quite different. The search rate for the MF is twice the chip rate; for direct search it is usually on the order of the bit rate which is typically orders of magnitude lower than the chip rate. Therefore the MF usually provides orders of magnitude faster acquisition than does direct search. Nonetheless a common expression can be obtained for T_{DS} and T_{MFS} by manipulating T_{DS} as follows:

$$\begin{aligned} T_{DS} &= \frac{2L}{SR_S} = \frac{2L}{S} \tau \\ &= \frac{2L}{S} \tau - \tau + \tau \\ &= \left(\frac{2L}{S} - 1 \right) \tau + \tau \\ &= \frac{1}{R_S} \left(\frac{2L}{S} - 1 \right) + \tau \end{aligned}$$

But τ is the time required for each correlation test, including the first one so that for direct search

$$\tau_0 = \tau$$

and

$$T_{DS} = \frac{1}{R_s} \left(\frac{2L}{S} - 1 \right) + \tau_0$$

which is the same as the MF expression. Therefore, a common expression for the search methods is

$$T_S = \frac{1}{R_s} \left(\frac{2L}{S} - 1 \right) + \tau_0 \quad (8.1-4)$$

8.2 The Data Transmission Method

An alternative to the search method of acquisition is the transmission of timing information as N bits of data, where

$$L \leq 2^N$$

using a fixed spreading function. The spreading function may be a fixed segment of a PN sequence, a fixed chirp waveform, etc. Transmitting the N bits of timing information at a bit rate of R_D bits per second results in an acquisition time (i.e., time to transmit the N bits) of

$$T_{DT} = \frac{N}{R_D}, \text{ seconds.} \quad (8.2-1)$$

The ratio of acquisition times for the data transmission method and the search method is

$$\frac{T_{DT}}{T_S} \cong \frac{R_s}{R_D} \frac{SN}{2L}$$

which for large N indicates many orders of magnitude faster acquisition by the data transmission method. This improved performance is of course due to the fact that there is no uncertainty in the spreading function, which also makes the receiver quite vulnerable to smart jamming.

8.3 The Combined Search and Data Transmission Method

Basically, the move from a search method of acquisition time to the data transmission has been one from great uncertainty in the spreading function, with correspondingly large acquisition time but considerable immunity to smart jamming, to no uncertainty in the spreading function, with correspondingly small acquisition time but considerable vulnerability to smart jamming. A combination of these two methods provides a reasonable compromise between these two extremes, and, under certain conditions, results in an even somewhat faster acquisition than even the data transmission method. Many so called rapid acquisition techniques employ some variation of this idea.

In this combined method acquisition of a long PN code with

$$L_{LC} = 2^{N_{LC}} \text{ chips} \rightarrow N_{LC} \text{ bits of timing information}$$

is achieved by: (1) transmitting a short PN code - driven spreading function with

$$L_{SC} = 2^{N_{SC}} \text{ chips} \rightarrow N_{SC} \text{ bits of timing information}$$

(2) acquiring this short code by a search method and (3) transmitting the remaining $(N_{LC} - N_{SC})$ bits of timing information as data on the short code spread signal. The time to acquire using this method therefore is the time to search over L_{SC} chips plus the time to transmit $(N_{LC} - N_{SC})$ bits of data. The time to conduct one search over the short code is

$$T_S = \frac{1}{R_S} \left(\frac{2L_{SC}}{S} - 1 \right) + \tau_0$$

and the time to transmit $(N_{LC} - N_{SC})$ bits of data is

$$T_{DT} = \frac{N_{LC} - N_{SC}}{R_D}$$

so that the total time to acquire the long PN code using this combined method is

$$T_C = T_S + T_{DT}$$

$$= \frac{1}{R_S} \left(\frac{2L_{SC} - 1}{S} \right) + \tau_D + \left(\frac{N_{LC} - N_{SC}}{R_D} \right). \quad (8.3-1)$$

The performance of this method relative to the other two is best demonstrated by an example.

8.4 Example

Consider the acquisition of a long code-driven DS system with

$$N = 50$$

$$L = 1.13 \times 10^{25} \text{ chips}$$

$$R_C = 10 \text{ megachips/second}$$

$$S = 10$$

Direct Search

Assume that the nominal data rate for the system is 5 Kbps and that acquisition must be accomplished with the same processing gain. Then the search rate is

$$R_S = 5 \times 10^3, \frac{1}{2}\text{-chip positions/second}$$

and the time for one search over the entire long code is

$$T_S = 4.5 \times 10^{10} \text{ seconds.}$$

Obviously, the direct search method is unsuitable for initial acquisition of the long code.

MF Search

With an MF, the search rate is twice the chip rate so that

$$R_S = 20 \times 10^6, \frac{1}{2}\text{-chip positions/second}$$

and

$$T_S = 11.3 \times 10^6 \text{ seconds.}$$

The MF thus provides a considerable improvement (approximately 4000 times) in acquisition time but is still unsuitable for this initial acquisition situation.

Data Transmission

With the 50 bits of timing information transmitted at a data rate of 5 Kbps, the data transmission method requires only

$$T_{DT} = 10 \text{ milliseconds}$$

This is a tremendous improvement in acquisition time but with considerable vulnerability to smart jamming since the spreading function is fixed.

Combined Method

The time to acquire using the combined method is a function of the short code length,

$$T_C = \frac{1}{20 \times 10^6} \left(\frac{2L_{SC} - 1}{10} \right) + 2 \times 10^{-4} + \frac{(50 - N_{SC})}{5 \times 10^3} \quad (8.4-1)$$

which is plotted in Figure 8.4-1. It is noted that a minimum occurs and the value of 7.4 milliseconds (corresponding to a short code length of approximately 28,000 chips) actually represents an improvement over the data transmission

method. This raises some interesting questions regarding optimization of the combined method and its general performance relative to that of the data transmission method.

8.5 The Optimum Combined Method

The optimum value of the short code length in the combined method can be determined by expressing N_{SC} as

$$N_{SC} = \log_2 L_{SC}$$

in the expression for T_C , considering L_{SC} as a continuous variable and differentiating T_C with respect to L_{SC} . The resulting optimum value is

$$L_{SC \text{ OPT}} = \frac{SR_s}{(2 \ln 2) R_D} \quad (8.5-1)$$

and

$$N_{SC \text{ OPT}} = \log_2 \frac{S R_s}{(2 \ln 2) R_D}$$

(It is interesting to note that the optimum short code length is not a function of the long code length.) The corresponding optimum acquisition time using the combined method is

$$T_C \text{ OPT} = \frac{1}{R_D} \left\{ \frac{1}{\ln 2} + R_D \left(\tau_0 - \frac{1}{R_S} \right) + N_{LC} - \log_2 \left[\frac{SR_s}{(2 \ln 2) R_D} \right] \right\} \quad (8.5-2)$$

For the example considered earlier

For the example considered earlier

For the example considered earlier

$$L_{SC \text{ OPT}} = 28,854 \text{ chips}$$

$$T_C \text{ OPT} = 7.4 \text{ milliseconds}$$

which match the values indicated in Figure 8.4-1.

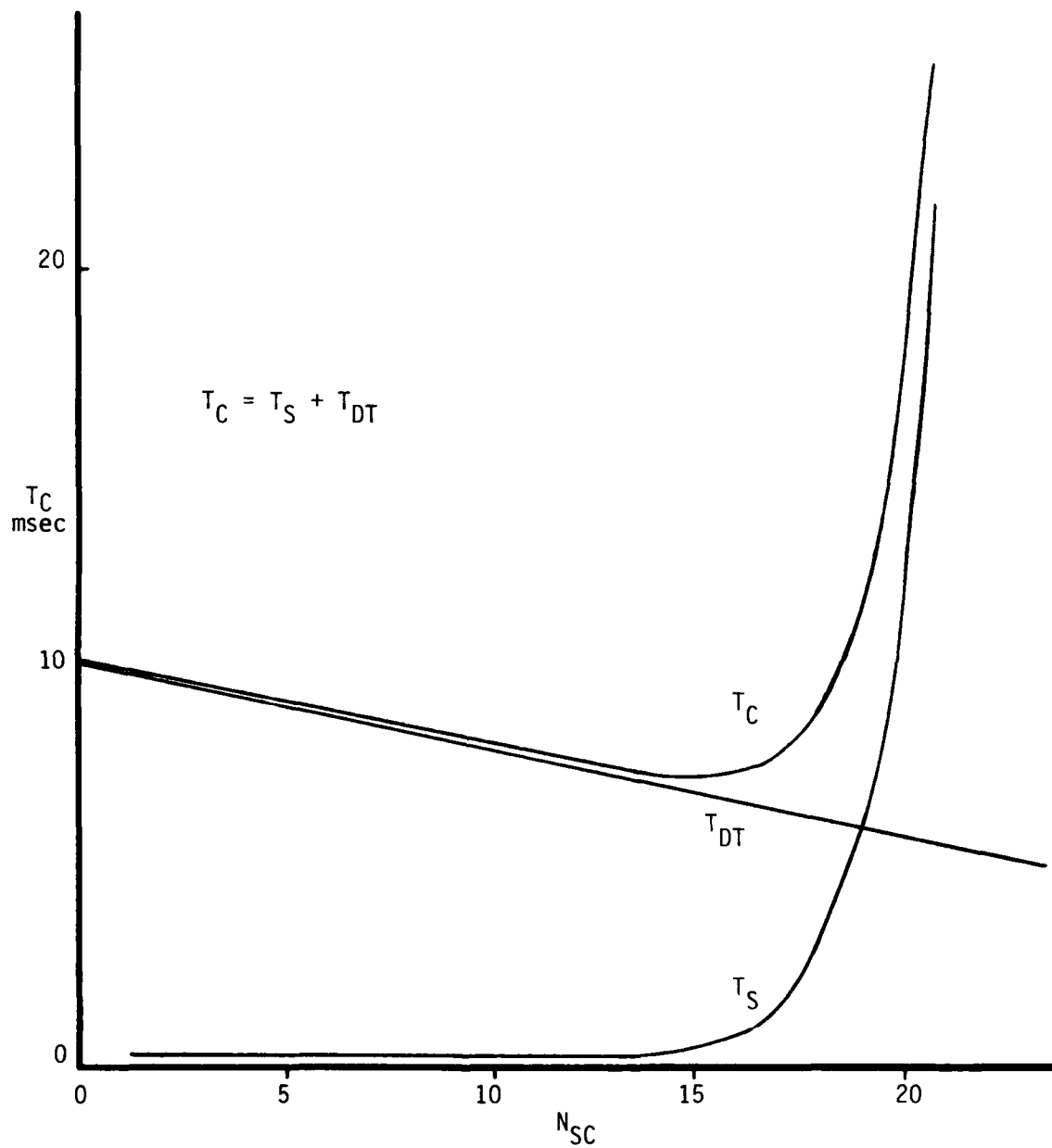


Figure 8.4-1. Performance of the Combined Method

The next question of interest is: Under what conditions will the combined method be faster than the data transmission method? Since (1) T_C approaches the T_{DT} value as $L_{SC} \rightarrow 0$, (2) T_C approaches the large T_S value when $L_{SC} \rightarrow L_{LC}$, and (3) T_C vs. L_{SC} has a unique minimum, then T_C can be less than T_{DT} only if the slope of T_C vs. L_{SC} is negative at the origin, i.e.,

$$\left. \frac{dT_C}{dL_{SC}} \right|_{L_{SC} = 0} < 0$$

This leads to the condition

$$SR_S \geq (2 \ln 2) R_D = 1.39 R_D. \quad (8.5-3)$$

Note that R_S is the search rate of each of the S independent search devices so that SR_S is the total search rate. The requirement therefore is that the total search rate for the short code search be somewhat larger than the data rate for the data transmission method. R_S is usually several orders of magnitude greater than T_D for an MF search implementation so that the combined method would usually be faster than the data transmission method if an MF is employed. And, of course, the main advantage of the combined method is the increased protection against smart jamming.

8.6 Conclusions

As is widely recognized, an MF can provide a significant reduction in spread spectrum signal acquisition time over direct search techniques and for reacquisition or acquisition with small timing uncertainty may result in acceptable acquisition performance. However, for acquisition with large and possibly even total timing uncertainty even the MF performance may be acceptable by many orders of magnitude. In such cases the only alternative is to reduce the randomness in the spreading function and tradeoff smart jammer protection for decreased acquisition time. This basic conflict arises from the fact that any randomness placed in the spreading function to confuse a smart jammer also confuses an unsynchronized receiver. Completely removing this randomness, as in the data transmission method, results in very rapid

acquisition but also makes the system very vulnerable to smart jamming.
The combined method presents a means for compromising between the two.

I

SECTION 9.0
CODE VALIDITY INTERVAL TECHNIQUES

9.0 CODE VALIDITY INTERVAL TECHNIQUES

The acquisition problem can obviously be circumvented by using fixed spreading waveforms; for example, by using a different but fixed segment of a PN sequence to represent each symbol in the data symbol alphabet. The receiver is then simply a bank of time invariant matched filters, one matched to each symbol sequence, and relative timing between transmitter and receiver becomes completely irrelevant insofar as despreading is concerned. But obviously the use of fixed spreading waveforms makes the system quite vulnerable to jamming by intelligent jammers. This vulnerability can be reduced in systems with limited timing uncertainty by periodically changing the spreading functions. The trick is to change the set of spreading functions at a rate which is fast enough to confuse the jammer but slow enough so that both the transmitter and receiver are using the same set of spreading functions "most of the time." Thus the trade-off is between speed of the smart jammer and timing accuracy in the communications system. The time interval over which each set of spreading waveforms is valid is referred to as the Code Validity Interval (CVI).

9.1 Hard Edge CVI

In conventional (so-called hard edge) CVI systems the waveforms are fixed throughout each CVI and changed abruptly at the end of each CVI. Thus the MFs in the receiver are exactly matched to the transmitter's set of waveforms during that part of the CVI in which both the transmitter and receiver are using the same set, and not matched during that part in which they are using adjacent sets due to timing errors. The problem occurs at the beginning and end of each CVI so that data loss can be avoided by providing a guard band around the transition point during which no transmissions occur. However, inclusion of a guard band reduces the available transmission time so that the transmitted symbol rate must increase (if the data rate is to remain constant) and the processing gain decreases correspondingly. For example, to protect against data loss in a system with maximum timing offset between transmitter and receiver of $\pm 30\%$ of the CVI would require a total guard band of 60% of the CVI. This would require a 2.5 times increase in transmitted symbol rate, producing a 4 dB decrease in processing gain. In general the loss in processing gain due to inclusion of a guard band to protect against an offset of $\pm X\%$ of the CVI is

$$pg_{\text{loss}}, \text{ dB} = -10 \log_{10} \left(1 - \frac{2x}{100} \right)$$

which is illustrated in Figure 9.1-1. Of course, the CVI should be made as small as possible in order to minimize the amount of time the jammer has to observe and process a particular set of spreading waveforms and then use the extracted parameters in a jamming signal. But the minimum CVI is constrained by the amount of processing gain loss which can be tolerated which is a function of both the CVI length and the maximum timing error anticipated in the system. A major disadvantage of the hard edge CVI approach is that in systems which include a mix of high precision clock units and low precision clock units the guard band is usually fixed for all data links at a value which will accommodate the lowest precision clock. Therefore even the high precision clock units pay the penalty of reduced processing gain. This situation can be avoided through a modified CVI approach in which changes in the spreading waveform set are evolutionary rather than abrupt. This technique is referred to as soft edge CVI.

9.2 Soft Edge CVI

In the soft edge CVI method small changes are continually introduced in the spreading waveforms throughout the CVI in such a way that the waveforms completely evolve from one set to the next in CVI. For example if in a hard edge CVI system the "0" symbol is represented by the PN segment $S_{0,i}$ during the i^{th} CVI interval and by $S_{0,i+1}$ during the next interval, the change from $S_{0,i}$ to $S_{0,i+1}$ is made abruptly at the end of the i^{th} interval. In an equivalent soft edge CVI system changes are made one chip at a time to $S_{0,i}$ so that at the end of the CVI $S_{0,i}$ has been completely changed to $S_{0,i+1}$. With $S_{0,i}$ and $S_{0,i+1}$ orthogonal, the two PN segments are alike in 50% of the chip positions and different in 50% of the chip positions. Therefore only 50% of the chips need be changed during each CVI, and they can be selected for change in a pseudo-random order which is common to transmitter and receiver. This evolutionary change therefore provides some additional processing gain against repeat jammers but more importantly, it provides, (1) a graceful degradation in performance as a function of timing error and, (2) performance of each unit is determined by the clock precision of the unit, not the precision of the

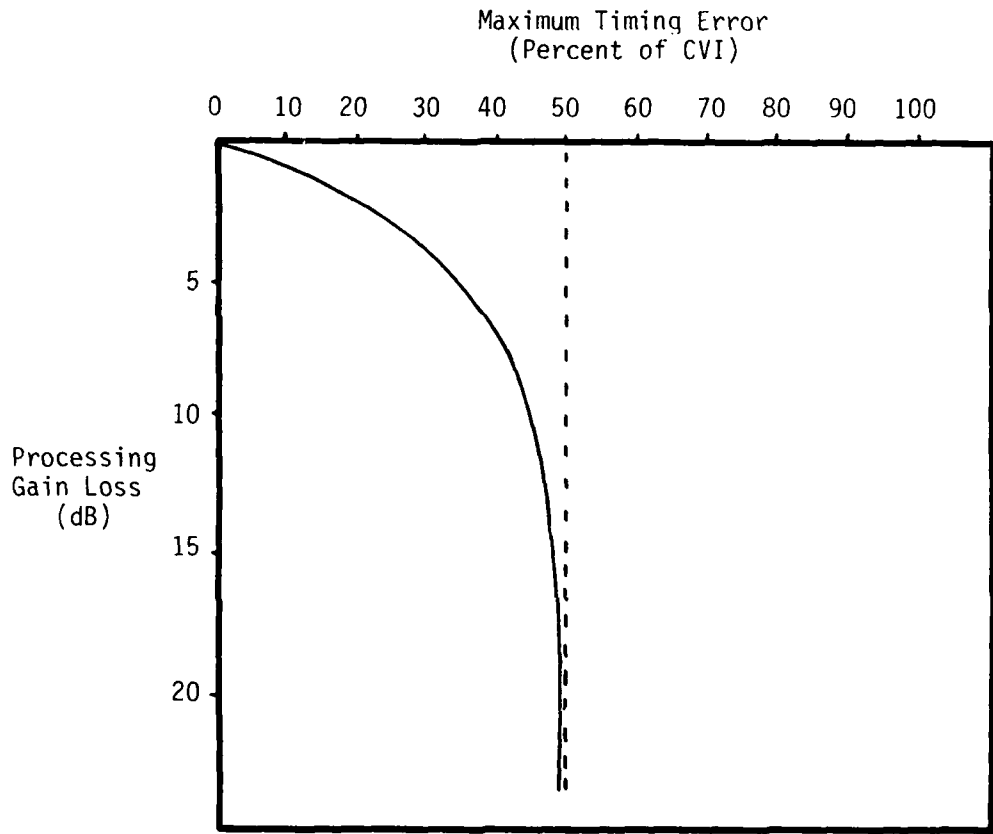


Figure 9.1-1. Processing Gain Loss in Hard Edge CVI System

lowest precision clock in the system. These advantages are illustrated as follows. Since 50% of the chips are changed in a CVI, 25% of the chips have changed by the mid-point of the CVI. Thus 75% of the chips in the mid-point "0" symbol match the initial $S_{0,i}$ PN segment and likewise 75% of the chips in the mid-point "0" symbol match the final $S_{0,i+1}$ PN segment. If the mid-point "0" symbol is correlated with either $S_{0,i}$ or $S_{0,i+1}$, 75% of the chips agree, 25% disagree so that the correlation value is one-half the maximum value, which indicates a loss in processing gain of 6 dB for a unit whose timing error is 50% of a CVI. For a unit whose timing error is zero the mid-point "0" received symbol would be correlated with the same PN segment so that there is no loss in processing gain. Thus the processing gain available to each unit is a function only of that unit's timing accuracy. Processing gain loss as a function of timing error is

$$pg_{\text{loss}}, \text{ dB} = -20 \log_{10} \left(1 - \frac{X}{100} \right)$$

where X is timing error expressed in percent of CVI. This function is plotted in Figure 9.2-1.

Note that a timing offset of $\pm 30\%$ in the soft edge CVI system results in a 3.1 dB loss in processing gain whereas as noted earlier a guard band to protect against a $\pm 30\%$ offset in the hard edge CVI system would result in a 4 dB loss in processing gain.

9.3 Acquisition Characteristics

No acquisition or reacquisition operations are required in CVI systems, and hence no time need be dedicated to acquisition, whenever the relative timing between the transmitter and receiver is within one CVI for hard edge systems or within some fraction of a CVI for soft edge systems. Under these conditions the MFs in the receiver are matched to the incoming symbols (or nearly matched in the case of soft edge systems) and symbol detection is accomplished immediately. Under conditions of larger timing uncertainties a search over the CVIs in the uncertainty region is required. But note that in DS systems the acquisition search is conducted in $\frac{1}{2}$ -chip increments and the timing resolution required for data demodulation is a small fraction of a chip, whereas in CVI systems the search is conducted in increments of some fraction of a CVI and timing

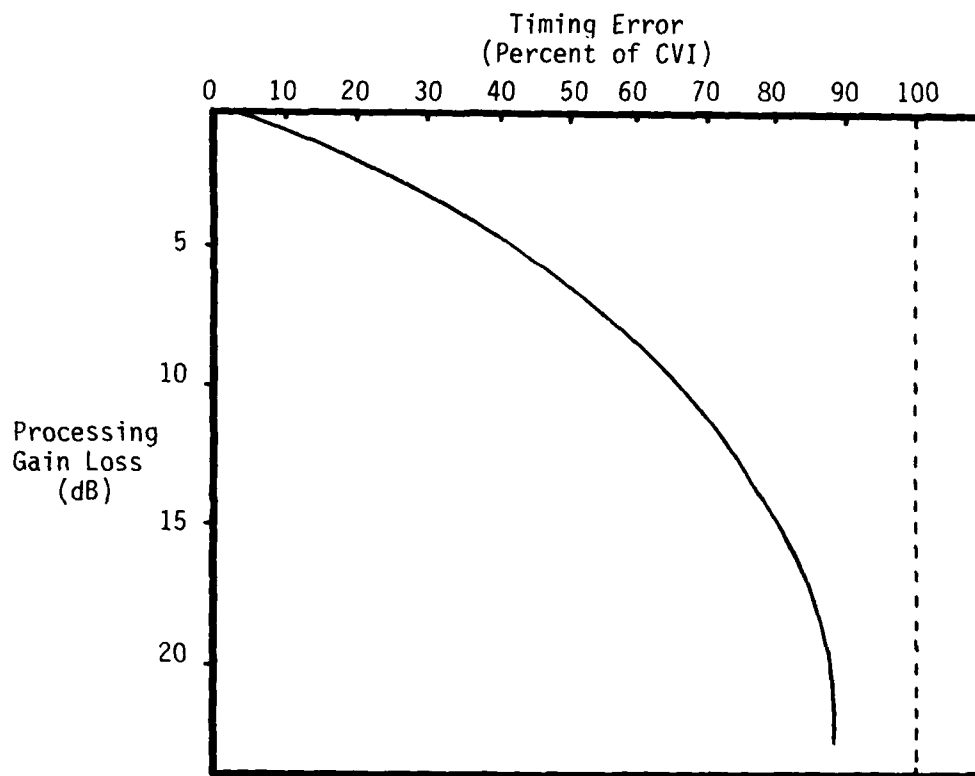


Figure 9.2-1. Processing Gain Loss in Soft Edge CVI System

need be resolved to only some fraction of a CVI. Since a CVI is typically many orders of magnitude greater than a chip width the search time is many orders of magnitude less for the CVI system. And, of course, the need for an acquisition search is greatly reduced in CVI systems since a much larger timing error can be tolerated.

SECTION 10.0

SUMMARY

10.0 SUMMARY

This investigation has focused on the fundamental principles of the acquisition process, mathematically quantifying potential acquisition performance as a function of (1) receiver structures and devices, (2) spreading waveforms and (3) specially structured acquisition signals. Certainly the most obvious conclusion is that MF devices offer a relatively straightforward means (for DS systems at least) of achieving two to three orders-of-magnitude improvement in acquisition time. These magnitudes of improvement are quite significant for reacquisition operations in which only "coarse" or "fine" timing uncertainties exist. In addition, acquisition with a MF results in the smallest residual timing uncertainty at the completion of the acquisition process. Therefore, every attempt should be made to exploit this rapidly developing technology, especially for application to DS data links which require both rapid reacquisition and precision ranging capabilities. A specific recommendation for further work in this area is presented in the next section.

Insofar as the influence of the spreading waveform is concerned direct search of FH was shown to provide the same acquisition speed advantage over direct search of DS as did a MF acquisition of DS. However, it was also seen that direct search of FH results in a larger residual timing uncertainty at the completion of the acquisition process than does a MF acquisition of DS. Basically direct search of FH has an acquisition speed advantage over direct search of DS, for the same initial timing uncertainties, simply because the timing accuracy required for data demodulation in FH systems is less than that required in DS systems. If the only purpose of the spread spectrum link is to provide data transfer, then a FH system employing direct search acquisition has an acquisition speed advantage over a DS system employing direct search acquisition. If precision ranging is a requirement then the FH system must employ a MF structure matched to the frequency hopping pattern which will result in acquisition time and residual timing uncertainty comparable to that provided by a DS system employing a MF receiver. The choice between FH and DS then must take into consideration the relative complexity of the two MF receiver structures, and here the DS system has a decided advantage. Evaluation of the FH/DS waveform for acquisition indicated that its performance falls between that of DS and FH with regard to both acquisition time and residual timing uncertainty. In addition, its receiver structure is more complex than

either of the others so that it cannot be considered an attractive approach to acquisition. The bottom line on these comparisons is that essentially the same acquisition performance can be achieved from DS and FH waveforms if the requirement is to resolve timing from the same initial value to the same final value; and FH/DS can be used to achieve similar acquisition speed but with larger residual timing uncertainty. Consequently, the choice of spreading function for a particular data link application should be much more strongly influenced by other system requirements than by acquisition performance.

Several approaches to specially structured acquisition signals are presented in the report. These methods are of particular interest for initial acquisition or for reacquisition with relatively large timing uncertainty, that is, conditions under which even the acquisition performance of a MF is not sufficient. As often noted in discussions of these methods, any structure in the transmitted signal can be used by a sufficiently intelligent jammer to increase his effectiveness. These techniques should, therefore, only be considered if acquisition or reacquisition with total or very large timing uncertainty is a real system requirement, and if the potential vulnerability is acceptable in light of the anticipated ECM environment. Given that the requirement exists and that the potential vulnerability is acceptable, the "Combined Search and Data Transmission Method" presented in Sections 8.3 through 8.5 provides a straightforward means of trading between waveform structure and acquisition time. In this method a short code spread signal is first acquired (preferably by a MF) and then the long code seed is transmitted as data on the short code spread signal. As shown in Section 8.5, the length of the short code can be selected to minimize the acquisition time, with longer short code lengths resulting in greatly increased acquisition time. An alternative to conventional short codes are the component codes described in Appendix B. These codes are generated by combining several codes in such a way that the period of the resulting code is equal to the least common multiple of the periods of all the components but that the acquisition time is essentially the time to acquire the longest component only. The result is an acquisition time significantly less than that of a comparable length PN code but the acquisition detector requires an acquisition device for each code component in order to fully realize the potential speed advantage. Further investigation of the implementation and vulnerability of these codes is required before a meaningful comparison can be made between them and conventional short code techniques.

The special waveform techniques which have the potential for making the greatest impact on tactical AJ data links are the CVI techniques discussed in Section 9. These techniques allow data demodulation with relatively large timing uncertainty between transmitter and receiver, thereby avoiding any reacquisition operations for most tactical scenarios. Direct utilization of the CVI methods would make the data link somewhat more susceptible to smart jamming but the inclusion of well designed message validation techniques can greatly reduce this vulnerability. These are areas for further study and are discussed in the next section.

SECTION 11.0
RECOMMENDATIONS FOR FUTURE WORK

11.0 RECOMMENDATIONS FOR FUTURE WORK

Having well established the fundamental principles of acquisition and identified areas of potential performance advantages, it is appropriate to now exploit the most promising techniques. The "ultimate" acquisition strategy is one which is fully AJ protected at all times and which provides instantaneous acquisition. Such a strategy would be the basis for a highly robust model which could meet a wide range of tactical communication requirements, including "push-to-talk" requirements. Such an acquisition strategy is obviously sometime off in the future but does represent a most significant and an achievable goal, and this section outlines a plan for achieving that goal.

Matched filter technology is recognized as one key to improved modem performance, for both acquisition and data demodulation. Devices which are either presently available or under development, CCDs, digital correlators, SAW convolvers and the hybrid array correlator, were described in this report and their utilization and performance as acquisition processors indicated. Investigation of new and more powerful MF concepts, such as the optical processing techniques described in Appendix D, should be encouraged and supported by the AJ systems community. The benefit to the AJ systems community would not only be the continual evaluation of the applicability of these new devices to AJ systems but also that development of the most promising concepts would be driven such that the end product is directly applicable to future AJ systems. These devices would represent powerful signal processing resources which could support multiple receiver functions including acquisition, data demodulation, carrier tracking and estimation of other pertinent system parameters.

Concurrent with the investigation of new MF devices, the performance advantages of present state-of-the-art devices should be verified and demonstrated through implementation, at the earliest opportunity, in a state-of-the-art AJ system. The Army's Modular Integrated Communication and Navigation System (MICNS) presently in development at Harris represents an excellent opportunity for near term application of a state-of-the-art MF to acquisition in a state-of-the-art DS system. Demonstration with the MICNS would be a relatively quick turnaround effort requiring a minimal design and breadboard effort for peripheral subsystems. This application would then provide the design experience and test data upon which to establish the requirements for new MF devices. This implementation activity would be supplemented by an analysis effort aimed at optimizing the effectiveness of the MF based acquisition processor. The correlation period of MFs is

limited by physical constraints on the devices and by signal decorrelation due to Doppler. In most applications the correlation period will be between 10 and 20 microseconds. For low symbol rates more than one correlation per acquisition test will be required in order to obtain a sufficiently high probability of acquisition detection at typical jammer to signal ratios. Therefore, the acquisition processor must include circuitry for sampling and processing the MF output. The process of converting the MF output to digital samples involves trade-offs between sample rate and sample quality, pulse shaping techniques, AGC, etc. The processing of the digital samples involves trade-offs between processing gain, probability of detection and probability of false alarm, and complexity of the processing hardware. Recent advances in LSI technology permit quite sophisticated processing. For example, it may be practical to keep track of past false alarm patterns and to use this information to dramatically reduce the dismissal time of future false alarms. In addition, the processor could be adaptive or programable such that its parameters (processing gain, sampling rate, etc.) could be changed to be compatible with the environment, either automatically or by user control. The inclusion of these signal processing capabilities into a MF acquisition processor would result in a greatly enhanced acquisition strategy, and could be accomplished with today's technology.

The next step towards the "ultimate" acquisition strategy is the formulation of receiver structures and waveform designs which will exploit the high speed, high density digital processing capabilities of the forthcoming VHSIC and VLSI technologies. These techniques will provide maximum processing power at minimum cost by performing most of the receiver functions in the relatively low cost digital domain rather than in the relatively high cost analog domain. The high speed of the devices will permit considerable processing of the received signal for enhanced message identification and smart jammer dismissal. This processing power will allow the use of more complex acquisition codes which will give a decided edge to the friendly receiver over the intelligent jammer. "Long" short codes and more complex component codes will be more attractive for acquisition. But the most attractive signalling techniques for this era of technology appear to be the CVI techniques. The basic techniques rely on a sufficiently high rate of code change to reduce susceptibility to smart jammers. Shortening the CVI increases the protection against smart jammers. However, clock instability and vehicle dynamics place a limit on how short the CVI can be made and still maintain the desired processing

gain. If moderately accurate position information is available, the clock is the limiting factor and the length of the CVI is a trade-off between clock accuracy and speed of the smart jammer. However, with the processing power of VHSIC and VLSI message validation techniques can be incorporated to significantly reduce the vulnerability of a relatively long CVI.

The final step in the plan is the merging of high accuracy clocks, high precision position estimation and powerful digital signal processing. At that point the CVI can be reduced and the small CVI, supported by the powerful message validation procedures, will result in the "ultimate acquisition strategy --- full AJ protection and instantaneous acquisition.

Harris is prepared to discuss, in detail, study activities which will support the areas outlined above.

APPENDIX A
FH ACQUISITION BY ASEAT

APPENDIX A
FH ACQUISITION BY ASEAT

An interesting technique for acquisition of FH, the Autoregressive Spectral Estimation Acquisition Technique (ASEAT), has recently been reported in the literature [1, 2]. A simplified block diagram of the system is shown in the attached figure with operation as follows. The N-stage linear feedback shift register (LFSR) in the transmitter provides the N-bit address for the frequency to be transmitted during each frequency interval. This allows 2^N different frequencies for hopping. Let the contents of the LFSR during the k^{th} interval be denoted by

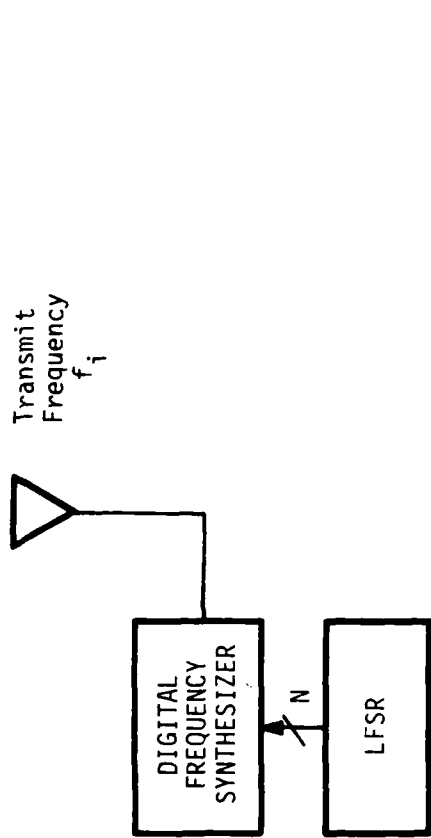
$$b_N \ b_{N-1} \ \dots \ b_2 \ b_1$$

where b_1 is the most significant bit (MSB) and b_N is the least significant bit (LSB). The corresponding transmitted frequency during this interval is f_k . For the $(k+1)^{\text{st}}$ interval the LFSR is shifted one bit so that the contents are

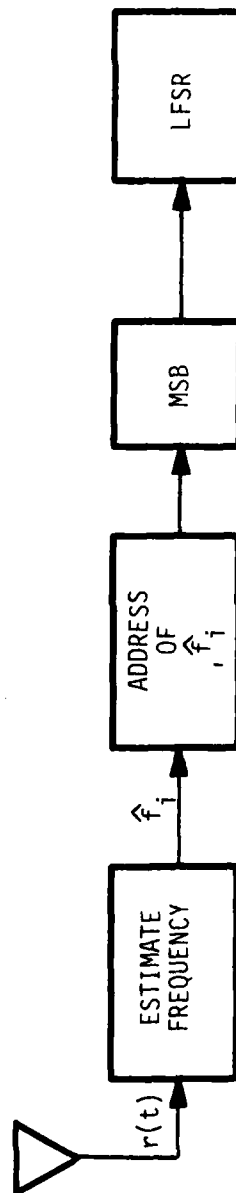
$$\begin{array}{ccc} \text{LSB} & & \text{MSB} \\ b_{N+1} & b_N & \dots \ b_2 \end{array}$$

producing the frequency f_{k+1} . For transmission intervals k through $k+N-1$ the LFSR contents and corresponding frequencies are:

<u>Interval</u>	<u>LFSR Contents</u>				<u>Frequency</u>
	<u>LSB</u>		<u>MSB</u>		
k	b_N	$b_{N-1} \ \dots$	$b_2 \ b_1$		f_k
k+1	b_{N+1}	$b_N \ \dots$	$b_3 \ b_2$		f_{k+1}
k+2	b_{N+2}	$b_{N+1} \ \dots$	$b_4 \ b_3$		f_{k+2}
⋮		⋮			⋮
k+N-1	b_{2N-1}	\dots	$b_{N+1} \ b_N$		f_{k+N-1}



(a) Transmitter



(b) Receiver

Figure A-1. FH Acquisition by ASEAT

I

Note that the list of MSBs constitute the LFSR contents during the initial interval. Thus, if the receiver can estimate the received frequencies f_k , f_{k+1} , ..., f_{k+N-1} with sufficient accuracy to have the MSB of the addresses correct, then the receiver will exactly know the initial contents of the transmitter's LFSR. Since all future contents of a LFSR are uniquely determined from the contents at any one instance, the receiver's LFSR can be loaded so as to match that of the transmitter. Thus acquisition is achieved in N intervals, by sending one bit of timing information (b_1 then b_2 then b_3 ... then b_N) during each interval. If the LFSR is connected to produce a maximal-length sequence the length is $2^N - 1$. Therefore, this technique is seen to be a data transmission method in which acquisition of a 2^{N-1} chip long code is achieved by transmission of N bits of timing data. Unfortunately a smart jammer can also use the ASEAT to obtain synchronization with the transmitter and can then exactly produce the FH pattern with any desired delay or advance. Thus such a system has a rapid acquisition capability but is also quite vulnerable to smart jamming. Normally the technique used to overcome this form of vulnerability is nonlinear code generation, in which case the MSBs of the sequence of received frequencies will not be the initial contents of the transmitter's shift register. Consequently the ASEAT does not appear to be a viable acquisition method for AJ systems.

REFERENCES

1. Takhar, G. S., A. K. Elhakeem and S. C. Gupta, "Frequency Hopping Acquisition by Autoregressive Spectral Estimation," Proc 1978 IEEE Int. Conf. Comm., Toronto, Canada, paper 16.4
2. _____, "New Code Acquisition Techniques in Spread-Spectrum Communication," IEEE Trans. on Comm., Vol COM-28, No. 2, February 1980, pp 249-257.

APPENDIX B
COMPONENT CODES

APPENDIX B COMPONENT CODES

Component codes offer a means of introducing structure into a DS spreading signal in such a way that it can be exploited by the receiver to reduce acquisition time. As emphasized throughout the report, any reduction in randomness of the spreading waveform increases the vulnerability to smart jammers so that the use of component codes does reduce the AJ protection. On the other hand they represent an alternative to the other structured waveform methods, such as conventional short codes, and may be employed when acquisition is to be performed in an environment of relatively unsophisticated jammers.

A component code (S) is one that is formed by performing some Boolean function (B) on several component codes (X_i), that is

$$S = B (X_1, X_2, \dots, X_n)$$

The period of the code S is equal to the least common multiple of the periods of all component codes. If the component code periods are chosen to be relatively prime, the period of S is equal to the product of the periods of the component codes. Furthermore, if B is chosen correctly the code S will have nearly equal numbers of 1's and 0's and the component code will exhibit a detectable cross correlation with each of its components. It is this last property which allows the component code to speed up the acquisition process.

At this point an example is in order. Consider a three component code and the Boolean function

$$S = X_1 \times X_2 + X_2 \times X_3 + X_3 \times X_1$$

where X_1 , X_2 and X_3 are the component codes. We could choose the component code periods as

$$\begin{aligned} P_{X_1} &= 2^7 - 1 = 127 && \text{(prime)} \\ P_{X_2} &= 2^9 - 1 = 511 && (= 7 \times 73) \\ P_{X_3} &= 2^{10} - 1 = 1023 && (= 3 \times 11 \times 31). \end{aligned}$$

Since these periods have no common factors they are relatively prime, thus the length of the composite code is

$$P_S = 127 \times 511 \times 1023 = 66389631.$$

This period is somewhat shorter than the period of a maximal length sequence having $7 + 9 + 10 = 26$ state variables, but longer than that of a 25 state variable maximal length sequence. For this particular code there are 358785 more 1's than 0's. It would appear that a maximal length sequence with 26 state variables is preferable to this composite code on the basis of slightly longer period and better 1/0 balance. This is true until one considers the acquisition process. Using the proper Boolean function allows acquisition of each of the component codes independently and simultaneously. Consider what happens when the composite code (transmitted as $1 \rightarrow +1$ and $0 \rightarrow -1$) is correlated with a replica of any of its components. This gives

$$R_{\hat{X}S} = 2 E[\hat{X} \oplus S] - 1$$

due to the translation $0 \rightarrow -1$. If \hat{X} is a time shifted version of a component (essentially uncorrelated) then

$$R_{\hat{X}S} \approx 0$$

while if \hat{X} is identical to a component

$$R_{\hat{X}S} \approx \frac{1}{2}.$$

Thus the problem of acquiring one component is simply the problem of acquiring a short code only with 6 dB less signal power (neglecting code self noise). Since all components may be acquired in parallel, the acquisition time is essentially equal to the time required to acquire the longest components. For our example code, the number of (half chip) cells to search is reduced from $\sim 2^{27}$ down to $\sim 2^{11}$ for a reduction of

$$\sim 2^{16} = 65536.$$

Of course acquisition is not 65000 times faster since the cells are searched with a 6 dB lower S/J, but considerably accelerated acquisition is possible.

APPENDIX C
TIMING UNCERTAINTY AT REACQUISITION

APPENDIX C

TIMING UNCERTAINTY AT REACQUISITION

The time required to reacquire a spread spectrum link after a period of link outage is directly proportional to the timing uncertainty which has accrued during the outage. It is, therefore, of interest to identify the sources of timing error and their relative contributions to the total error. In addition, an estimate of the total timing error is required to properly initialize the reacquisition processor. In a direct search reacquisition system the accrued timing error defines the uncertainty region which must be searched; in a MF reacquisition system it dictates the amount by which the local reference must be advanced. Underestimating the timing error may result in a missed acquisition; overestimating may result in unnecessarily long reacquisition time. The total timing uncertainty, T_u , is a function of PN clock offset, vehicle dynamics, error growth rate of any inertial navigation system (INS) used for position estimation and loss-of-link time.

The total timing error that accrues between two previously synchronized clocks is due to clock offset, aging and a randomly varying term which is characterized by the Allan variance. Clock offset consists of initial setting error, temperature stability, etc. and produces a timing error which is a linear function of loss-of-link time. Error due to aging can usually be neglected for the relatively short periods of link outage encountered in tactical communication systems. The randomly varying term is also usually negligible in comparison to the offset error for clocks of the quality used in tactical systems. Thus, the timing uncertainty contributed by the clocks is essentially that produced by clock offset and is a linear function of loss-of-link time. For example, considering the transmitter's clock to be a perfect reference, a clock offset in the receiver of 10^{-6} would produce 1 microsecond of timing offset per second of link outage. For MF reacquisition this would indicate that the local reference should be advanced 1 microsecond for each second of link outage, whereas for a direct search system the uncertainty region would grow at a rate of 2 microseconds per second since the direction of relative offset is unknown. Note that for this source of timing error, as is true for the other sources as well, the uncertainty region for direct search is twice as large as the reference advance for the MF. However, the MF may have to

wait an amount of time equal to twice its advance before coincidence occurs. In the following discussions of timing uncertainties only the one-sided error will be indicated, i.e., the amount of MF advance.

As noted above the timing uncertainty due to the PN clock is a linear function of the loss-of-link time

$$T_{uc} = C_o T_l \times 10^{+6} \quad (C-1)$$

where C_o is the clock offset, T_l is the loss-of-link time in seconds and T_{uc} is the timing uncertainty produced by the clock in microseconds. The timing uncertainty due to differential velocity between transmitter and receiver is also a linear function of loss-of-link time, with a rate of approximately 1.1 microseconds per second at Mach 1. Therefore, with differential velocity v in Km/hr the timing uncertainty in microseconds is

$$T_{uv} = 3.34 \times 10^{-3} v T_l \quad (C-2)$$

However, a second order tracking loop can accurately track out constant velocity, even over relatively long periods of link outage, so that this error may not be a significant factor. Differential acceleration produces timing uncertainty which is proportional to the square of T_l . For a differential acceleration of "a" gs,

$$T_{ua} = 32.0 \times 10^{-3} a T_l^2 \quad (C-3)$$

where again the timing uncertainty is in microseconds.

The timing uncertainties due to clock, differential velocity and differential acceleration are compared in Figure B-1 where the assumed system parameters are:

$$\begin{aligned} C_o &= 10^{-7} \\ v &= 200 \text{ Km/hr} \\ a &= 2 \text{ gs} \end{aligned}$$

It is noted that velocity is the driver for loss-of-link times up to about 11 seconds. However, as noted earlier, constant velocity can be tracked out by a second order loop while the link is established and very accurately estimated while the link is lost. Thus, the major contributions are actually acceleration and clock offset. Of these two, clock offset is the major factor for the first few seconds and then acceleration becomes the major factor.

Timing uncertainty due to acceleration can be greatly reduced by INS aided position estimation. A relatively low cost INS unit typically employed in RPVs can provide range estimation with a one σ error of

$$\sigma_{re} = 6 \times 10^{-3} T_1^2 \quad (C-4)$$

where σ_{re} is in feet and T_1 is in seconds. This produces a PN code timing uncertainty ($+3\sigma$) of

$$T_{uINS} = 18 \times 10^{-6} T_1^2 \quad (C-5)$$

where T_{uINS} is in microseconds and T_1 in seconds. With such a unit providing range information the timing uncertainties due to velocity and acceleration are replaced by T_{uINS} , and the total timing uncertainty is due to the clock and the INS. Obviously the clock offset is the dominant factor for most link outages. Equating T_{uc} and T_{uINS} and solving for T_1 indicates that the INS does not become the dominant factor until the link has been out for over 1.5 hours. Thus, in the case of INS aided positioning the clock offset is, in reality, the only significant factor in timing uncertainty for reasonably long link outages.

The maximum acceptable timing uncertainty at reacquisition is an important system parameter in that it establishes the minimum update rate. If, for example, the maximum uncertainty is 10 microseconds and the total uncertainty is due to clock offset and differential acceleration then the maximum period of link outage is 11.7 seconds for the example cited above. If INS aided positioning is available only clock offset need be considered and the maximum T_1 becomes 100 seconds. On the other hand, if a CVI technique is employed with a CVI length of hundreds of milliseconds the system can operate for days between timing updates based on these considerations.

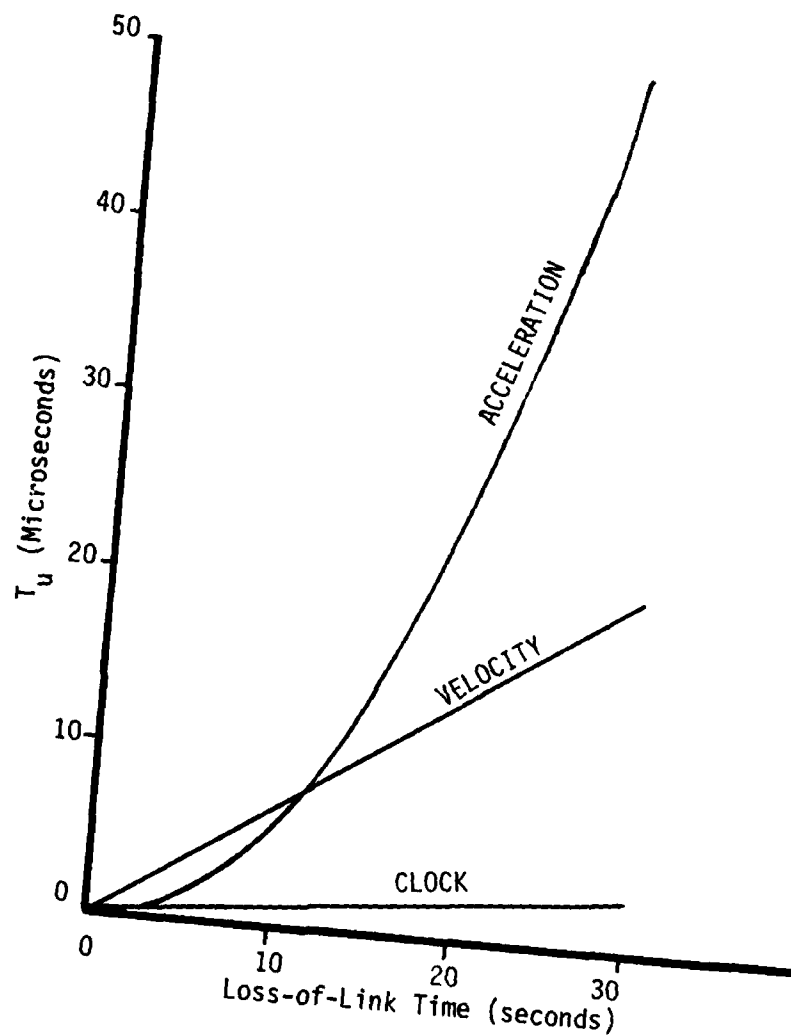


Figure C-1. Timing Uncertainties

APPENDIX D
OPTICAL PROCESSING

APPENDIX D
OPTICAL PROCESSING

In addition to the CCD and SAW convolvers, digital correlators and hybrid array technologies cited in Section 5, optical approaches warrant further study for performing high-speed, parallel processing. The key element in optical processing is a Bragg cell which, in most implementations functions as an analog or a digital delay line. Generally these devices have bandwidths in the 50-300 MHz range, delay times ranging from 1 to 40 sec and time-bandwidth products in the range of 1000-2000.

For some communication applications the integration time, which is basically the delay time, is too short. In recent years, however, a new class of processing architectures have evolved in which the integration time can be extended appreciably to provide additional correlation gain. This class of optical systems are generally called time-integrating optical systems (TIC). One attractive feature of optical processing is that the operations are naturally performed in parallel. Of equal significance for rapid acquisition is the fact that optical systems are two-dimensional so that the orthogonal axis can be used to display doppler if the principal axis is used to display time delay.

We first describe an optical system that performs a matched filtering operation similar to that described before; this example will illustrate some of the basic principles of optical processing. Figure D-1 shows an optical system in which light from a point source is collimated by lens L_1 . The source might be a small solid state light emitting diode or an injection laser diode. Suppose that we modulate the source with the PN sequence $f_1(t)=C(t)$ and that this light illuminates a Bragg cell which is driven by the received signal $f_2(t)$ which is the same sequence, with a large starting time uncertainty, plus noise. For the moment, suppose we treat the noise free case; the Bragg cell operates so that the waveform within the cell is $C(t-x/v)$ where x is a space coordinate in the plane of the Bragg cell and v is the velocity of the acoustic wave. The light emerging from the Bragg cell is then $C(t)C(t+\tau)$ where $\tau=-x/v$.

If we image the Bragg cell onto a linear photodetector array containing N elements, we can associate a given time delay τ_j with the j th element in the array. If we integrate for a time T , where T may be much longer than the delay time of the Bragg cell, we have that the output of the j th element is

$$R_j = R(\tau_j) = \int_0^T C(t)C(t+\tau_j)dt .$$

Since the number of elements in the array may be of the order of 1000 and if we measure the correlation at $\frac{1}{2}$ chip intervals, we see that we can dismiss 500 chip intervals in each time interval of duration T.

By using multiple sources or multi-channel Bragg cells, along with a multi-channel or two dimensional photodetector array, we can increase the time delay searched in parallel by a corresponding factor. Alternatively, different dopplers could be provided in each channel with the same PN sequence phasing to give a simultaneous doppler/delay output.

It should be noted that this optical system performs the matched filtering operation without the need to time reverse the reference PN sequence which is typical of many other approaches. Very long sequences can therefore be correlated easily.

If it is desirable to rapidly acquire a PN sequence when the doppler range is large (or when fine doppler increments must be tested), a different optical configuration might be useful. Such a system, not shown here, is called a "triple-product processor." Its configuration is similar to that shown in Figure X except that the first Bragg cell is imaged onto a second Bragg cell that is oriented along the axis orthogonal to the first cell. Both cells are then imaged onto a two-dimensional photodetector array. This system has the interesting property that it displays the ambiguity function as given by the combination of equations (3.4-8) and (3.4-9). The integrated output is given as

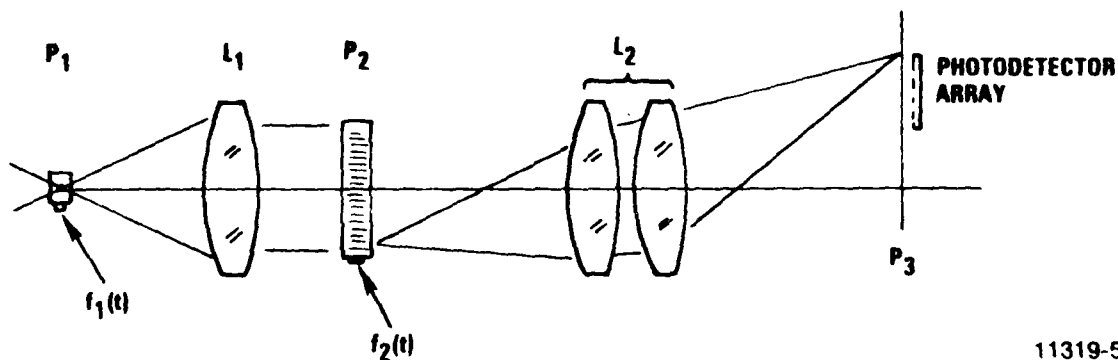
$$R(\tau, \omega_d) = \int_0^T C(t) C(t+\tau) e^{j\omega_d t} dt$$

where τ is a continuous variable in the horizontal direction and ω_d is a continuous variable in the vertical direction. For a 1000x1000 photodetector array, we can examine of the order of $(500)^2=250,000$ doppler/delay bins in a time interval of T.

Other optical configurations can be used to handle frequency hopped signals. For example, it is well-known that a coherently illuminated optical system displays the instantaneous Fourier transform of that portion of a signal resident within the Bragg cell at any instance in time. As the frequency is hopped, the position of the focused beam in the Fourier plane also hops, with a

unique one-to-one mapping of hop frequency and spatial position. Schemes for activating photodetectors based on the hopping sequence or the use of a second Bragg cell to introduce a reference of the hopped sequence may be useful to dehop and despread the signal in a single system.

To date very little effort has been applied toward investigating the potential uses of the features of two-dimensional or multi-channel optical processing. We propose to examine this potential by studying and adding to the existing class of optical processing architectures for implementing rapid acquisition algorithms. The focus will be to develop techniques that provide high-speed, parallel searches for doppler and time delay simultaneously. Although we currently envision using the optical techniques primarily for acquisition, there are also possibilities for demodulation and detection as well. Efforts will also be directed toward system configurations that are compact and low-cost, but these considerations are of less importance at this time.



11319-5

Figure D-1. Time-Integrating Correlator

